1988

Quantitation of maltooligosaccharides and determination of glucoamylase activity using pulsed amperometric detection for glucose

Larry Arnold Larew
Iowa State University

Order Number 8909166

Quantitation of maltooligosaccharides and determination of glucoamylase activity using pulsed amperometric detection for glucose

Larew, Larry Arnold, Ph.D.

Iowa State University, 1988

U·M·I
300 N. Zeeb Rd.
Ann Arbor, MI 48106

Quantitation of maltooligosaccharides and determination of glucoamylase activity using pulsed amperometric detection for glucose

by

Larry Arnold Larew

A Dissertation Submitted to the

Graduate Faculty in Partial Fulfillment of the

Requirements for the Degree of

DOCTOR OF PHILOSOPHY

Department: Chemistry
Major: Analytical Chemistry

Approved:

Signature was redacted for privacy.

In Charge of Major Work

Signature was redacted for privacy.

For the Major Department

Signature was redacted for privacy.

For the Graduate College

Iowa State University
Ames, Iowa

1988

TABLE OF CONTENTS

GENERAL INTRODUCTION

Carbohydrates and Starch Hydrolyzing Enzymes

Carbohydrates represent one of the major classes of biologically important compounds. They participate in virtually all aspects of cellular life. They are the primary products of plant photosynthesis and, thus, are the metabolic precursors of all other organic compounds. Carbohydrates are stored as the source of energy that maintains life and they also have many important structural and regulatory roles in living systems (1). Carbohydrates are the primary natural resource of many important industries, including the manufacture of foods and food processing, fermentation, paper and wood processing, textiles, plastics, and pharmaceuticals and drugs (2).

A carbohydrate is defined as a polyhydroxy aldehyde or ketone (2). Some of the more common carbohydrates include: sucrose (table sugar), glucose, maltose, ribose, fructose, lactose, starch and cellulose (1). Derivatives of polyhydroxy aldehydes or ketones are also considered to be carbohydrates. Some of the more common derived carbohydrates contain a reduced (3) or oxidized (4) carbonyl group or an amino (5), thiol (6), hydrogen (7), or halide (8) group substituted for a hydroxyl group.

Carbohydrates can be divided into three major classes based upon the size of the carbohydrate molecule (1): the monosaccharides (2), which include all simple sugars (i.e., glucose and ribose); the oligosaccharides (9), which include the polymeric carbohydrates ranging in size from 2 to *ca.* 20 polymer units (i.e., sucrose, maltose, maltotriose, malto-

tetraose, etc.); and the polysaccharides (10, 11), which include the polymeric carbohydrates with more than *ca.* 20 polymer units (i.e., starch, cellulose and dextran).

One of the largest and most important polysaccharides is starch which is composed of hundreds of glucose units (11). The glucose units are linked primarily *a*-1,4 with *a*-1,6 branch points. Dextrins are the products of partial starch hydrolysis (enzymatic or chemical) (11). A dextrin is composed of a mixture of maltooligosaccharides which vary in their size from 2 to several (*ca.* 50) glucose units. Starch is produced by plants from a part of the energy captured from the sun during photosynthesis and is stored as a food reserve. Starch provides the link between non-photosynthesizing organisms and energy from the sun (12). Starch represents the primary raw material for the starch processing, food processing and the fermentation industries. Enzymes which catalyze the hydrolysis of the glycosidic bonds between the glucose units found in starch are required for organisms to utilize starch as a food source (12). Several of these starch hydrolyzing enzymes (amylases) are used by the starch processing industries in the production of high-fructose, high-glucose, and high-maltose syrups (13). The enzyme of primary interest in this dissertation is glucoamylase from the fungal species Aspergillus niger (14). Glucoamylase catalyzes the hydrolysis of *a*-1,4, *a*-1,6 and *a*-1,3 glycosidic bonds of glucose polymers producing *b*-glucose from the non-reducing end of the polymer chain (14). For a complete discussion of the properties and uses of glucoamylase the interested reader should refer to the excellent reviews by Reilly (13, 14).

Principles of Amperometric Detectors

Electrochemistry is the study of the interconversion of chemical and electrical energy. A change in the chemical energy (dG, change in the Gibbs free energy) of a system (usually a solution) results in a change in the ability of the system to do electrical work (w_{elec}). Conversely, when electrical work is done on a system, the energy of the system is changed. In fact, the change in the energy is equal to the electrical work done on the system. Electrical work is defined as the product of the total charge (Q) passed to (or from) the system and the potential difference (E) through which the charge is passed:

$$w_{elec} = QE \qquad (1)$$

If electrons are the carriers of the charge, then:

$$Q = nF \qquad (2)$$

where n is the number of moles of electrons passed and F is the charge per mole of electrons. When the electrical work is done by the system, then the change in the energy of the system is:

$$dG = - w_{elec} = - nFE \qquad (3)$$

Therefore, changes in chemical energy can be directly detected by an electrochemical probe (called an electrode) which is capable of doing and/or measuring electrochemical work.

The above discussion illustrates how electrochemistry is a useful tool for chemical analysis. Since dG is a function of the concentrations

of reactants and products for any chemical reaction, the electrode is used to detect changes in concentrations. Consider the following general reaction:

$$A + B = C + D \qquad (4)$$

for which we can write $K_{eq} = CD / AB$. When the reaction proceeds to the right,

$$dG = dG^{o} + RT \ln CD/AB \qquad (5)$$

where R is the ideal gas constant and T is the absolute temperature. At equilibrium $dG = 0$ and $dG^{o} = - RT \ln K_{eq}$. Combining equations (5) and (3) yields

$$E = E^{o} + RT/nF \ln AB/CD \qquad (6)$$

where $E^{o} = RT/nF \ln K_{eq}$. Equation (6) (known as the Nernst equation) is used to relate changes in potential differences to changes in concentrations. For a more complete discussion on the fundamentals of electrochemistry, the interested reader should refer to the excellent monographs by Rieger (15) and Bard and Faulkner (16). Also, for a description of how electrochemical measurements are made, the reader is referred to the monographs which detail electrochemical instrumentation (15, 16, 17, 18, 19).

The electrochemical detector of primary interest in this dissertation is one which measures current (charge/time). An amperometric detector measures the flow of current to (or from) a chemical system

when a potential difference (voltage) is applied to the system at the electrode. The value of the potential difference is controlled (independent variable) and the current is measured as the dependent variable. The applied potential is the driving force for the electrochemical reactions which occur at the electrode. The current is a measure of the net rate of the electrochemical reactions. The electrode current (I, coul sec^{-1}) is related to the rate of the electrochemical reaction by Faraday's law:

$$I = nFAN \qquad (7)$$

where n is the number of moles of electrons passed per mole of reactant (equiv mol^{-1}), F is the faraday constant (96,486.6 coul $equiv^{-1}$), A is the geometrical area of the electrode (cm^2), and N is the total flux of the reactant to the electrode surface (moles cm^{-2} sec^{-1}). The value of N is dependent upon the diffusion coefficient (D, cm^2 sec^{-1}), and the solution concentration of the reactant (C^b, M). For the general reaction, Ox + ne --> Red, occurring in a quiescent solution at a planar electrode with $E >> E^o$:

$$N = DC^b / d \qquad (8)$$

where $d = (3.14Dt)^{1/2}$ and t is the time (sec) elapsed since the application of E. Combining equations (7) and (8) yields the Cottrell equation:

$$I = nFADC^b / (3.14Dt)^{1/2} \qquad (9)$$

Thus, in theory, the solution concentration of Red can be determined if I is measured after the application of a potential difference capable of supporting the electrochemical oxidation of Red at the electrode surface (assuming the values of all the constants are known). In practice, however, exact values for n and D are often not known, so that a calibration experiment with known concentrations of Red is required to determine the proportionality constant (K) for the equation:

$$I = KC^b \qquad (10)$$

before unknown concentrations of Red can be determined. Also, some separation technique (i.e., chromatography) is usually required prior to amperometric detection to eliminate contributions to I from other components which may be present in real samples. This requirement results from the inherently non-selective nature of amperometric detectors, i.e., many types of compounds are capable of reacting at similar potentials.

From examination of the Cottrell equation, I is predicted to decay to zero at a rate proportional to the square root of time. This relationship results from the rapid depletion of Red near the electrode surface as the oxidation reaction proceeds. Diffusional mass transport of Red from the bulk solution is a slow process and is usually much less than the rate of the electrochemical oxidation of Red. Thus, a finite concentration of Red can not be maintained near the electrode and I decays to zero shortly (t = *ca.* 100 msec) after the application of the potential to the electrode. For the measurement of I to be an accurate estimater of C^b, convective mixing of the solution is used to replenish

the concentration of Red near the electrode. The current resulting from the oxidation of Red remains finite and becomes constant at t > 100 msec with the addition of convective mass transport to the total value of the flux. Convection effectively decreases the value of *d* (the diffusion layer thickness) so that the rate of mass transport of Red to the electrode is of the same magnitude as the rate of the electrochemical reaction.

Two types of electrodes were used to measure I in the experiments described in this dissertation. A flow-through cell (20) containing a circular gold disc electrode was used for flow injection and chromatographic determinations of glucose and glucose polymers. Convective mass transport of analyte to this type of electrode was effected by the flow of the solution over the electrode surface. Therefore, the current produced was a function of the flow rate through the cell (21):

$$I = 1.47nFC^{b}(DA / b)^{2/3}u^{1/2} \qquad (11)$$

where b is channel height or thickness of the cell (cm), u is the average volume flow rate (mL sec^{-1}) through the cell, C^{b} is the mM concentration of the analyte, and I is the current in uA. The second type of electrode was a circular gold disc on the end of a cylindrical stainless steel shaft. The steel shaft was insulated with Teflon so that it could not contact the solution. Convective mass transport to this type of electrode was effected by rotation of the electrode. The convective-diffusion equation has been solved rigorously for the steady state current produced at the rotated disc electrode (RDE) (16):

$$I = 0.62nFAD^{2/3}w^{1/2}v^{-1/6}C^{b} \qquad (12)$$

where w is the rotation velocity of the electrode (rad sec^{-1}), v is the kinematic viscosity of the solution (cm^2 sec^{-1}), C^b is the M concentration of the analyte and I is the current in mA. Equation (11) is known as the Levich equation (16).

Pulsed Amperometric Detection

Most aliphatic compounds, including the carbohydrates determined in this dissertation, have traditionally been considered to be electrochemically inactive at constant applied potentials (22). Currents for these compounds at noble metal electrodes are initially large, but, fall to zero within a few seconds after the application of $E >> E^{o}$ (even in the presence of large flux) (23). This behavior has been attributed to fouling of the electrode surface by strongly adsorbing reaction intermediates (free radicals) which prevent further electrode activity (22).

It is now well established that a significant anodic (oxidation) current can be obtained for carbohydrates at a gold electrode in an alkaline solution if the potential is cycled or pulsed to maintain an active electrode surface (24, 25, 26, 27). The cycling or pulsing of the electrode potential effects the oxidative desorption of the adsorbed free radical and the reactivation of the electrode (26). Pulsed amperometry was first reported for carbohydrate detection at Pt electrodes by Hughes and Johnson in 1981 (28). Since then, pulsed amperometric detection (PAD) has been applied with much success to the detection of many types of aliphatic compounds, including alcohols, thiols,

amines, and amino acids (26). Instrumentation for PAD has recently been commercialized by the Dionex Corporation (20).

The triple-step potential waveform commonly applied for PAD is shown in Figure 1. The detection potential (E_1) for carbohydrates at a gold electrode in alkaline solution is typically 0.15 V (versus SCE). This potential is applied to the electrode for a total of 420 msec. The current is sampled over the last 200 msec of the application of E_1. Oxidative cleaning of the electrode is effected by pulsing to a potential value (E_2) near the region of oxygen evolution (*ca.* 0.75 V). Reactivation of the electrode is effected by pulsing to a potential value (E_3) near the region of hydrogen evolution (*ca.* - 1.0 V). Both E_2 and E_3 are applied for 120 msec.

The determination of carbohydrates is of importance in many diversified areas of science and industry because carbohydrates are so widespread in nature. A few of these areas include: the paper, textile and wood processing industries (29); the brewing (30) and food processing industries (31); and medicinal and clinical chemistry (32). The traditional methods for determining carbohydrates have been reviewed elsewhere (27, 32, 33, 34, 35). PAD combined with high performance anion exchange chromatography for the determination of carbohydrates has been shown to have significant advantages over the more traditional methods (20, 22, 26, 27). These advantages include: much lower limits of detection, high sensitivity, excellent precision, and rapid analysis times (20).

Figure 1. Typical triple-step potential waveform applied for PAD

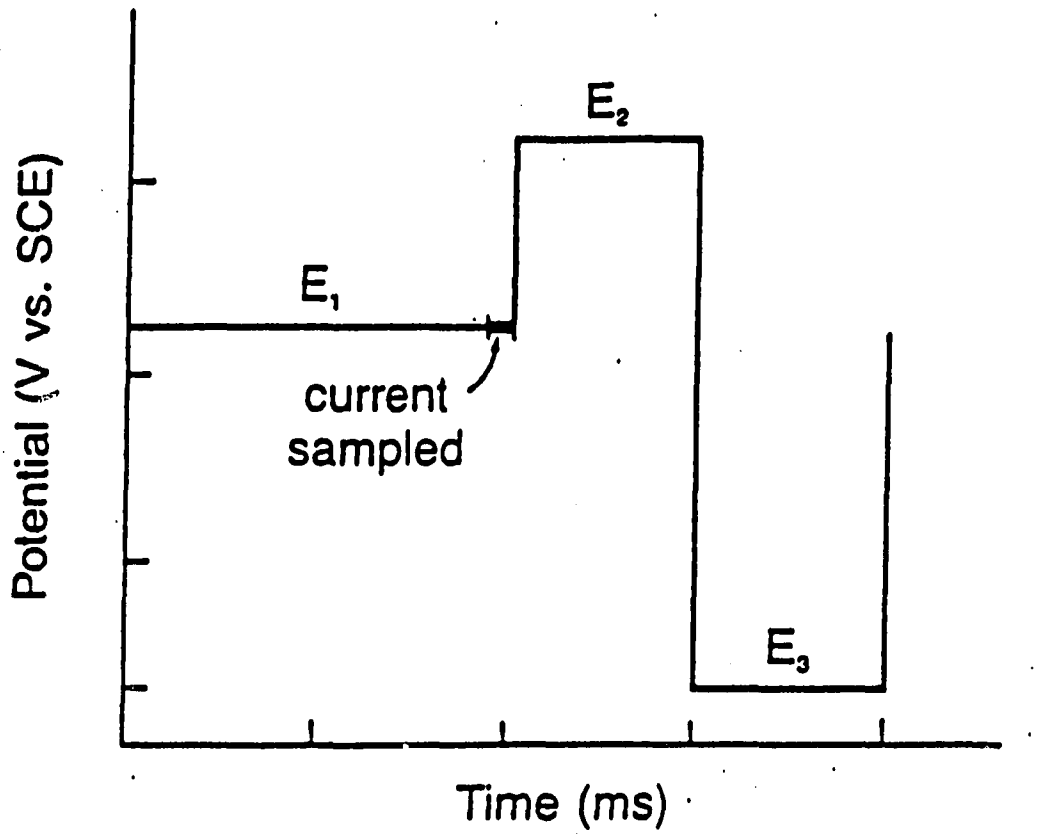
Potential (V vs. SCE)
E2
E1
current
sampled
E3
Time (ms)

Explanation of Dissertation Format

This dissertation follows the alternate format. The sections detail the research completed under Dr. Dennis C. Johnson from fall of 1986 to fall of 1988. Research completed prior to the fall of 1986 under Dr. Rodney R. Walters is not included (36). The sections are arranged in reverse chronological order with Section I representing the work completed in the fall of 1988. Because of this arrangement, a few of the questions asked in the final sections are answered in the first sections. It is neccessary to make the reader aware of this arrangement in advance to avoid possible confusion or misunderstanding. However, it is believed that the reverse chronological order should result in a better understanding of the research described in the final sections.

Section I represents the fundamental basis for amperometric detection of carbohydrates. It describes the mechanism of glucose oxidation at gold electrodes in alkaline solutions and, thus, answers the questions of how and why glucose is detected by PAD. The results discussed in Section I explain why PAD calibration curves are nonlinear for large glucose concentrations (C^b > *ca.* 5 mM).

Section II describes the extension of PAD for glucose to solutions of low buffer capacity having neutral or acidic pH values. This extension of PAD allowed the direct, in situ, assay of the hydrolysis of starch by glucoamylase. The results discussed in this section explain why detection of glucose by PAD was previously limited to only those solutions having high alkalinity.

Section III describes the determination of the maltooligosaccharides found in corn syrup. Maltooligosaccharides were quantified with a single glucose calibration curve after they were separated by anion exchange chromatography and eluted through an immobilized glucoamylase reactor for conversion to glucose prior to being detected by PAD.

Section IV describes the determination of starch and total carbohydrate in beer samples by flow injection analysis. Samples containing starch were eluted through an immobilized glucoamylase reactor and the glucose produced was detected by PAD.

SECTION I.

CONCENTRATION DEPENDENCE OF THE MECHANISM OF GLUCOSE OXIDATION AT GOLD ELECTRODES IN ALKALINE MEDIA

SUMMARY

The catalytic oxidation of glucose in alkaline solution at a gold electrode was studied by performing cyclic voltammetry at a rotating disc electrode. The voltammetric response of glucose was studied as a function of glucose concentration and rotation velocity. Concentrations < 2 mM produced mass transport limited currents at a potential of *ca.* 0.4 V versus NHE with n = *ca.* 8 equiv mol^{-1}. Concentrations > 30 mM produced currents limited by a kinetic step involved in the electron transfer reaction with n = *ca.* 2 equiv mol^{-1}. From comparison of the voltammetric responses of glucose and glucose derivatives, the mass transport limited reaction was concluded to proceed by first the pairing of the enediol conformation of glucose, via hydrogen bridges, to the catalytic hydrous gold oxide, followed by oxidative cleavage of the enediol and oxidation of the primary hydroxyl group. The kinetically limited reaction for large glucose concentrations was concluded to effect only the oxidation of the aldehyde or hemiacetal group producing gluconic acid or gluconolactone. The rate determining step for this process was concluded to be the transfer of an electron from an adsorbed carbohydrate radical species to the electrode. The concentration dependence of the mechanism of glucose oxidation is explained by a decrease in the number of interactions between each glucose molecule and the catalytic hydrous gold oxide as the glucose concentration is increased.

INTRODUCTION

Extensive work has been done during the last 20 years on the oxidations of alcohols, poly-alcohols, and carbohydrates at noble metal electrodes, both in the development of analytical sensors and hydrocarbon fuel cells (1, 2). It is now well established that significant anodic currents can be obtained from glucose at gold electrodes in alkaline solution if the potential is cycled or pulsed to maintain a catalytic electrode surface (3 - 6). However, gold has been shown to be a poor catalyst for glucose oxidation in acidic solution (3, 7). This observation has been explained by the lack of formation of the catalytic hydrous gold oxide in acidic solution (3, 7). The catalytic oxide, AuOH, has been reported to form only in alkaline solution by chemisorption of hydroxide ions onto gold (2, 3, 7, 8). Alternatively, AuOH could form by the adsorption of hydroxy radicals produced by anodic discharge of water.

Mechanistic studies have been reported for the oxidations of n-propanol (2) and glucose (3) in alkaline solution at Au electrodes. Both studies concluded that the mechanism proceeds by first the pairing of surface -OH species, via hydrogen bridges, with either the hydroxyl of the alcohol or the aldehyde of the carbohydrate. The rate determining step for n-propanol was concluded to be radical formation produced by dehydrogenation of the adsorbed hydrocarbon (2). The final products of these electrooxidations were reported to be propanoic acid from n-propanol (2) and gluconic acid (or gluconolactone) from glucose (3). Here, we present evidence from cyclic voltammetric studies which

shows that the extent of glucose oxidation is diminished as the glucose concentration is increased. A mechanism is presented which is consistent with results for oxidation of glucose at Au.

MATERIALS AND METHODS

Apparatus

Current-potential curves were obtained by cyclic voltammetry using a RDE 3 potentiostat and a Au rotated disc electrode (RDE) (AFMD19, 0.196 cm^2) in a MSR rotator (Pine Instrument Co.; Grove City, PA). Voltammetric data were traced with a Model 100 X-Y recorder (Houston Instruments; Austin, TX). All potentials were recorded and are reported versus a calomel electrode with a potential of 0.326 V versus the normal hydrogen electrode (NHE). A coiled Pt wire (2.8 cm^2) was the counter electrode.

Reagents

All chemicals were reagent grade. Glucose was from Fischer Scientific (Fair Lawn, NJ). 2-Deoxy-D-glucose was from Aldrich Chemical Company (Milwaukee, WI). Glucuronic acid, glucaric acid, gluconic acid and gluconic acid lactone were from Sigma Chemical Company (St. Louis, MO). Water was condensed from steam and purified further in a Milli-Q system from Millipore (Bedford, MA).

Procedure

The voltammetric response of the carbohydrates was studied at the RDE as a function of concentration and rotation velocity in aqueous solutions of NaOH. All measurements were made at 25° C. The electrolysis cell was made from Pyrex with the working, counter and reference compartments separated by porous glass frits. The Au working electrode was activated prior to each experiment as follows: after gentle polishing with alumina on microcloth, it was rinsed with deionized water and

placed into the electrolysis cell; a cyclic potential scan between the potential limits for oxygen and hydrogen evolution was applied for several minutes until no further changes were detected on the voltammogram.

RESULTS AND DISCUSSION

Voltammetry of Glucose

The voltammetric response of glucose at Au in 0.1 M NaOH is shown in Figure 1. During the positive scan of potential (E), glucose oxidation begins at approximately -0.75 V and continues at a constant rate, as evidenced by the anodic current plateau, to *ca.* -0.35 V. As the potential is swept further positive, the rate of glucose oxidation increases and the anodic wave develops into a broad peak with a maximum at *ca.* 0.1 V. The rate of glucose oxidation decreases rapidly as the potential becomes more positive and glucose oxidation virtually ceases at $E \geq 0.35$ V. The electrode processes which catalyze glucose oxidation are concluded to be the formation of incipient AuOH, which is concomitant with the onset of glucose oxidation (8), the increased surface coverage of chemisorbed -OH, and the greater polarization of the AuOH bond for $E > -0.35$ V (2). The formation of higher Au-oxides (Au_2O_3) causes the catalytic oxidations to cease at $E > 0.35$ V.

The current produced from glucose oxidation is greatly dependent upon both glucose and NaOH concentration. A plot of the maximum oxidation current at 0.1 V versus glucose concentration in 0.1 M NaOH is shown in Figure 2. The shape of this curve will be explained in detail below. A plot of current sensitivity (maximum current divided by glucose concentration) versus NaOH concentration is shown in Figure 3. The shape of this curve is explained by the dependence of the rate of formation of the catalyst, AuOH, upon the flux of hydroxide ions transported to the electrode surface. As shown in Fig. 3, the rate of

Figure 1. Fischer structure (A) and voltammetric response at Au RDE (B) for glucose. Conditions: 0.1 M NaOH, $w = 167.5$ rad sec^{-1}, $v = 5.0$ V min^{-1}. Curves (B): (a) residual response, (b) air-saturated 0.4 mM glucose, (c) He-saturated 0.4 mM glucose

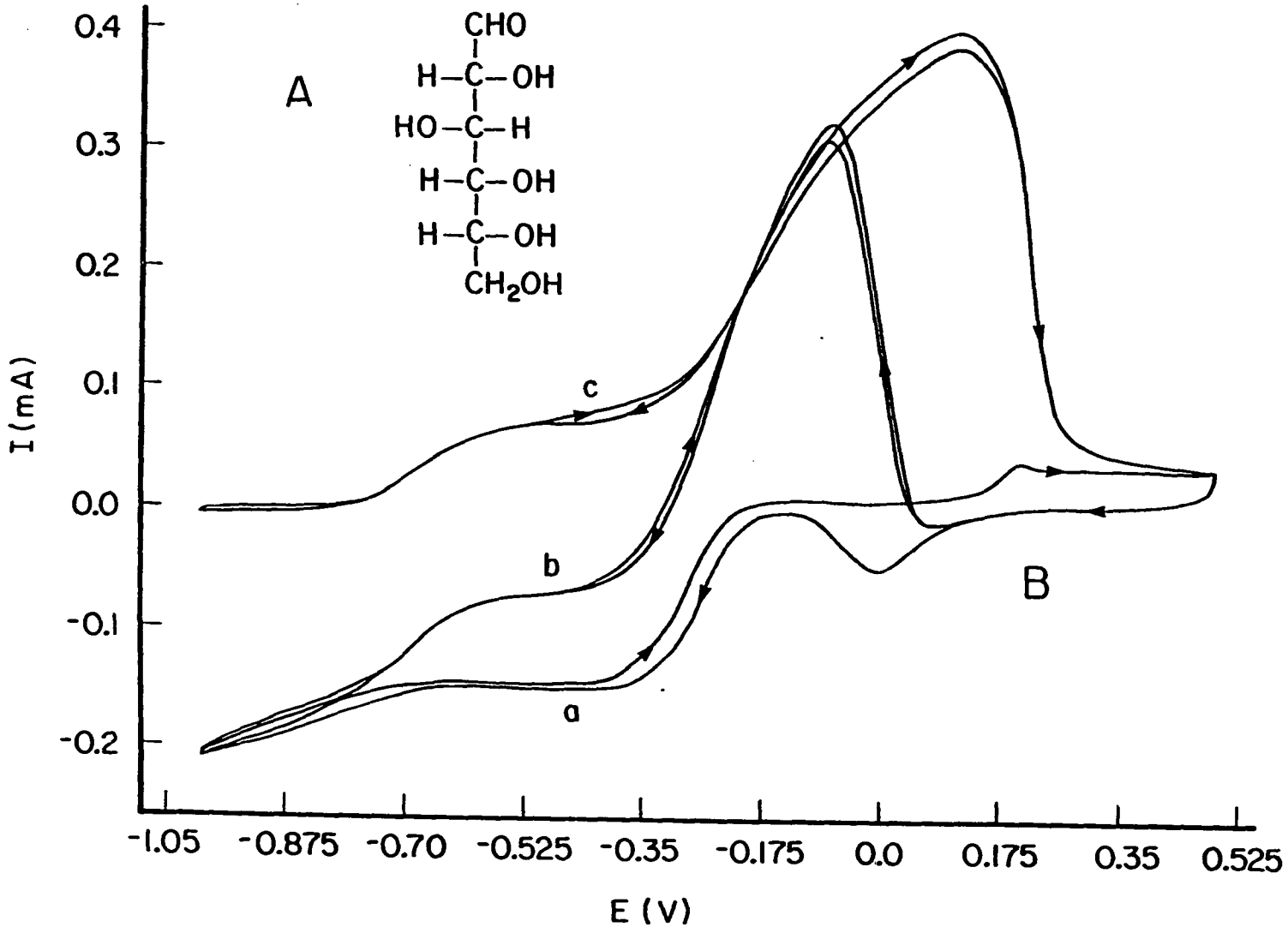
A
CHO
H–C–OH
HO–C–H
H–C–OH
H–C–OH
CH2OH
B
a
b
c
0.4
0.3
0.2
0.1
0.0
-0.1
-0.2
I (mA)
-1.05
-0.875
-0.70
-0.525
-0.35
-0.175
0.0
0.175
0.35
0.525
E (V)

Figure 2. Voltammetric current for glucose as a function of glucose concentration. Conditions: 0.1 M NaOH, $w = 167.5$ rad sec^{-1}, $v = 5.0$ V min^{-1}

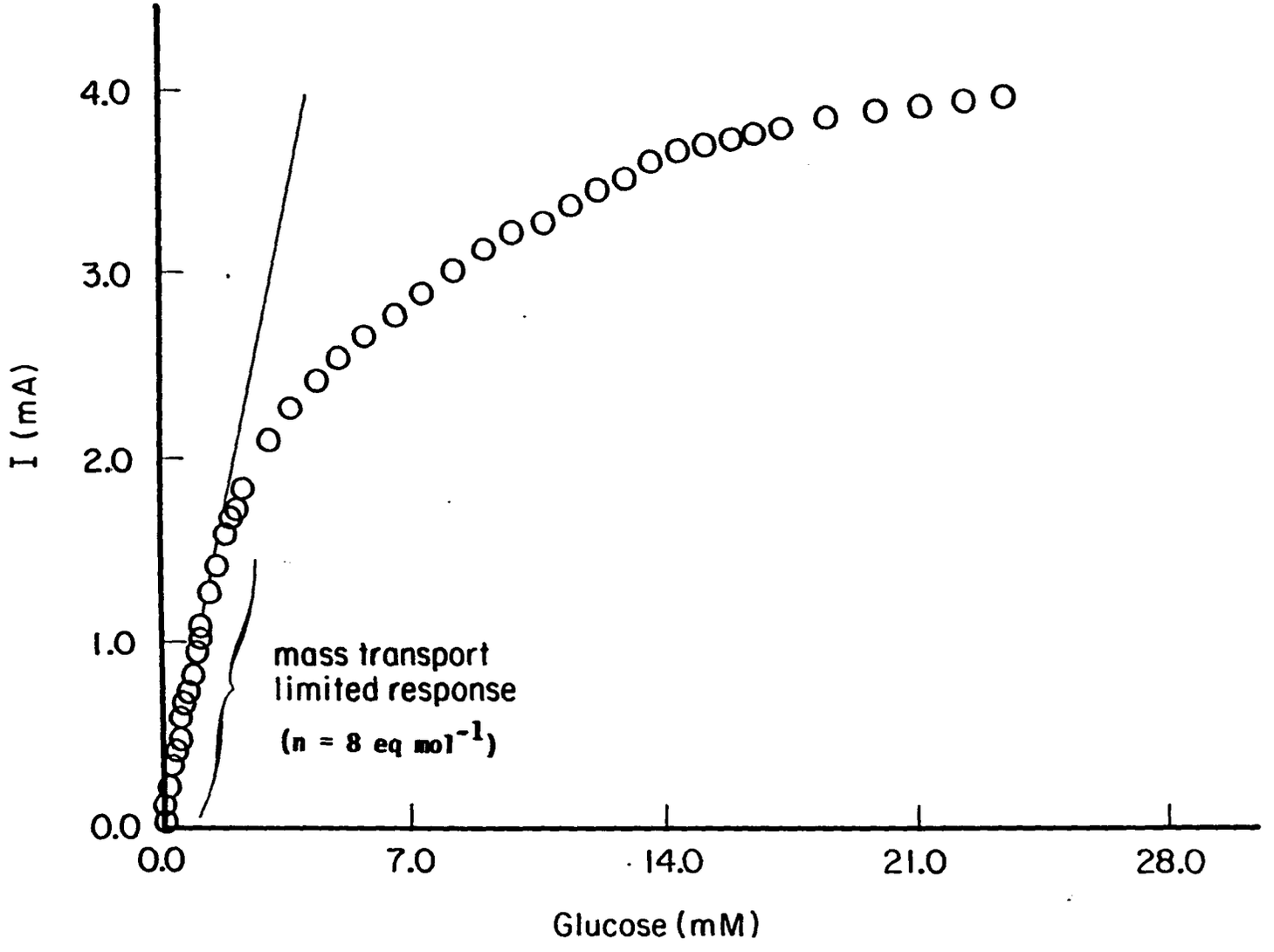
4.0
3.0
2.0
1.0
0.0
I (mA)
mass transport
limited response
(n = 8 eq mol^{-1})
0.0
7.0
14.0
21.0
28.0
Glucose (mM)

Figure 3. Voltammetric current sensitivity for glucose as a function of NaOH concentration. Conditions: 9.5 mM glucose, $w = 104.7$ rad sec^{-1}, $v = 5.0$ V min^{-1}

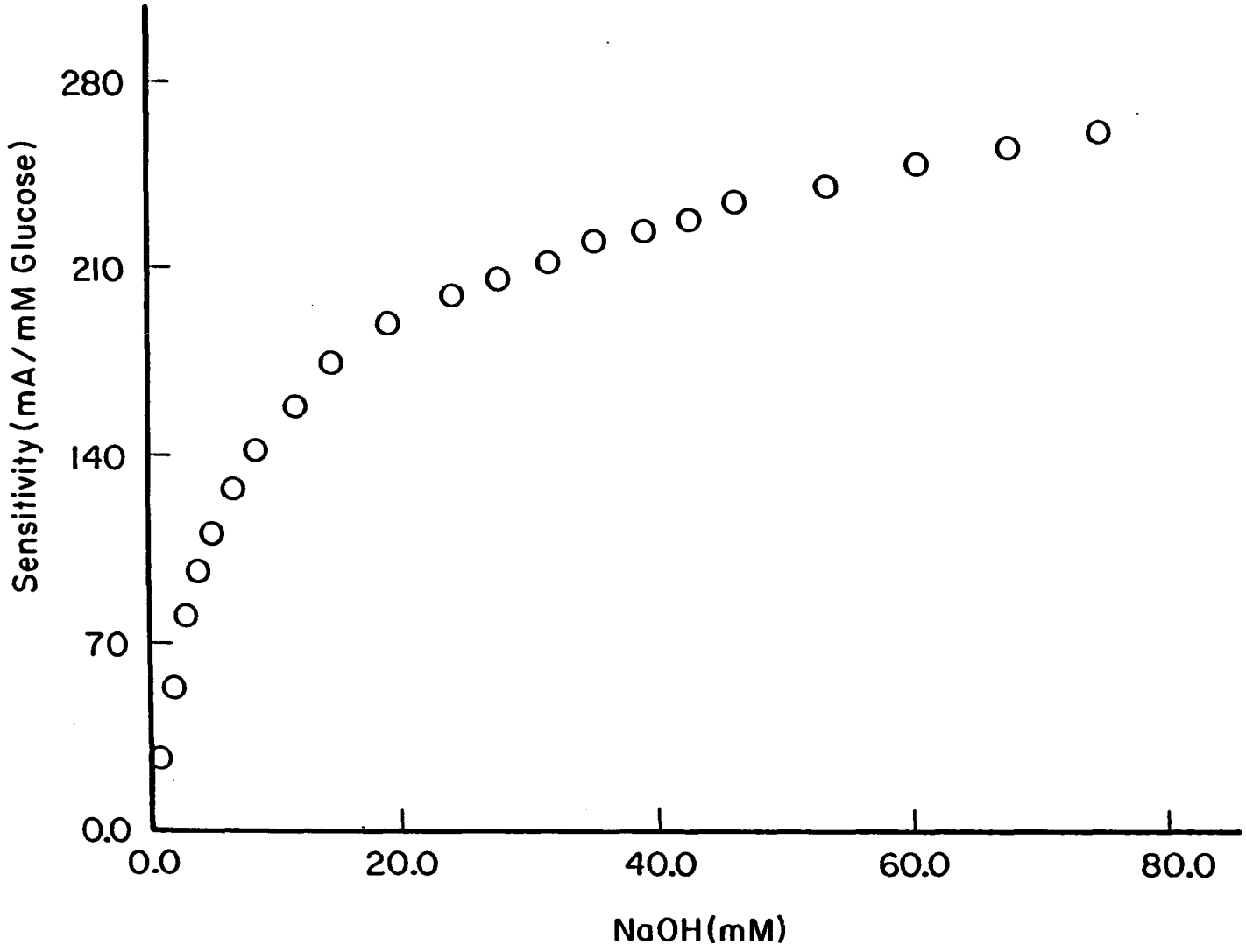
Sensitivity (mA / mM Glucose)
280
210
140
70
0.0
0.0
20.0
40.0
60.0
80.0
NaOH(mM)

glucose oxidation was limited by the flux of hydroxide ions when the ratio of glucose to NaOH was > *ca.* 1/2 (i.e., NaOH < 20 mM for *ca.* 10 mM glucose). Thus, the formation of the catalyst is concluded to be the rate determining step (rds) in the anodic reaction mechanism for $C^b_{glucose} \gg C^b_{NaOH}$. However, for ratios of glucose to NaOH < 1/2 (i.e., NaOH > 20 mM for *ca.* 10 mM glucose) the anodic process is concluded to be limited by a step in the glucose oxidation mechanism, as is discussed below.

The Levich equation (9) describes the mass transport limited disc current (I_{lim}; mA) as a function of: the number of electrons per molecule oxidized (n, equiv mol^{-1}); the surface area of the electrode (A, cm^2); the diffusion coefficient of the molecule oxidized (D, cm^2 sec^{-1}); the rotation velocity of the electrode (w, rad sec^{-1}); the kinematic viscosity of the solution (v, cm^2 sec^{-1}); and the bulk concentration of the oxidized molecule (C^b, M). For a totally mass-transfer limited process:

$$I_{lim} = 0.62nFAD^{2/3}w^{1/2}v^{-1/6}C^b \qquad (1)$$

where F is the faraday constant (96486.6 coul $equiv^{-1}$). A plot of I_{lim} versus C^b is predicted to be linear with a positive slope and an intercept at the origin. As shown in Fig. 2, in 0.1 M NaOH glucose produced mass transport limited currents when C^b < *ca.* 2 mM. The plot was linear with slope = 910 ± 7 mA M^{-1}, y-intercept = 0.027 ± 0.004 mA, standard error = 0.0014 mA, and correlation coefficient = 0.99941 (C^b = 0.05 to 1.0 mM, N = 20). Uncertainties given are ± one standard

deviation. The experiment was repeated five times and the average value of n was calculated from the slopes of the I_{lim} - C^b plots to be 7.9 ± 0.4 equiv mol^{-1}, using the values D = $6.7x10^{-6}$ for glucose and v = 0.01023 for 0.1 M NaOH (10). Only 2 electrons would be produced per molecule if gluconic acid was the primary oxidation product. Therefore the extent of oxidation of glucose was greater for low concentrations of glucose in the presence of excess NaOH.

It can be concluded from the shape of the I_{lim} - C^b curve (Fig. 2) that a kinetic step involved in the electron transfer reaction, rather than mass transfer, becomes rate determining for glucose concentrations > 2 mM. The current produced at an RDE by a process under mixed kinetic and mass transport control is described by the following equation (9):

$$I_k = \frac{nFADC^b}{d + D/k} \qquad (2)$$

where $d = 1.61D^{1/3}v^{1/6}w^{-1/2}$ and k is the apparent rate constant (cm sec^{-1}). A linear correspondence is predicted for $1/I_k$ versus $1/w^{1/2}$ with an intercept for $1/w^{1/2}$ -> 0 which is inversely related to k as given by:

$$1/I_k = 1/n_{eff}kFAC^b + 1/0.62n_{eff}FAD^{2/3}w^{1/2}v^{-1/6}C^b \qquad (3)$$

where n_{eff} is the effective number of electrons transfered up to and including the rate determining step. Thus, from linear plots of $1/I_k$ versus $1/w^{1/2}$, values of n_{eff} and k can be estimated from the slope and intercept, respectively. Applications of Equation 3 should be

considered as empirical at best for kinetic studies of multi-electron processes wherein coupled homogeneous and/or heterogeneous chemical reactions are possible. Values of k so obtained are to be interpreted as the average value for the passage of n_{eff}. Linear regression parameters are given in Table 1 for plots of $1/I_k$ versus $1/w^{1/2}$ for glucose concentrations in the range 0.06 to 30.1 mM. The average value of n_{eff} obtained for each glucose concentration is also given in Table 1. Values of n_{eff} were calculated from the slopes (m) of the respective plots as follows:

$$n_{eff} = 1/0.62mFAD^{2/3}v^{-1/6}C^b \qquad (4)$$

A plot of n_{eff} versus glucose concentration is shown in Figure 4. As shown, n_{eff} -> *ca.* 8 as C^b -> 0 and n_{eff} -> *ca.* 2 for C^b > 30 mM. Therefore, gluconic acid is concluded to be the primary oxidation product for C^b > 30 mM, but the extent of oxidation of glucose is greater for C^b < 30 mM. A plot of k, calculated from the intercepts shown in Table 1, versus n_{eff} is shown in Figure 5. As shown, the reaction becomes mass transport limited (i.e., k -> ∞) as n_{eff} -> *ca.* 8 and electron-transfer limited (i.e., k = 0.003) as n_{eff} -> *ca.* 2. For intermediate values of n_{eff}, the reaction is under mixed kinetic and mass transport control.

Voltammetry of Glucose Derivatives

Voltammetric experiments were performed on glucose derivatives to elucidate the electrochemical steps which produce the more extensive oxidations of glucose. Fischer structures of the carbohydrates studied are shown in Figure 6. The sugar acids shown (A, C and G) result when

Table 1. Linear regression parameters and effective number of electrons transferred obtained from results of current versus rotation velocity studies at various glucose concentrations in 0.1 M NaOH; equation: $1/I = mw^{-1/2} + b$

Glucose (mM)	m ($rad^{1/2}\ sec^{-1/2}\ mA^{-1}$)	b (mA^{-1})	Standard error (mA^{-1})	Correlation coefficient (r)	n_{eff} (eq. mol^{-1})
0.06	226.3 ± 8.3	2.51 ± 0.34	4.520	.99961	8.2 ± 0.3
0.30	48.0 ± 1.8	1.07 ± 0.26	0.935	.99902	7.8 ± 0.3
0.75	19.6 ± 0.3	0.57 ± 0.07	0.388	.99953	7.6 ± 0.1
3.50	5.2 ± 0.1	0.29 ± 0.04	0.034	.99919	6.1 ± 0.1
8.00	3.1 ± 0.2	0.26 ± 0.05	0.065	.99777	4.5 ± 0.3
15.00	2.0 ± 0.2	0.25 ± 0.05	0.044	.99929	3.8 ± 0.4
22.80	1.6 ± 0.1	0.19 ± 0.03	0.032	.99870	3.1 ± 0.2
30.10	1.3 ± 0.1	0.18 ± 0.03	0.025	.99845	2.8 ± 0.2

Conditions: v = 5.0 V min^{-1}, w 20.9 - 209.3 rad sec^{-1} (N = 10).
Each concentration done in duplicate; average m, b and n_{eff} given ± one standard deviation.

Figure 4. Effective number of electrons transferred (n_{eff}) for glucose as a function of glucose concentration

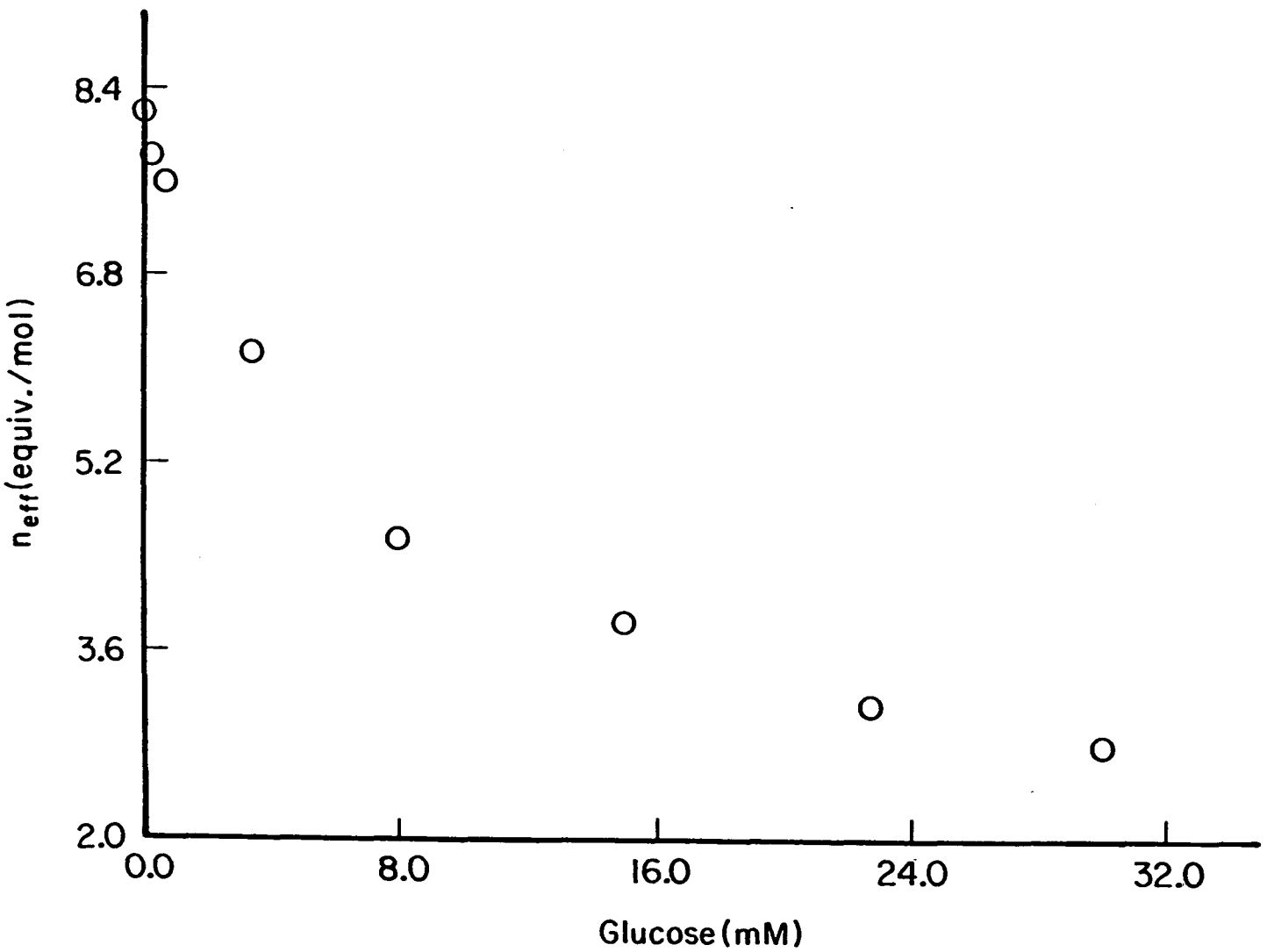
8.4
6.8
5.2
3.6
2.0
n_{eff}(equiv./mol)
0.0
8.0
16.0
24.0
32.0
Glucose (mM)

Figure 5. Heterogeneous rate constant (k) for the oxidation of glucose at the Au RDE as a function of the effective number of electrons transferred (n_{eff})

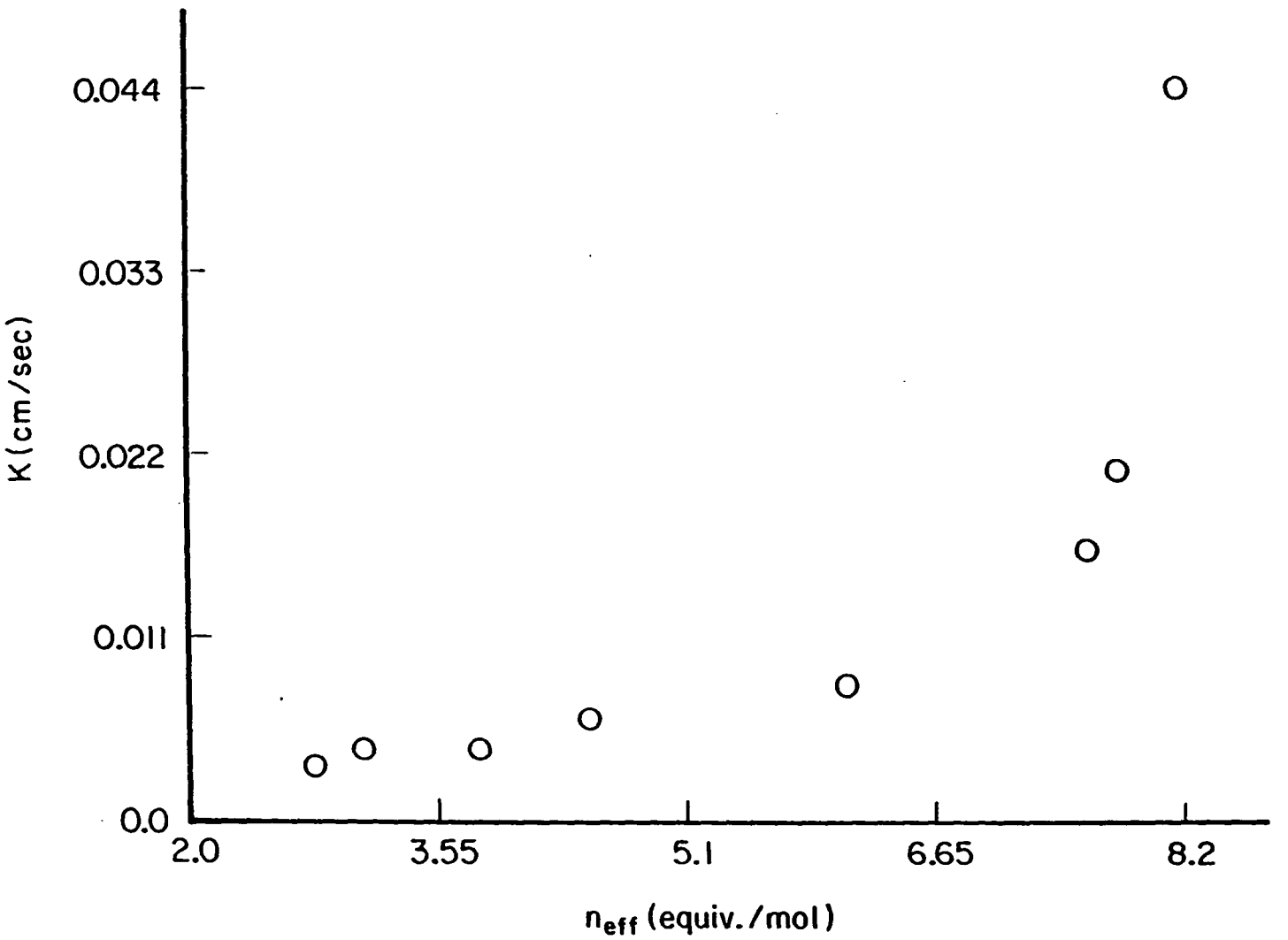
0.044
0.033
0.022
0.011
0.0
K (cm/sec)
2.0
3.55
5.1
6.65
8.2
n_{eff} (equiv./mol)

Figure 6. Fischer structure (A) and voltammetric response at Au RDE (B) for gluconic acid. Conditions: 0.1 M NaOH, w = 167.5 rad sec^{-1}, v = 5.0 V min^{-1}. Curves (B): (a) residual response, (b) air-saturated 0.4 mM gluconic acid, (c) same as (b) except He-saturated

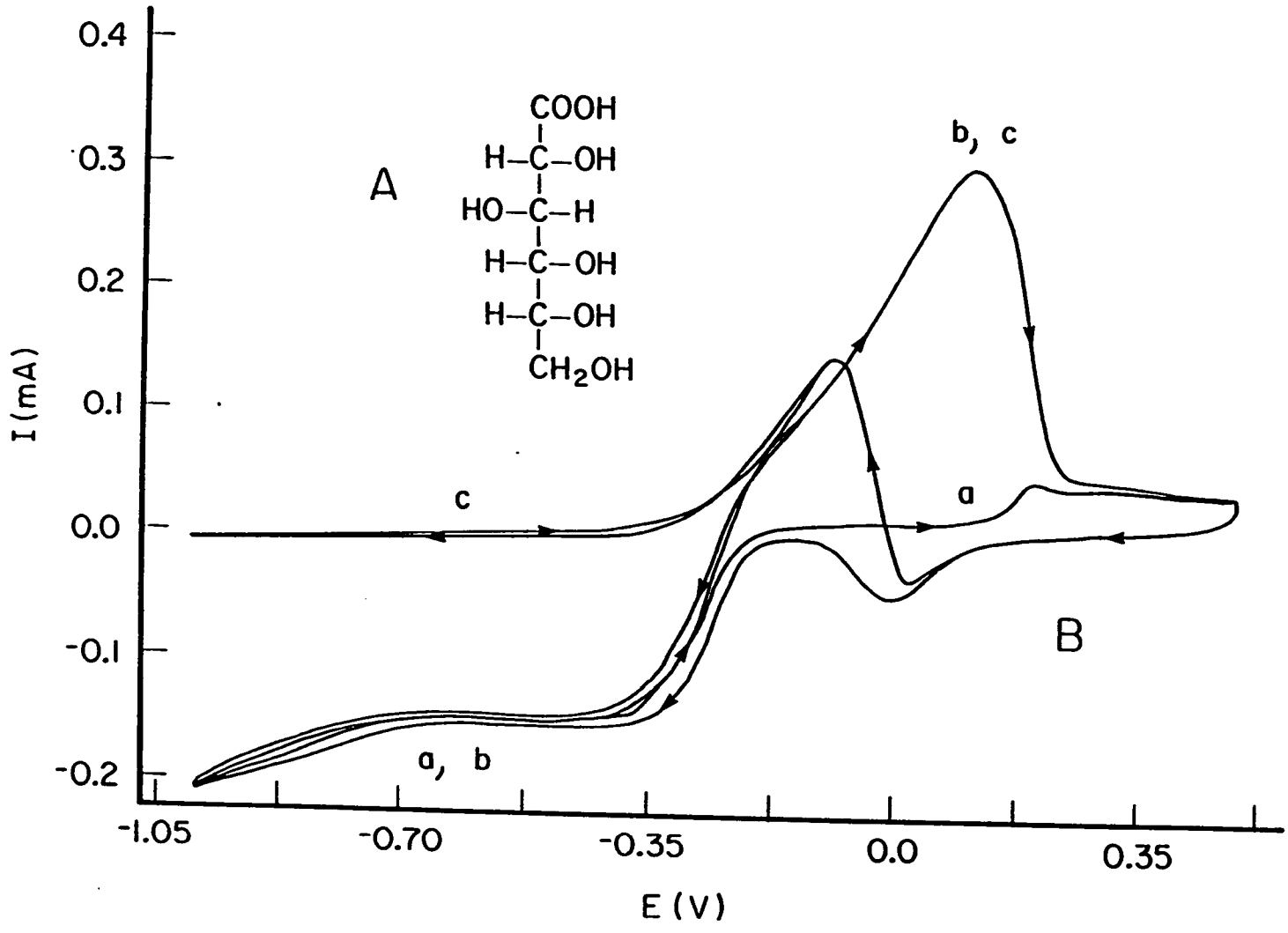
0.4
0.3
0.2
0.1
0.0
-0.1
-0.2
I (mA)
A
COOH
H–C–OH
HO–C–H
H–C–OH
H–C–OH
CH2OH
b, c
c
a
B
a, b
-1.05
-0.70
-0.35
0.0
0.35
E (V)

Figure 6. Fischer structure (C) and voltammetric response at Au RDE (D) for glucuronic acid. Conditions: 0.1 M NaOH, $w = 167.5$ rad sec^{-1}, $v = 5.0$ V min^{-1}. Curves (D): (a) residual response, (b) air-saturated 0.45 mM glucuronic acid, (c) same as (b) except He-saturated

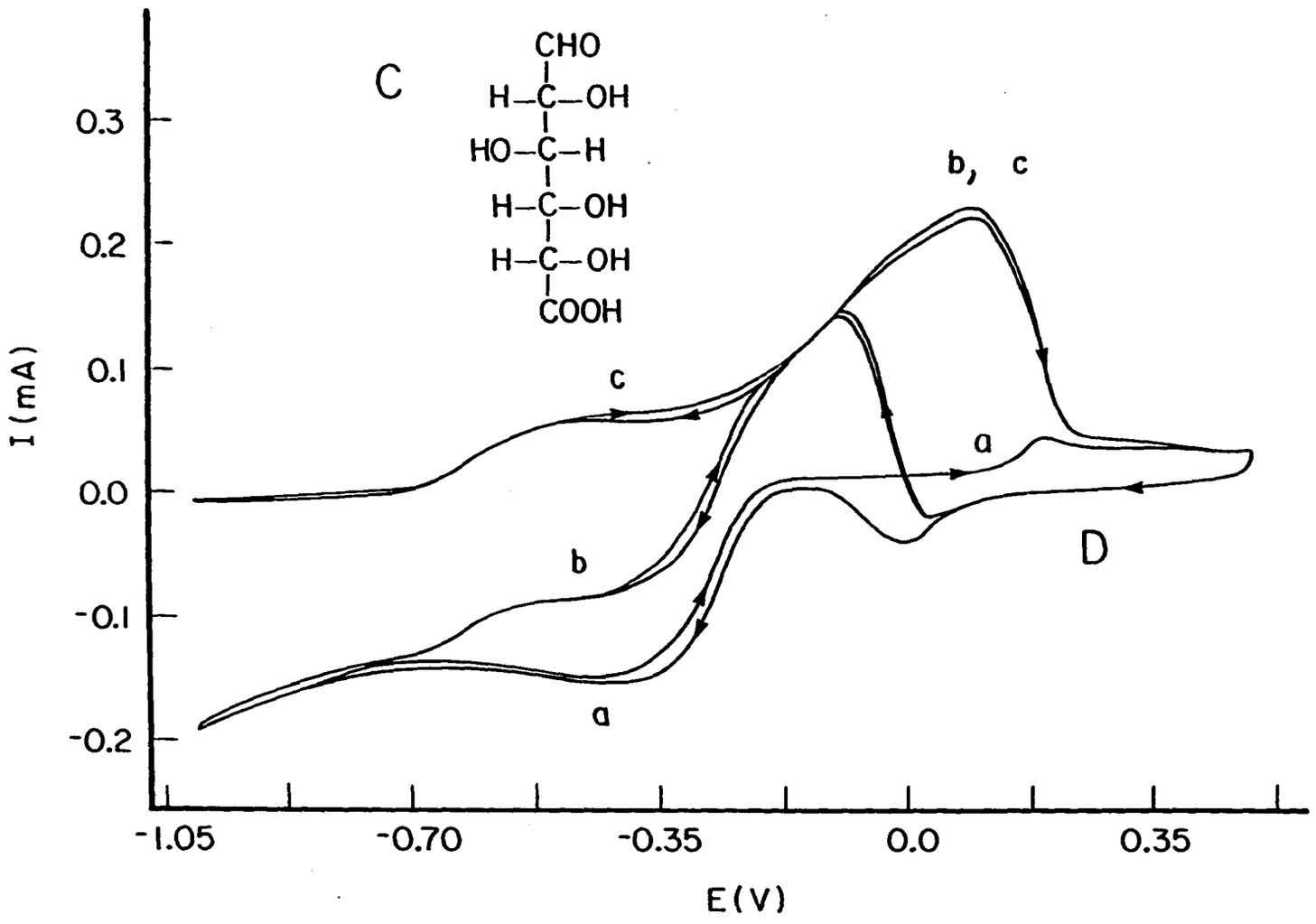
C
CHO
H–C–OH
HO–C–H
H–C–OH
H–C–OH
COOH
b, c
c
a
b
a
D
0.3
0.2
0.1
0.0
-0.1
-0.2
I (mA)
-1.05
-0.70
-0.35
0.0
0.35
E (V)

Figure 6. Fischer structure (E) and voltammetric response at Au RDE (F) for 2-deoxy-D-glucose. Conditions: 0.1 M NaOH, $w = 167.5$ rad sec^{-1}, $v = 5.0$ V min^{-1}. Curves (F): (a) residual response, (b) air-saturated 0.38 mM 2-deoxy-D-glucose, (c) same as (b) except He-saturated

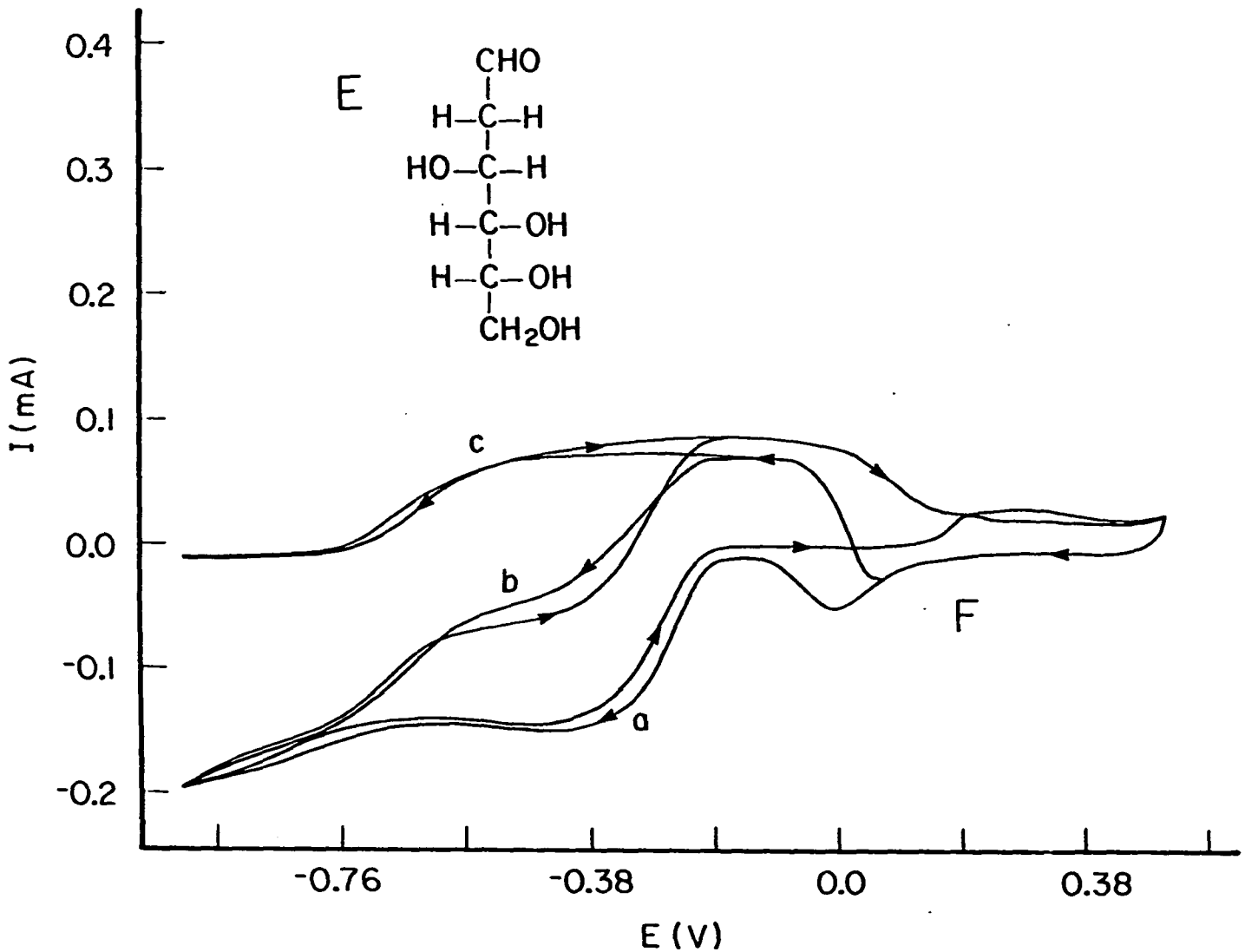
E
CHO
H–C–H
HO–C–H
H–C–OH
H–C–OH
CH2OH
0.4
0.3
0.2
0.1
0.0
-0.1
-0.2
I (mA)
c
b
a
F
-0.76
-0.38
0.0
0.38
E (V)

Figure 6. Fischer structure (G) and voltammetric response at Au RDE (H) for glucaric acid. Conditions: 0.1 M NaOH, $w = 167.5$ rad sec^{-1}, $v = 5.0$ V min^{-1}. Curves (H): (a) residual response, (b) air-saturated 0.33 mM glucaric acid, (c) same as (b) except He-saturated

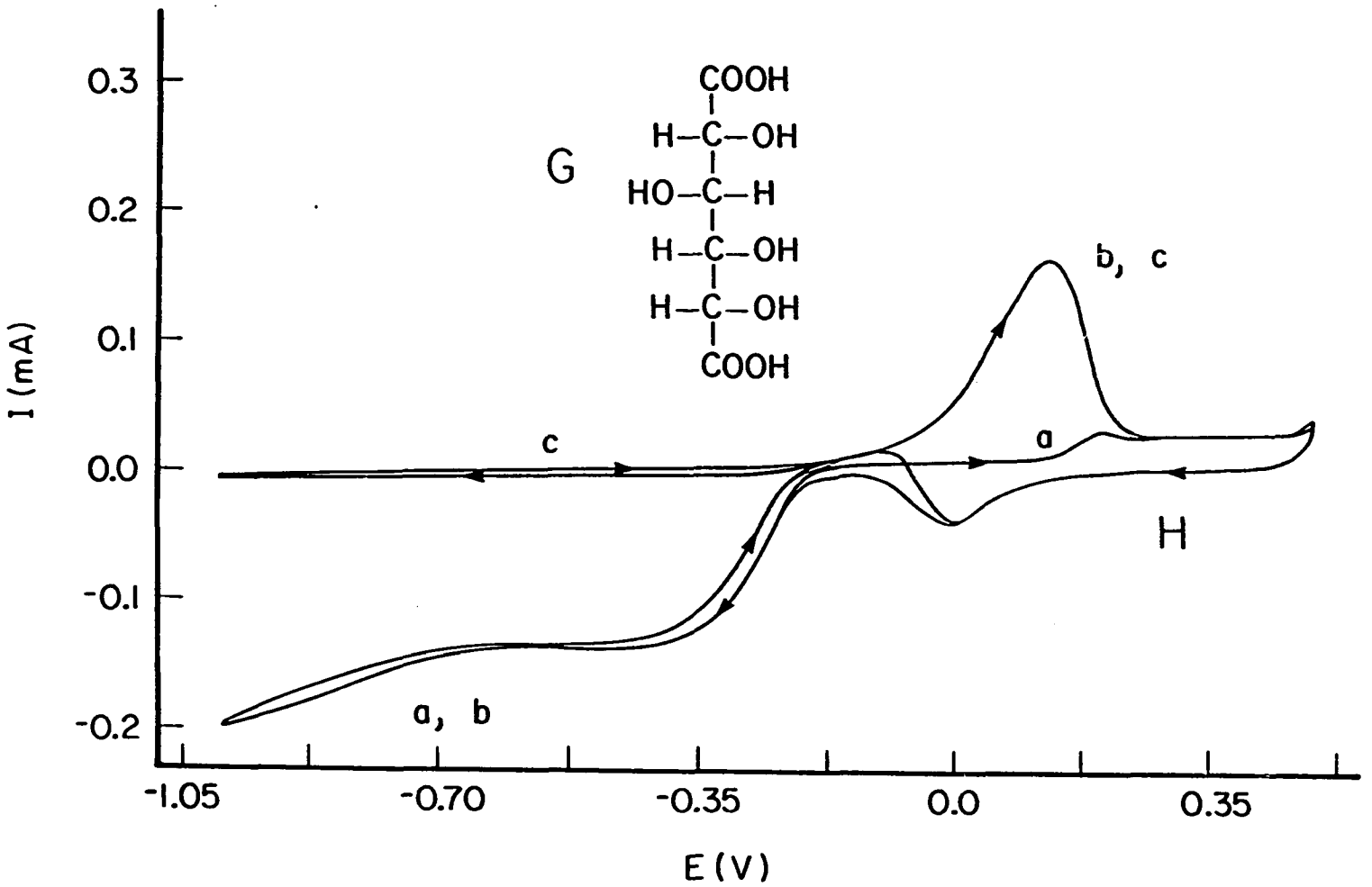
0.3
0.2
0.1
0.0
-0.1
-0.2
I (mA)
-1.05
-0.70
-0.35
0.0
0.35
E (V)
G
COOH
H–C–OH
HO–C–H
H–C–OH
H–C–OH
COOH
c
a
b, c
H
a, b

the aldehyde group, primary alcohol group, or both of glucose (Fig. 1A) are oxidized. The deoxy-sugar shown (E) is produced when the hydroxy group at carbon atom C_2 of glucose (Fig. 1A) is replaced by a hydrogen atom. The oxidation of the aldehyde group to the aldonic acid (A) is easily effected by treatment of glucose with mild oxidants, e.g., Br_2 in water (11). The oxidation of both the aldehyde and the primary alcohol to the aldaric acid (G) is effected by treatment of glucose with strong oxidants, e.g., warm HNO_3 (11). Oxidation of glucose by O_2 in alkaline solution containing platinized carbon yields glucaric acid (G) along with 4- and 5-carbon aldonic and aldaric acids as products (12). Clearly, if these derivatives (A, C and G) can be oxidized at the Au RDE, then oxidations of glucose can occur beyond the formation of gluconic acid (A).

Aqueous solutions of the carbohydrates shown in Fig. 6 contain a mixture of their various possible conformations. For example; glucose (Fig. 1A), glucuronic acid (6C), and 2-deoxy-D-glucose (6E) exist primarily as hemiacetals, but, gluconic (6A) and glucaric (6G) acids exist as a mixture of the acid and the lactone (11). However, the transformation rates between the various conformations are greatly accelerated in alkaline solutions (13). Also, the proton attached to carbon atom C_2 of glucose (Fig. 1A) and glucuronic acid (6C) becomes acidic in solutions with pH > 12 which results in the formation of a 1,2-enediol (14). The oxidation of glucose by O_2 in alkaline solution proceeds first through the formation of an enediol intermediate followed by oxidative cleavage of the bond between carbon atoms C_1 and C_2 (13). Oxidative cleavage of

the bond between atoms C_1 and C_2 of 2-deoxy-D-glucose (6E) is not possible because an enediol intermediate can not be formed. Thus, 2-deoxy-D-glucose was included to determine the significance of the enediol intermediate for the more extensive oxidations of glucose at the Au RDE.

Voltammograms obtained from the derivatives of glucose are shown in Figure 6. The response of gluconolactone was identical to that of gluconic acid (Fig. 6B). Therefore, the rate of transformation between the different conformational forms was greater than the rate limiting step of the electrochemical reaction. As shown, only glucuronic acid (Fig. 6D) and 2-deoxy-D-glucose (Fig. 6F) produced anodic currents similar to glucose (Fig. 1B) in the region from -0.75 to -0.35 V. Gluconic acid (Fig. 6B) and glucaric acid (Fig. 6H), which contain an oxidized carbon atom C_1, produced no net anodic current in this region. Therefore, the oxidation of the aldehyde (or hemiacetal) at carbon atom C_1 is the primary reaction occurring at $E < -0.35$ V. Further evidence to support this conclusion comes from application of Eq. 1 to the voltammetric results obtained for glucose at -0.45 V. The I_{lim} - C^b plot was linear with slope = 200 $\pm$ 8 mA M^{-1}, y-intercept = 0.002 $\pm$ 0.001 mA, standard error = 5×10^{-6} mA, and correlation coefficient = 0.99741 (C^b = 0.05 - 0.35 mM, N = 7). The experiment was repeated three times and the average value of n was calculated from Eq. 1 to be 1.8 $\pm$ 0.1. Hence, oxidation of the aldehyde (or hemiacetal) at carbon atom C_1 is concluded to result in the formation of gluconic acid (or gluconolactone). As shown in Figs. 6B and 6D, respectively, the onset of gluconic acid

oxidation occurred at approximately the same potential that the rate of glucuronic acid oxidation increased (i.e., E > -0.35 V). Therefore, the electrochemical processes which produce more extensive oxidations of glucose (n_{app} > 2; Fig. 1B) also effect oxidations of these compounds. The onset of glucaric acid oxidation (Fig. 6H) occurred at *ca.* -0.2 V; however, the rate of oxidation is quite small until E > *ca.* 0.0 V. Oxidation of glucaric acid results in cleavage of the bonds between adjacent carbon atoms. Hence, this reaction proceeds at slower rates and requires more positive potential values than the oxidation of the aldehyde and the primary hydroxyl groups. As shown in Fig. 6F, only the aldehyde group at carbon atom C_1 of 2-deoxy-D-glucose is oxidized. More extensive oxidations of this derivative did not occur since no increase in anodic current was observed at E > -0.35 V. Therefore, the inability to form the enediol intermediate prevented both oxidative cleavage of the bond between carbon atoms C_1 and C_2 and oxidation of the primary hydroxyl group. It is concluded from Fig. 6 that more extensive oxidations of glucose occur beyond formation of gluconic acid at the Au RDE. Furthermore, these more extensive oxidations require the enediol intermediate.

Equation 1 was applied to voltammetric results obtained from the derivatives shown in Fig. 6. The linear regression parameters of the I_{lim} - C^b plots are given in Table 2. As shown, the linear fits were quite good and all y-intercepts were *ca.* zero. Thus, mass transport limited oxidations occurred for each derivative over the concentration range studied and use of Eq. 1 was justified. The average value of n

Table 2. Linear regression parameters and apparent number of electrons transferred obtained from results of current versus concentration studies for derivatives of glucose; equation: $I = mC^b + b$

Derivative	m ($mA\ M^{-1}$)	b ($mA \times 10^3$)	standard error ($mA \times 10^5$)	Correlation coefficient (r)	n ($eq.\ mol^{-1}$)
gluconic acid	670 ± 29	3 ± 2	440	.99985	5.8 ± 0.3
glucaric acid	430 ± 24	8 ± 1	2.0	.99905	3.7 ± 0.2
glucuronic acid	481 ± 28	9 ± 3	3.1	.99868	4.2 ± 0.3
2-deoxy-D-glucose	218 ± 27	5 ± 2	1.8	.99945	1.9 ± 0.2

Conditions: 0.1 M NaOH, $v = 5.0\ V\ min^{-1}$, C^b 0.05 - 0.4 mM (N = 7). Maximum net I_{lim} plotted. Each derivative done in triplicate; average value of m, b and n given, ± one standard deviation.

obtained from the slope of the I_{lim} - C^b plots is also given in Table 2. From comparison of the values of n obtained for the derivatives and for glucose (Table 1), we conclude that the oxidation of glucose proceeds as follows: oxidation of the aldehyde at carbon atom C_1 results in the formation of gluconic acid with the net production of 2 electrons; oxidation of the primary hydroxyl at carbon atom C_6 results in the formation of an aldaric acid with the net production of 4 electrons; oxidative cleavage of the bond between carbon atoms C_1 and C_2 results in the formation of formic acid and an aldaric acid containing one less carbon atom with the net production of 2 electrons. Oxidation of the primary hydroxyl and oxidative cleavage of the carbon-carbon bond are concluded to occur concurrently after gluconic acid formation from comparison of the voltammograms obtained (Figs. 1 and 6). Thus, it is concluded that the more extensive oxidations of glucose produced at the Au RDE by voltammetry are similar to those produced by O_2 in the presence of platinized carbon (12). It should be noted from the glucaric acid results (Table 2) that the bonds between the first two carbon atoms (C_1 and C_2) and the last two (C_5 and C_6) are equally capable of undergoing oxidative cleavage with the net production of 4 electrons. Thus, a 4-carbon aldaric acid along with a second molecule of formic acid would be expected from the oxidation of glucose with a total electron transfer of 10. However, the breaking of the bond between the last two carbon atoms is concluded not to occur at a significant rate at the RDE as evidenced by the values of n obtained for glucose (Table 1) and glucuronic acid (Table 2). The 5-carbon aldaric acid resulting from glucose oxidation

is concluded to be displaced from the electrode surface by a more strongly adsorbing functional group (i.e., aldehyde or primary hydroxyl), preventing the cleavage of a second carbon-carbon bond.

Mechanism of Glucose Oxidation

The mechanism proposed for the oxidation of glucose at the Au RDE must be consistent with the experimental facts presented in the previous sections. The mechanism must account for the following:

(a) at high glucose concentrations gluconic acid is the primary oxidation product;

(b) at low glucose concentrations and E < -0.35 V, gluconic acid is the primary oxidation product;

(c) at low glucose concentrations and E > -0.35 V, oxidative cleavage of the bond between the first two carbon atoms occurs concurrently with the oxidation of the primary hydroxyl at carbon atom C_6; and

(d) formation of an enediol intermediate is required for the more extensive oxidations of glucose.

It is apparent from the experimental facts (a - c) that the mechanism of glucose oxidation is dependent upon both glucose concentration and electrode potential. In fact, a different mechanism must be occurring at high and low glucose concentrations. Likewise, a different mechanism must be occurring at E < -0.35 V and at E > -0.35 V for low glucose concentrations. These different mechanisms are the result of the electrode processes which catalyze glucose oxidation. The aldehyde group is concluded to be preferentially adsorbed onto the catalytic AuOH at E > -0.75 V. But, through the enediol intermediate a single glucose

molecule is concluded to interact with more than one AuOH site. Thus, when the number of catalytic sites exceeds the number of glucose molecules on the electrode suface, multiple oxidation of each glucose molecule can occur.

The steps involved in the proposed mechanism for high glucose concentrations (a) are shown in Figure 7. Step 1 is the formation of the catalytic AuOH at E > -0.75 V. Step 2 is the adsorption of glucose onto the AuOH site by pairing of the aldehyde with the surface -OH. The aldehyde is used to represent the adsorption of glucose for simplicity of discussion, but, it should be kept in mind that all of the possible conformations are involved and that the transformation rate between the different conformations is much greater than the rate of glucose oxidation. Step 3 is the dehydrogenation of the adsorbed glucose molecule producing an adsorbed radical species. Step 4 is the rate determining step (rds) which involves the transfer of an electron from the radical to a bare Au site producing a positively charged organic species. Step 5 involves the transfer of the surface oxygen to the positively charged organic species concomitant with the regeneration of the AuOH species. The aldonic acid is displaced from the catalytic site by the aldehyde group of another glucose molecule and the reaction is repeated starting with Step 2. The mechanism outlined in Fig. 7 is the primary one occurring when the number of glucose molecules at the surface are greater than the number of catalytic sites. The aldehyde group is preferentially adsorbed and the catalytic oxidations which occur result in the production of gluconic acid with n = 2 equiv. mol^{-1}. The rds for n-propanol

Figure 7 I. Steps 1 and 2 of the proposed mechanism for the catalytic oxidation of glucose for concentrations of glucose > 30 mM; and for concentrations of glucose < 2 mM and potential < - 0.35 V

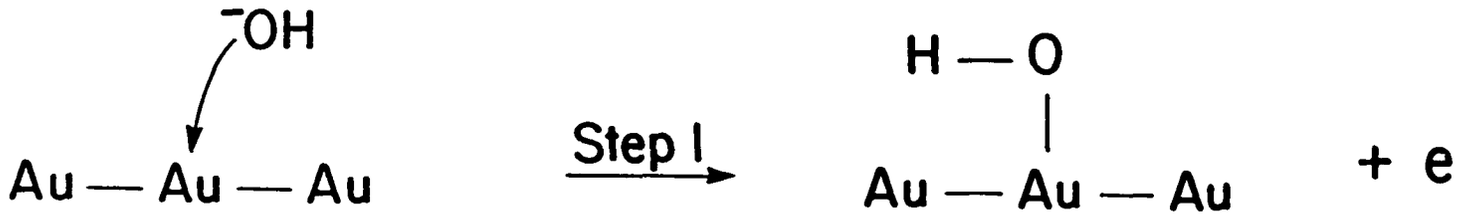
⁻OH
Au — Au — Au
Step 1
H — O
Au — Au — Au
+ e

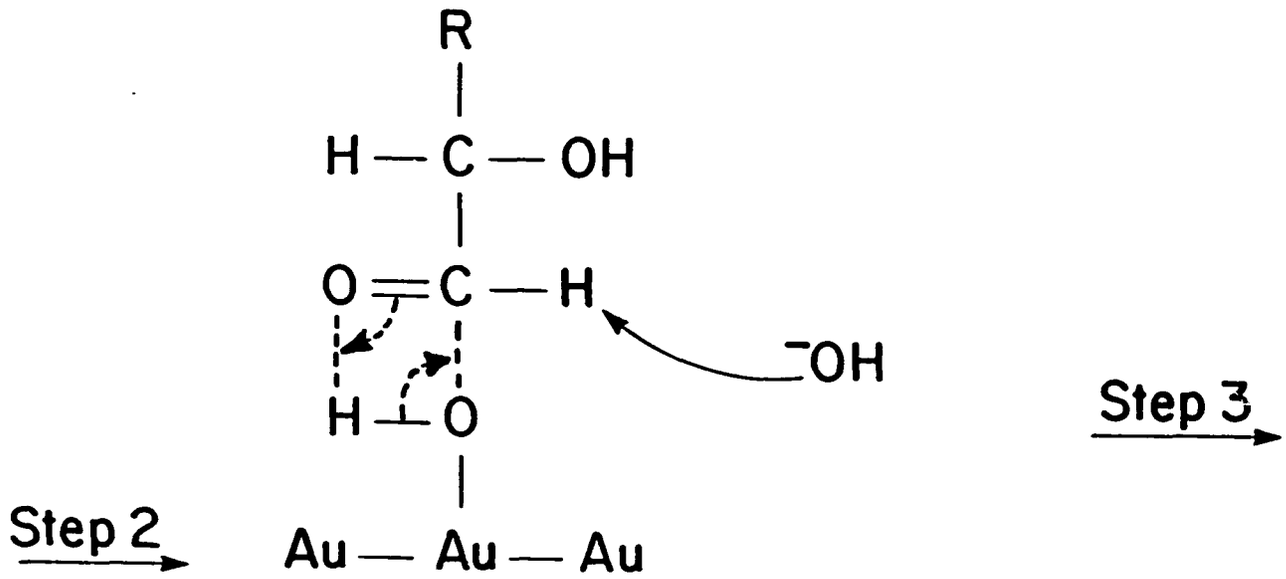
R
H — C — OH
O = C — H
⁻OH
H — O
Step 2
Au — Au — Au
Step 3

Figure 7 II. Steps 3 and 4 of the proposed mechanism for the catalytic oxidation of glucose for concentrations of glucose > 30 mM; and for concentrations of glucose < 2 mM and potential < - 0.35 V

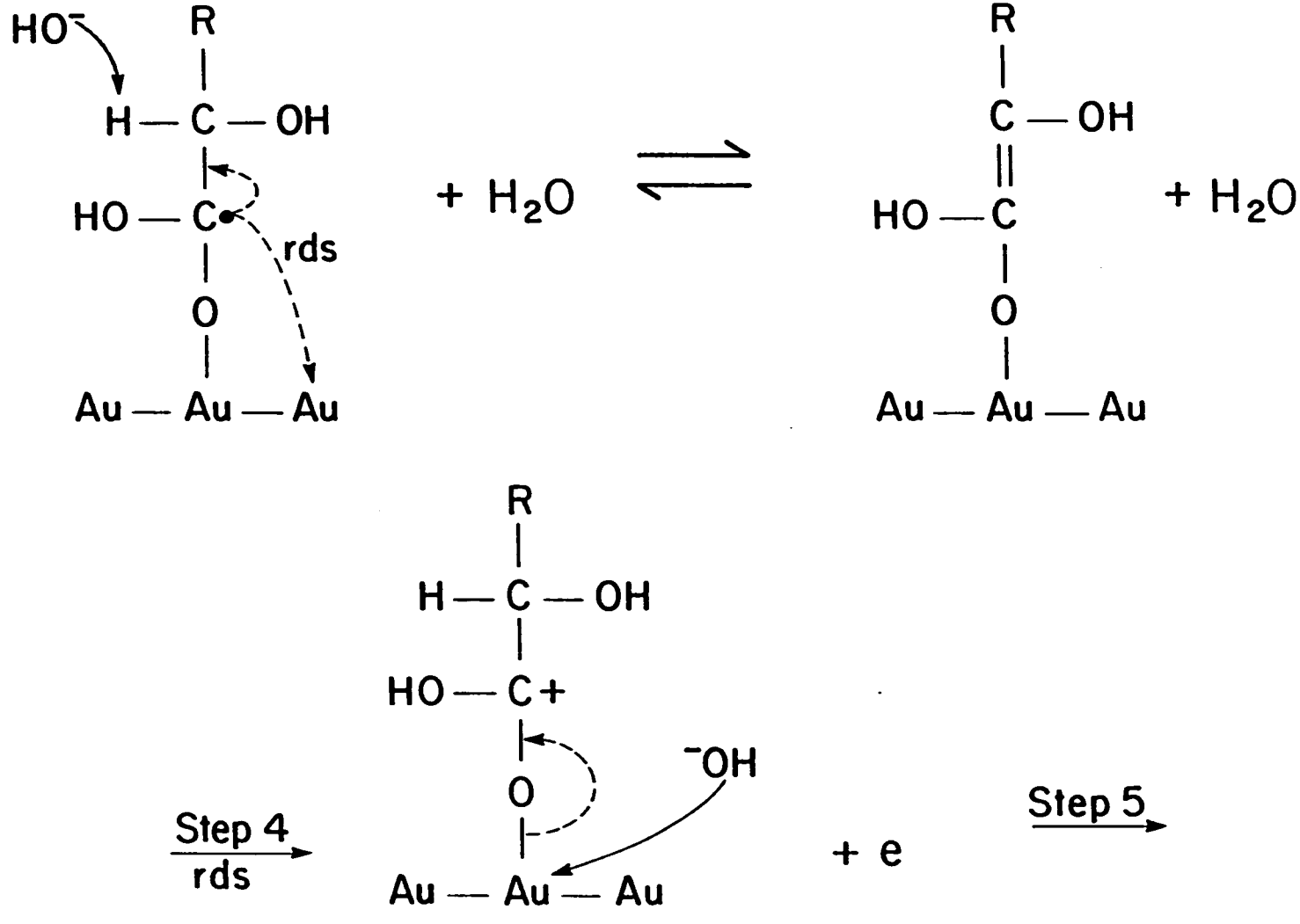
HO⁻
R
H — C — OH
HO — C
rds
O
Au — Au — Au
+ H2O
C — OH
HO — C
+ H2O
Step 4
rds
H — C — OH
HO — C+
⁻OH
Step 5
+ e

Figure 7 III. The final step (Step 5) of the proposed mechanism for the catalytic oxidation of glucose for concentrations of glucose > 30 mM; and for concentrations of glucose < 2 mM and potential < - 0.35 V. Also shown is step 2 for the glucose molecule that displaced the product molecule (gluconic acid)

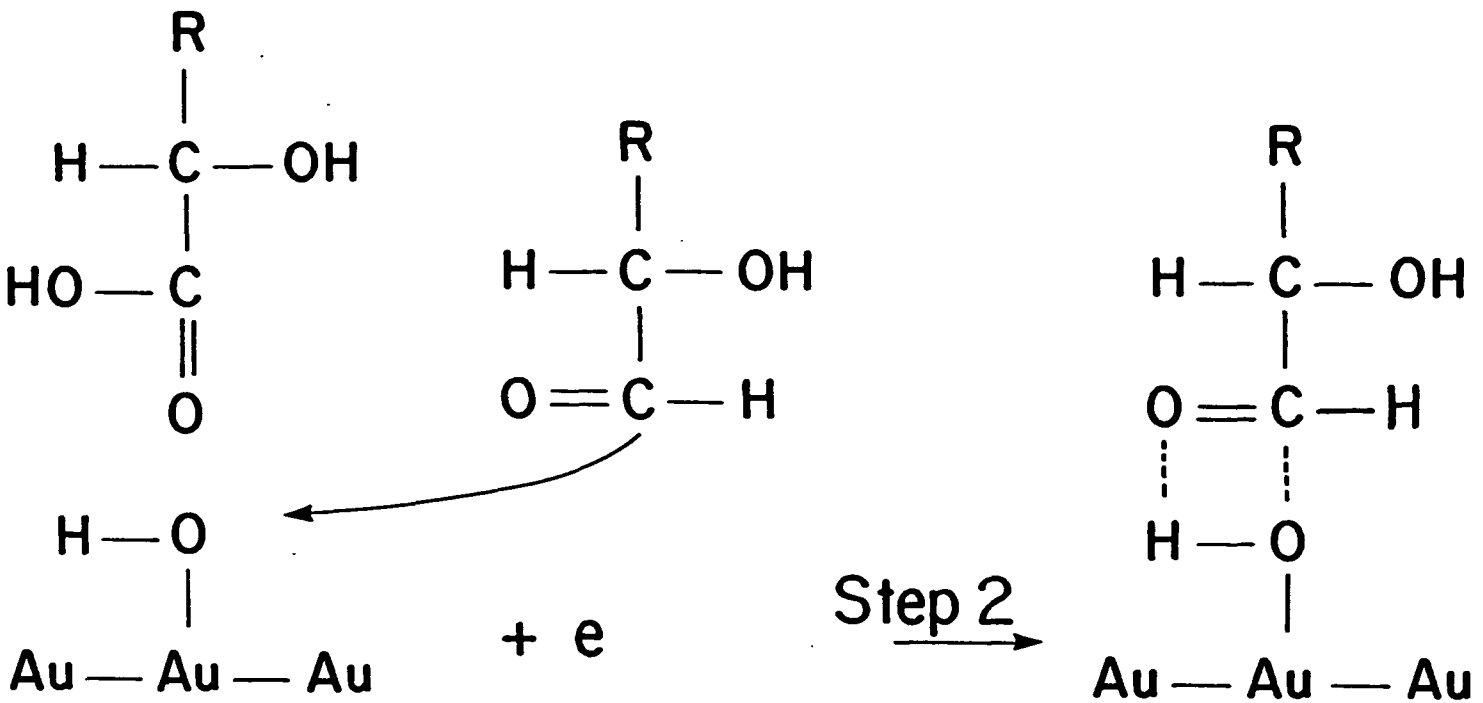
R
H — C — OH
HO — C
O
R
H — C — OH
O = C — H
H — O
Au — Au — Au
+ e
Step 2
R
H — C — OH
O = C — H
H — O
Au — Au — Au

was concluded to be dehydrogenation and the formation of the radical species (2). However, for glucose the radical species is stabilized by the enediol conformation as shown in Step 3. This intermediate cannot be formed by n-propanol. Also, since 2 electrons are produced up to and including the rds (Fig. 4), transfer of the electron (Step 4) must be the rds.

The steps involved in the mechanism of glucose oxidation at low concentrations and $E < -0.35$ V (b) are identical to those discussed above (Fig. 7). The surface coverage by chemisorbed -OH is concluded to be small at $E < -0.35$ V. Therefore, the distance between catalytic sites is large and it is not possible for a glucose molecule to interact with more than a single site even though the number of sites may be greater than the number of glucose molecules at the surface. Hence, aldehyde groups are preferentially adsorbed onto the catalytic sites and oxidations beyond the formation of gluconic acid do not occur at significant rates.

The steps involved in the proposed mechanism for low glucose concentrations and $E > -0.35$ V (c) are shown in Figure 8. Under these conditions, the catalytic sites are near enough to one another to allow interaction between a single glucose molecule and more than one site. The number of sites must be greater than the number of glucose molecules (aldehyde groups) near the surface for this to occur. As shown in Fig. 8, Step 1 is the formation of AuOH. Step 2 is the adsorption and concomitant pairing of the enediol conformation of glucose with 4 AuOH sites. All the conformations are involved in the process, but, based on

Figure 8 I. Step 1 of the proposed mechanism for the catalytic oxidation of glucose for concentrations of glucose < 2 mM and potential > - 0.35 V

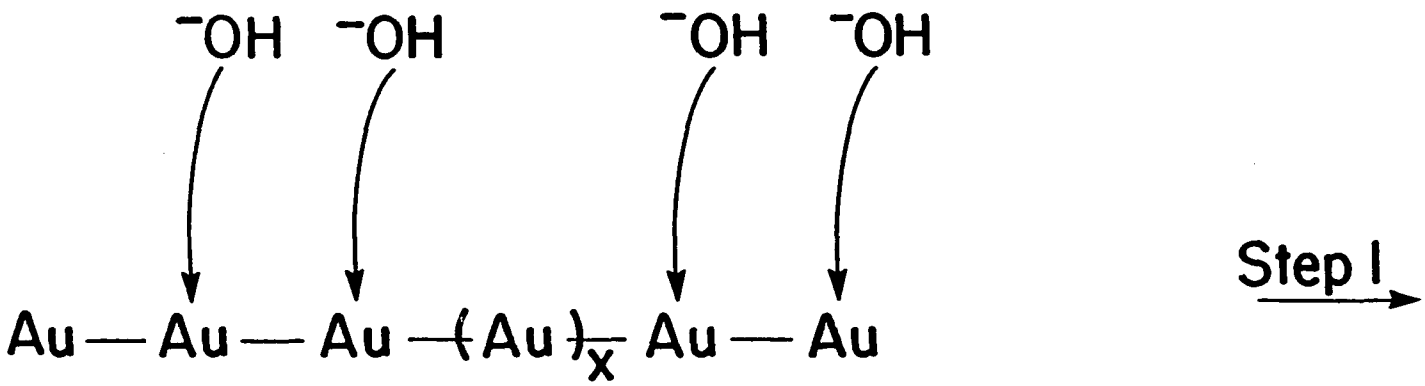
⁻OH ⁻OH ⁻OH ⁻OH
Au — Au — Au — (Au)x — Au — Au
Step I

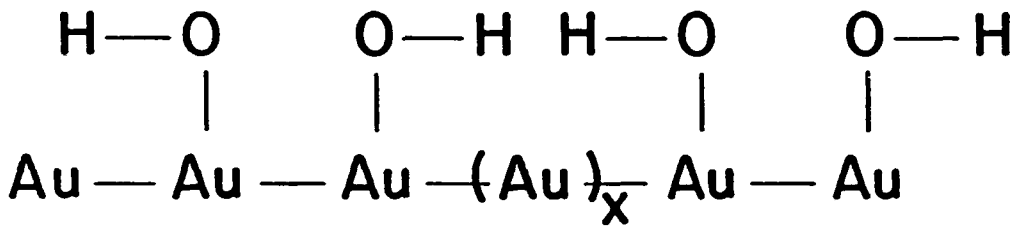
H — O O — H H — O O — H
Au — Au — Au — (Au)x — Au — Au

Figure 8 II. Steps 2 and 3 of the proposed mechanism for the catalytic oxidation of glucose for concentrations of glucose < 2 mM and potential > - 0.35 V

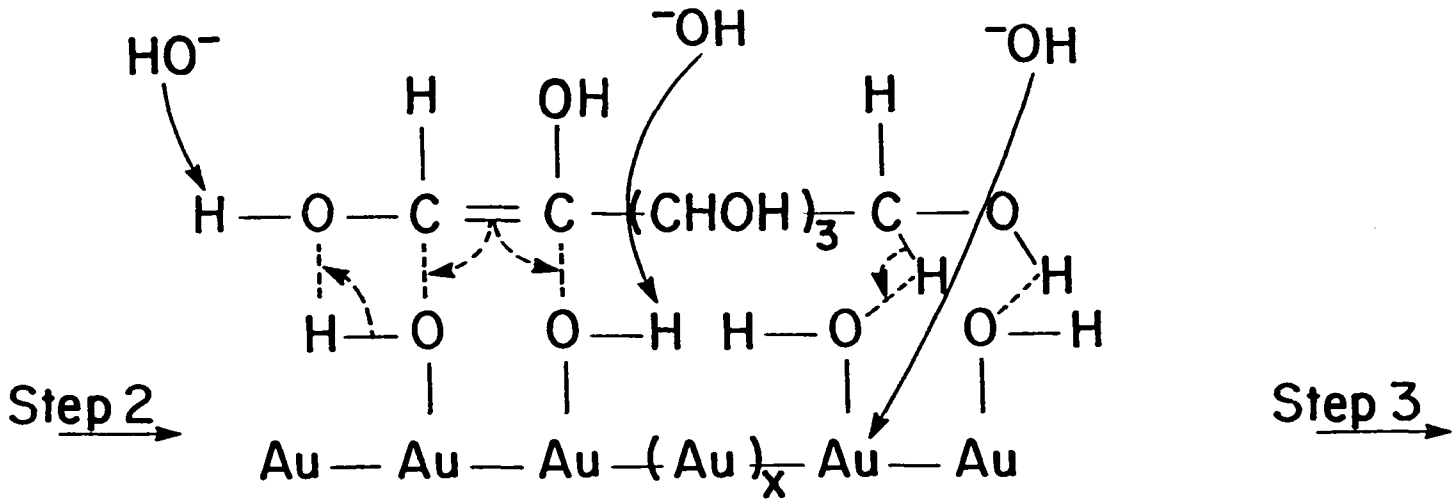
HO⁻
⁻OH
⁻OH
Step 2
Step 3
Au — Au — Au — (Au)x — Au — Au

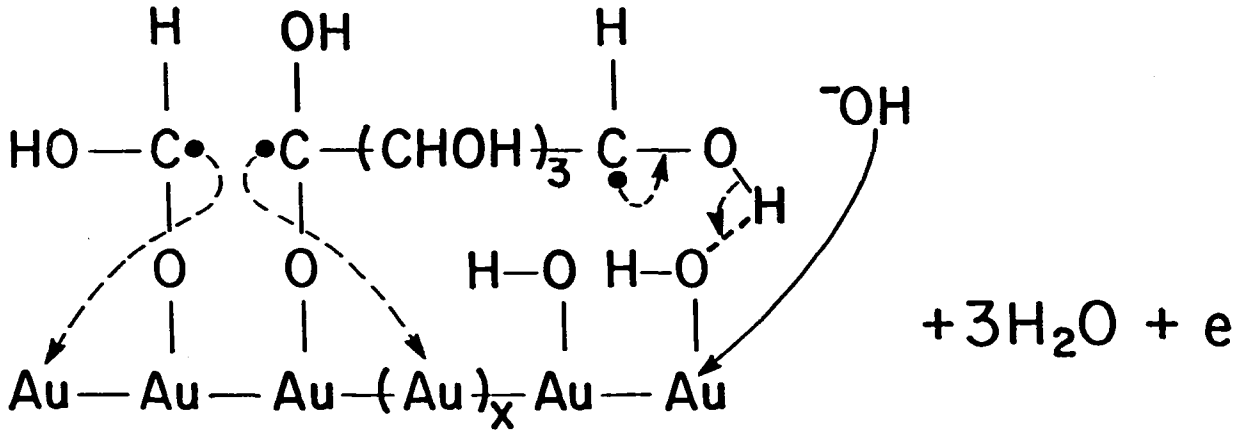
⁻OH
Au — Au — Au — (Au)x — Au — Au
+3H2O + e

Figure 8 III. Steps 4 and 5 of the proposed mechanism for the catalytic oxidation of glucose for concentrations of glucose < 2 mM and potential > - 0.35 V

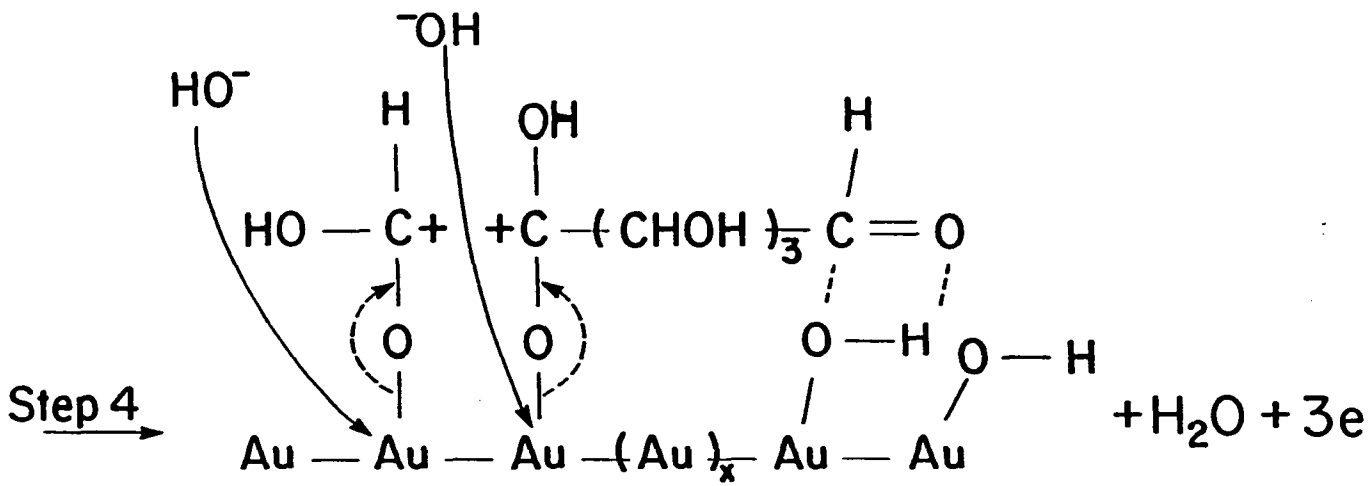
HO⁻
⁻OH
H
OH
H
HO — C+
+C —(CHOH)3— C = O
O
O
O — H
O — H
Step 4
Au — Au — Au —(Au)x— Au — Au
+H2O + 3e

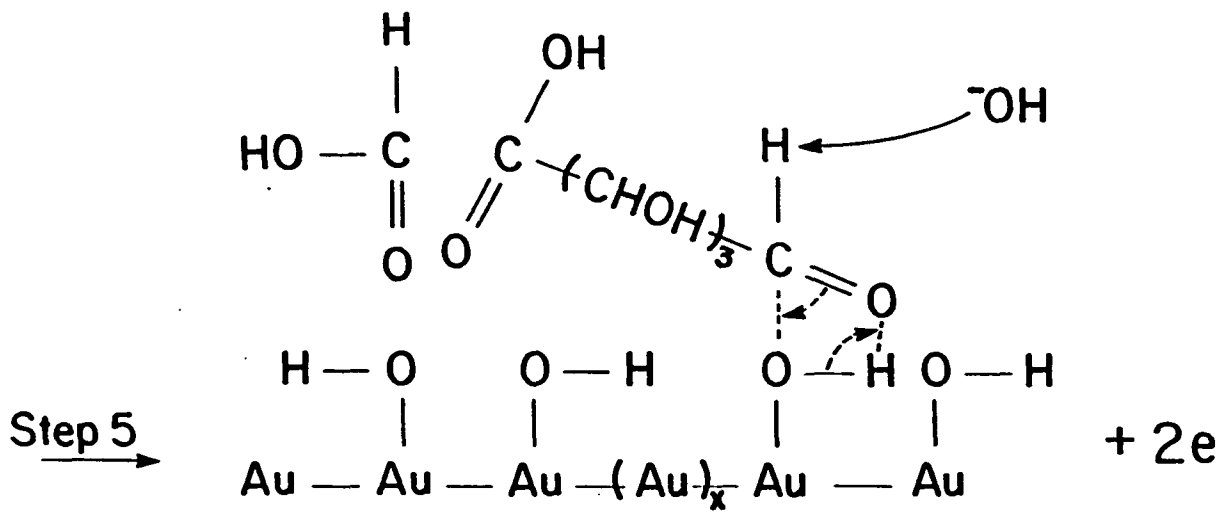
H
OH
⁻OH
HO — C
C —(CHOH)3
H
O
O
C
O
H — O
O — H
O — H
O — H
Step 5
Au — Au — Au —(Au)x— Au — Au
+ 2e

Figure 8 IV. Steps 6, 7 and 8 of the proposed mechanism for the catalytic oxidation of glucose for concentrations of glucose < 2 mM and potential > - 0.35 V

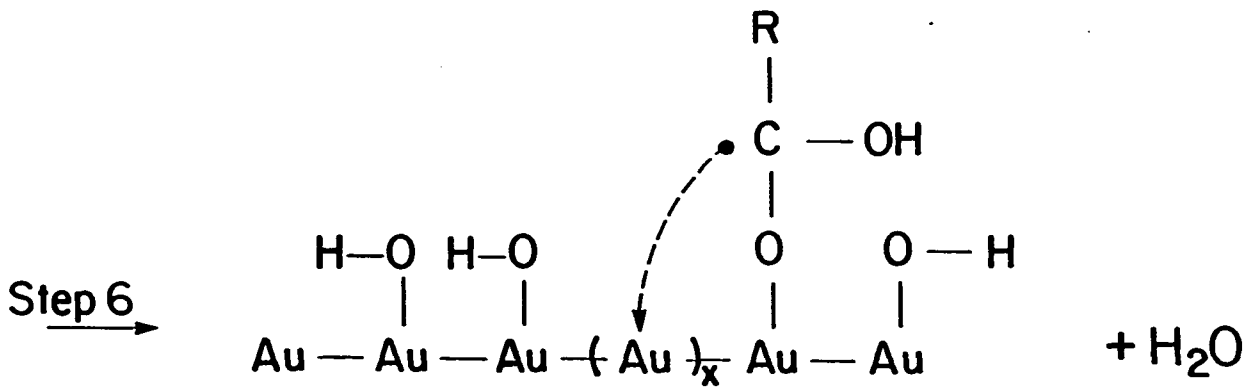
Step 6
R
C — OH
H—O H—O
O
O — H
Au — Au — Au — (Au)x Au — Au
+ H2O

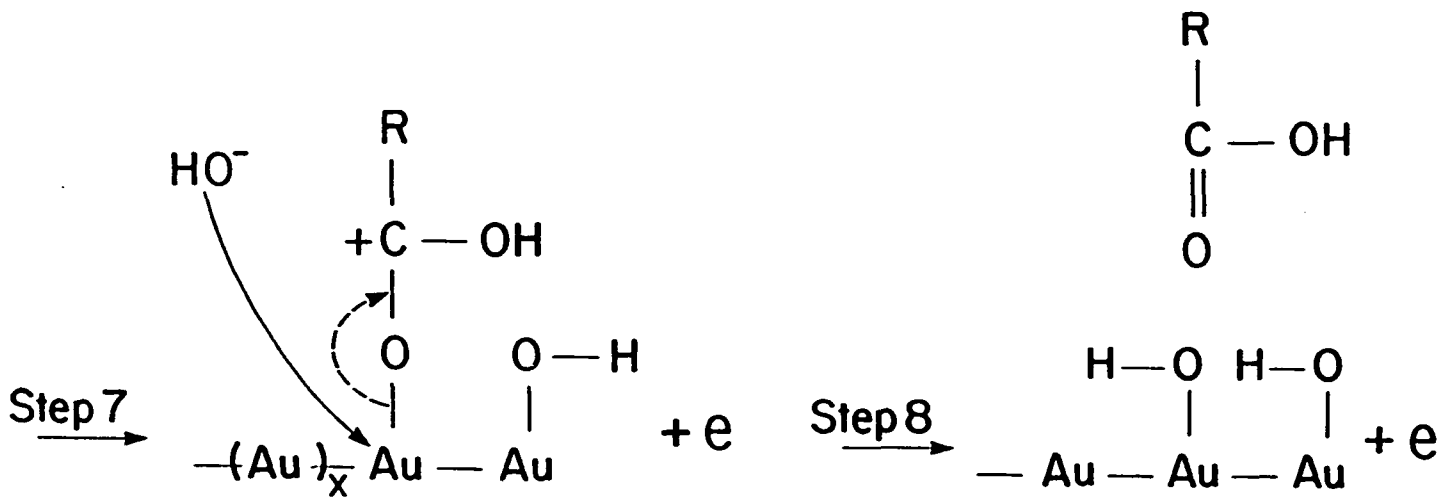
Step 7
HO⁻
R
+C — OH
O
O — H
—(Au)x Au — Au
+ e
Step 8
R
C — OH
O
H—O H—O
— Au — Au — Au
+ e

the results obtained for 2-deoxy-D-glucose and from the literature reports on the importance of the enediol intermediate in glucose oxidations (13), the enediol is concluded to be the primary one involved in the mechanism. Step 3 involves dehydrogenation and radical formation along with splitting of the bond between carbon atoms C_1 and C_2. Undoubtedly, all of these processes do not occur simultaneously and they are illustrated here as a single step for conciseness only. Step 4 involves the transfer of electrons from the radicals to bare Au sites producing positively charged organic species. Step 5 involves the transfer of the surface oxygen to the positively charged organic species concomitant with the regeneration of the AuOH sites. The aldehyde remaining at carbon atom C_6 undergoes further oxidation in Steps 6 - 8 similar to those discussed above in (a) producing a total of 8 electrons transferred. The formic and aldaric acids produced are displaced from the electrode surface before further oxidation can occur by a more strongly adsorbing enediol and the reaction is repeated starting with Step 2. The processes outlined in Fig. 8 are quite similar to the ones shown in Fig. 7. However, a far greater number of steps are involved in case (c). The complexity of the mechanism shown in Fig. 8 explains why the mass transport limited rate is only observed for small glucose concentrations ($C^b < 2.0$ mM). Fewer glucose molecules undergo multiple oxidations as C^b is increased (Fig. 2) and the rds becomes electron transfer as shown in Fig. 7.

ACKNOWLEDGMENTS

This work was supported by the National Science Foundation under contract CHE-8612314.

REFERENCES

1. Y. B. Vassilyev, O. A. Khazova and N. N. Nikolaeva, J. Electroanal. Chem., 196 (1985), 105.
2. P. Ocon, C. Alonso, R. Celdran and J. Gonzalez-Velasco, J. Electroanal. Chem., 206 (1986), 179.
3. Y. B. Vassilyev, O. A. Khazova and N. N. Nikolaeva, J. Electroanal. Chem., 196 (1985), 127.
4. E. B. Makovos and C. C. Liu, J. Electroanal. Chem., 211 (1986), 157.
5. D. C. Johnson and T. Z. Polta, Chromatogr. Forum, 1 (1986), 37.
6. G. G. Neuburger and D. C. Johnson, Anal. Chem., 59 (1987), 150.
7. B. Beden, I. Cetin, A. Kahyaoglu, D. Takky and C. Lamy, J. Catal., 104 (1987), 37.
8. R. R. Adzic and M. Avramov-Ivic, J. Catal., 101 (1986), 532.
9. A. J. Bard and L. R. Faulkner, "Electrochemical Methods; Fundamentals and Applications", John Wiley and Sons, New York, 1980, chapt. 8.
10. R. C. Weast (Ed.), "CRC Handbook of Chemistry and Physics", 64th ed., CRC Press, Boca Raton, 1983, pp. F-46 and D-261.
11. O. Theander, in W. Pigman and D. Horton (Eds.), "The Carbohydrates; Chemistry and Biochemistry", Vol. 1B, Academic Press, New York, 1980, chapt. 23.
12. J. Dirkx, H. S. Van Der Baan and J. Van Den Broek, Carbohydr. Res., 59 (1977), 63.

13. H. S. Isbell, in R. F. Gould (Ed.), "Carbohydrates in Solution", Adv. in Chem. Series, Vol. 117, ACS, Washington, D.C., 1973, chapt. 5.

14. J. A. Rendleman, Jr., in R. F. Gould (Ed.), "Carbohydrates in Solution", Adv. in Chem. Series, Vol. 117, ACS, Washington, D.C., 1973, chapt. 4.

SECTION II.

TRANSIENT GENERATION OF DIFFUSION LAYER ALKALINITY FOR THE PULSED AMPEROMETRIC DETECTION OF GLUCOSE IN LOW CAPACITY BUFFERS HAVING NEUTRAL AND ACIDIC PH VALUES

SUMMARY

The alkaline condition necessary for the anodic detection of glucose at gold electrodes can be generated electrochemically within the diffusion layer by cathodic stripping of surface oxide and reduction of dissolved oxygen. The cathodic generation of hydroxide and the anodic detection of glucose are alternated within the control of the three-step potential waveform traditionally used for pulsed amperometric detection (PAD) of carbohydrates. The detection limit for glucose in dilute acetate buffer (pH 4.8) was determined to be ca. 0.8 uM. The technique was applied to the direct determination of glucose in a continuous glucoamylase assay in the presence of the active enzyme and the starch substrate at pH 4.8. This method for glucoamylase activity was found to be accurate, more precise, and much faster than the traditional ferricyanide assay.

INTRODUCTION

Pulsed amperometric detection (PAD) has been applied with great success to the detection of carbohydrates at Au electrodes in liquid chromatography (1,2,3). Carbohydrates, and most aliphatic organic molecules, are considered to be electroinactive under conditions of dc detection (1). This apparently results from fouling of the electrode surface by adsorbed reaction products and intermediates (3). PAD allows the direct anodic detection of carbohydrates by application of a three-step potential waveform which incorporates the detection process with electrode reactivation (3). The initial (detection) potential (E_1) in the PAD waveform is set at a value where the signal from carbohydrate oxidation is large for small time values and there is little background oxidation of the Au electrode (e.g., 0.15 V vs. SCE in 0.1 M NaOH). The potential is then pulsed to a value (E_2) in the vicinity of O_2 evolution to achieve Au-oxide formation with concurrent oxidative cleaning of the electrode surface. The final potential pulse is to a value (E_3) in the region of O_2 reduction with simultaneous regeneration of the reduced Au surface. The waveform is repeated at a frequency of ca. 1 Hz. Instrumentation for PAD is available commercially (2).

PAD has its greatest sensitivity for carbohydrates at Au electrodes in alkaline solutions (pH > ca. 10) (4,5). This fact is consistent with the production of H^+ in the anodic reaction mechanism in steps up to and including the rate controlling step. The requirement of high pH for carbohydrate detection has been satisfied in chromatographic analyses by separations on low capacity anion-exchange columns using alkaline mobile

phases (2). However, the requirement of high pH prevents direct in situ application of PAD to many systems of biochemical and clinical interest because most of the enzymes that catalyze biological processes become denatured at high alkalinity. Previously, the activity of a starch hydrolyzing enzyme, glucoamylase, was determined by injection of aliquots from a reaction mixture into a carrier stream of 0.1 M NaOH prior to detection by PAD of the glucose produced (6). An attempt to analyze the enzyme reaction solution directly by PAD failed because the enzyme required a pH of 4.8 for activity and PAD is unable to detect glucose at pH < ca. 10.

Here, we present a method for the determination of glucose by PAD in low capacity buffers of neutral and acidic pH values. The method utilizes the electrochemical generation of OH^- in the diffusion layer by the reductions of Au-oxide and O_2 during the cathodic reactivation step at E_3 in the PAD waveform. The method is somewhat analogous to reverse pulse polarographic (RPP) determinations of halogenated hydrocarbons (7,8) in which halide ions, produced in the diffusion layer by reduction of the halogenated species at the initial potential, are detected at a Hg electrode following a positive potential step by anodic reactions to form insoluble mercurous salts (8).

MATERIALS AND METHODS

Apparatus

Current-potential curves were obtained by cyclic voltammetry using a Model RDE 3 or RDE 4 potentiostat at Au rotated disc electrodes (RDE) (AFMD10, 0.008 cm^2; or AFMD19, 0.196 cm^2) in a PIR or MSR rotator (Pine Instrument Co.; Grove City, PA). Voltammetric data were traced with a Model 100 (Houston Instruments; Austin, TX) or a Model 7035B (Hewlett-Packard; Palo Alto, CA) X-Y recorder. A coiled Pt wire (2.8 cm^2) served as the counter electrode. A calomel electrode with a potential of 0.326 V versus the normal hydrogen electrode (NHE) and a saturated calomel electrode (SCE) served as reference electrodes for the voltammetric and the PAD studies, respectively. A Model PAD-2 potentiostat (Dionex Corp.; Sunnyvale, CA) was used to generate three-step waveforms at the Au RDE and the PAD signal was recorded by a Series 5000 stripchart recorder (Fisher Scientific; Fair Lawn, NJ). The current response in PAD was sampled during a 200 msec period (t_s) at the end of the detection period (t_1).

Reagents

Glucoamylase (EC 3.2.1.3, *a*-(1,4) glucan glucohydrolase, ex. Aspergillus niger) was from Novo Industri (Bagsvaerd, Denmark). All other chemicals were reagent grade. Water was condensed from steam and purified further in a Milli-Q system from Millipore (Bedford, MA).

Procedures

The voltammetric response of glucose was studied as a function of pH and buffer capacity at Au RDEs in aqueous solutions of NaOH, HNO_3, sodium acetate (pH 4.8), and sodium phosphate (pH 7.2).

The following PAD waveforms were used to detect glucose. In 0.1 M NaOH: E_1 = 0.15 V (t_1 = 420 ms, t_s = 200 ms), E_2 = 0.75 V (t_2 = 120 ms), and E_3 = -1.0 V (t_3 = 120 ms). In sodium acetate buffer (pH 4.8): E_1 = 0.35 V (t_1 = 420 ms, t_s = 200 ms), E_2 = 1.20 V (t_2 = 120 ms), and E_3 = - 0.80 V (t_3 = 480 ms). The detector output for both waveforms was filtered with a 3.0 s time constant.

The initial activity of glucoamylase was determined at 25 ^{o}C by adding 10 uL of a solution containing 0.0105 g mL^{-1} enzyme to 50 mL of 1.0% (wt/vol) corn starch. Both enzyme and starch were prepared in 1.0 mM acetate buffer (pH 4.8) containing 50 mM $NaNO_3$. The increase in glucose concentration with time was followed by PAD at a Au RDE. The system response for glucose was calibrated in a separate experiment by addition of 100 uL aliquots of 5.0 mM glucose to 50 mL of the reaction solution containing starch but no enzyme.

RESULTS AND DISCUSSION

Voltammetry of Glucose

The voltammetric response for glucose is shown in Figure 1 for a Au RDE in well-buffered solutions of various pH values. During the positive potential scan in 0.1 M NaOH (Fig. 1A), oxidation of glucose occurs beginning at ca. - 0.5 V, but nearly ceases with the onset of Au-oxide formation at ca. 0.2 V. The maximum glucose signal appears at ca. 0.1 V. The maximum anodic sensitivity for glucose was 30 mA M^{-1} at pH ca. 13 in 0.10 M NaOH (Fig. 1A). The sensitivity decreased to 0.1 mA M^{-1} at pH 7.2 (Fig. 1B), and further to ca. 0.0 mA M^{-1} for pH < 4.8 (Figs. 1C & D). As shown also in Figure 1, both the onset of Au-oxide formation (positive scan) and the cathodic stripping of the oxide film (negative scan) are shifted to more negative potential values with the increase of solution alkalinity. Au-oxide formation commences at ca. 1.0 V at pH 1, 0.8 V at pH 4.8, 0.6 V at pH 7.2, and 0.1 V at pH 13. Au-oxide stripping peaks occur at ca. 0.8 V at pH 1, 0.5 V at pH 4.8, 0.3 V at pH 7.2, and 0.0 V at pH 13. Onset of the reduction of dissolved O_2 on the negative scan also is shifted to more negative values with increased pH, e.g., ca. 0.1 V at pH 1, -0.05 V at pH 4.8, -0.10 V at pH 7.2, and -0.20 V at pH 13. However, this shift for O_2 reduction is not as large as that observed for oxide stripping. The voltammetric response for glucose shown in Figure 1A is useful in approximating the appropriate values of potential for each step in the PAD waveform applied to 0.1 M NaOH.

The anodic current maximum for glucose oxidation was studied at a Au RDE as a function of glucose concentration and rotational velocity

Figure 1A. Voltammetric response for glucose in air-saturated 0.1 M NaOH. Conditions: $w = 94.2$ rad sec^{-1}, $v = 6.0$ V min^{-1}, $A_d = 0.008$ cm^2. Curves: (a) residual response, (b) 0.25 mM glucose

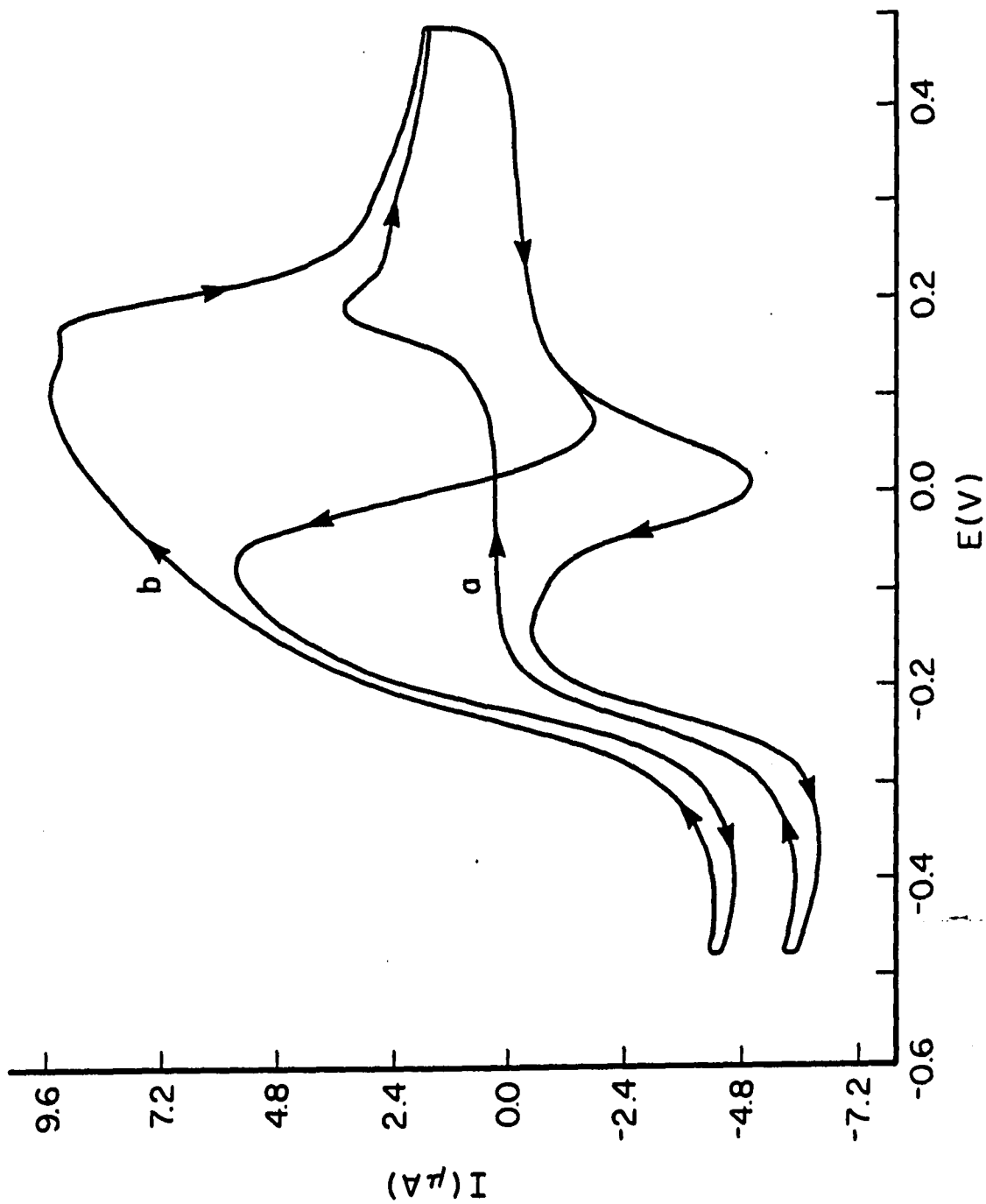
9.6
7.2
4.8
2.4
0.0
-2.4
-4.8
-7.2
I(μA)
-0.6
-0.4
-0.2
0.0
0.2
0.4
E(V)
a
b

Figure 1B. Voltammetric response for glucose in air-saturated 0.1 M sodium phosphate at pH 7.2. Conditions: $w = 94.2$ rad sec^{-1}, $v = 6.0$ V min^{-1}, $A_d = 0.008$ cm^2. Curves: (a) residual response, (b) 10.0 mM glucose

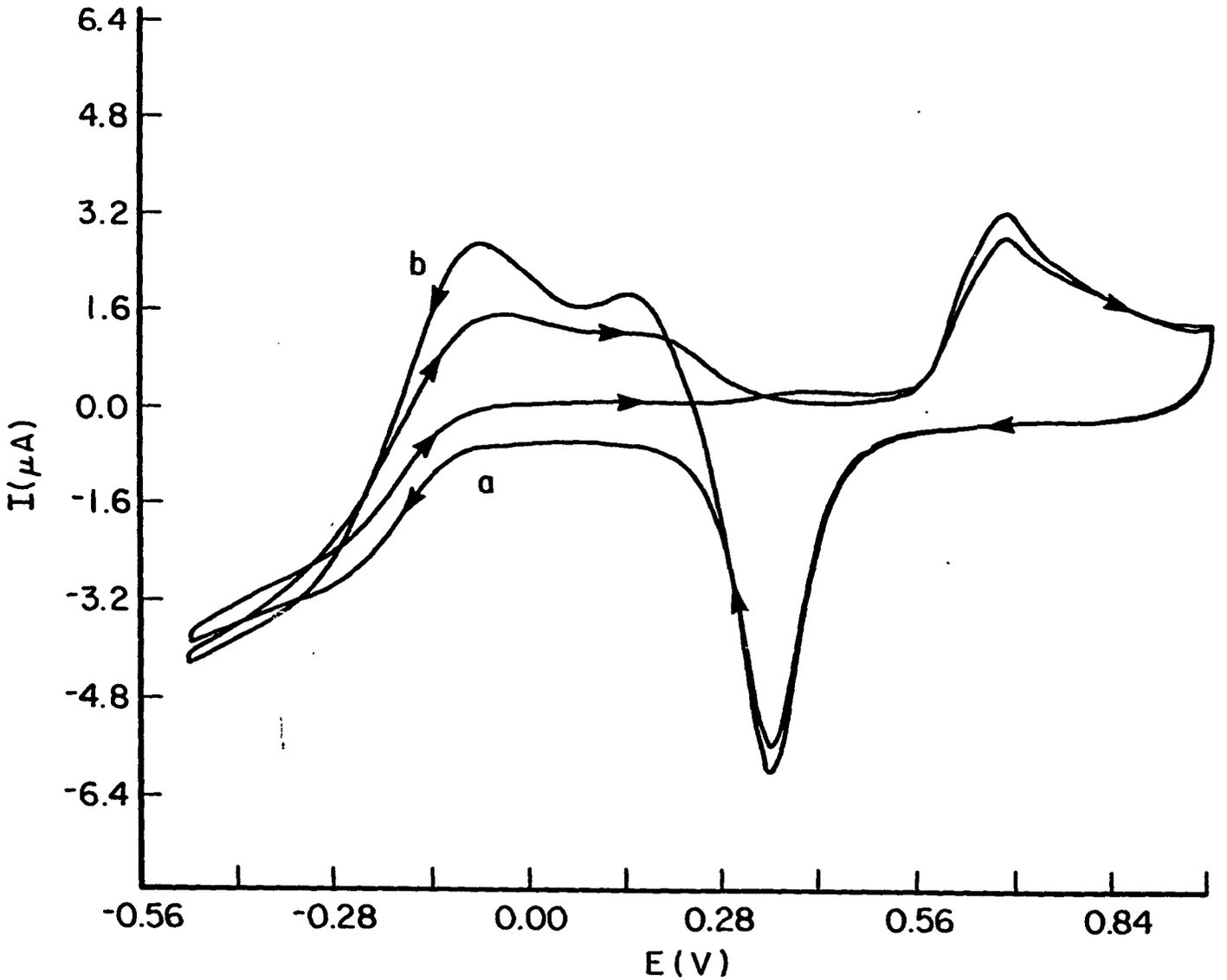
6.4
4.8
3.2
1.6
0.0
-1.6
-3.2
-4.8
-6.4
I(μA)
b
a
-0.56
-0.28
0.00
0.28
0.56
0.84
E (V)

Figure 1C. Voltammetric response for glucose in air-saturated 0.1 M sodium acetate at pH 4.8. Conditions: $w = 94.2$ rad sec^{-1}, $v = 6.0$ V min^{-1}, $A_d = 0.008$ cm^2. Curves: (a) residual response, (b) 10.0 mM glucose

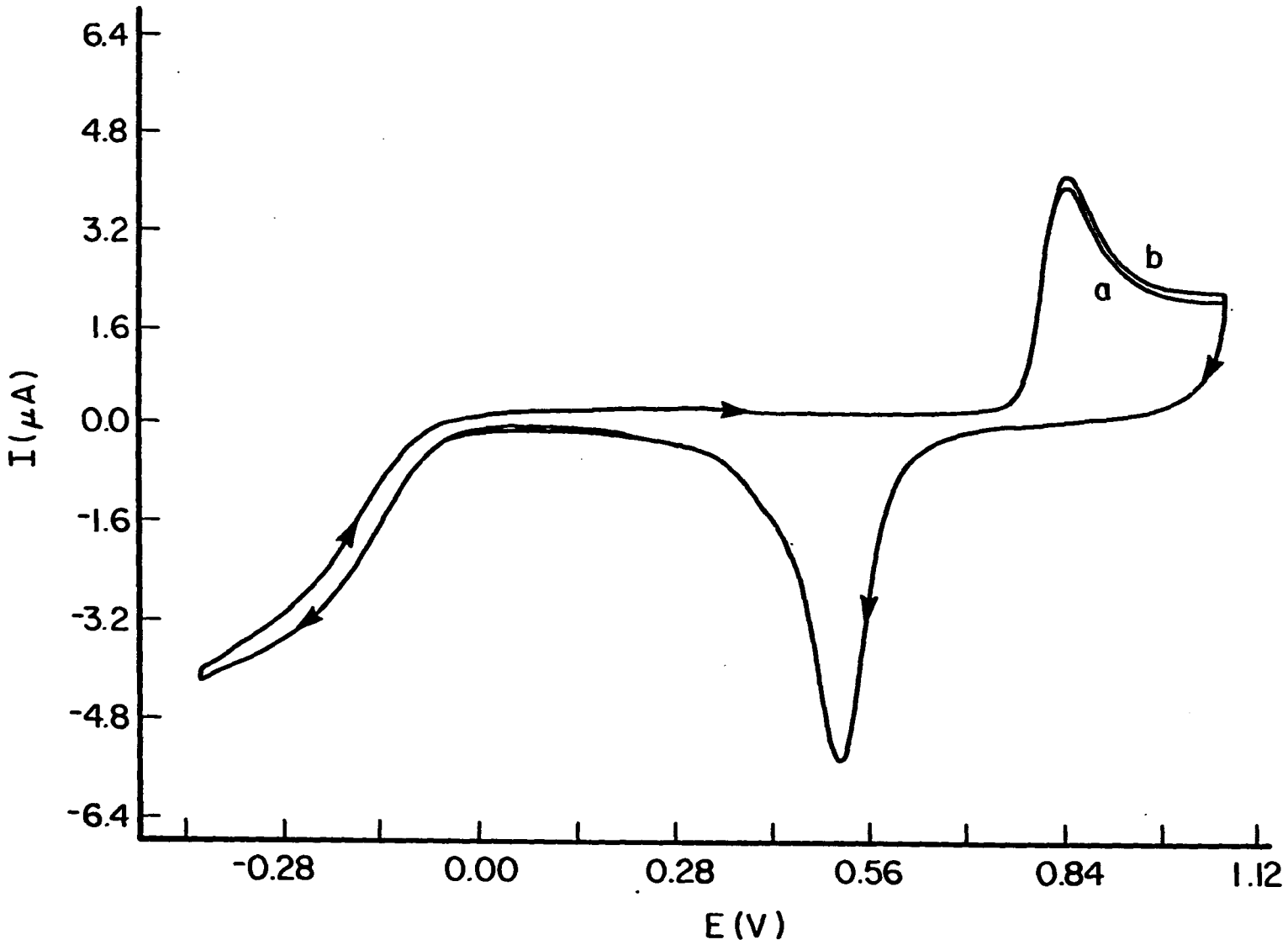
6.4
4.8
3.2
1.6
0.0
-1.6
-3.2
-4.8
-6.4
I(μA)
-0.28
0.00
0.28
0.56
0.84
1.12
E(V)
a
b

Figure 1D. Voltammetric response for glucose in air-saturated 0.2 M HNO_3. Conditions: $w = 94.2$ rad sec^{-1}, $v = 6.0$ V min^{-1}, $A_d = 0.008$ cm^2. Curves: (a) residual response, (b) 10.0 mM glucose

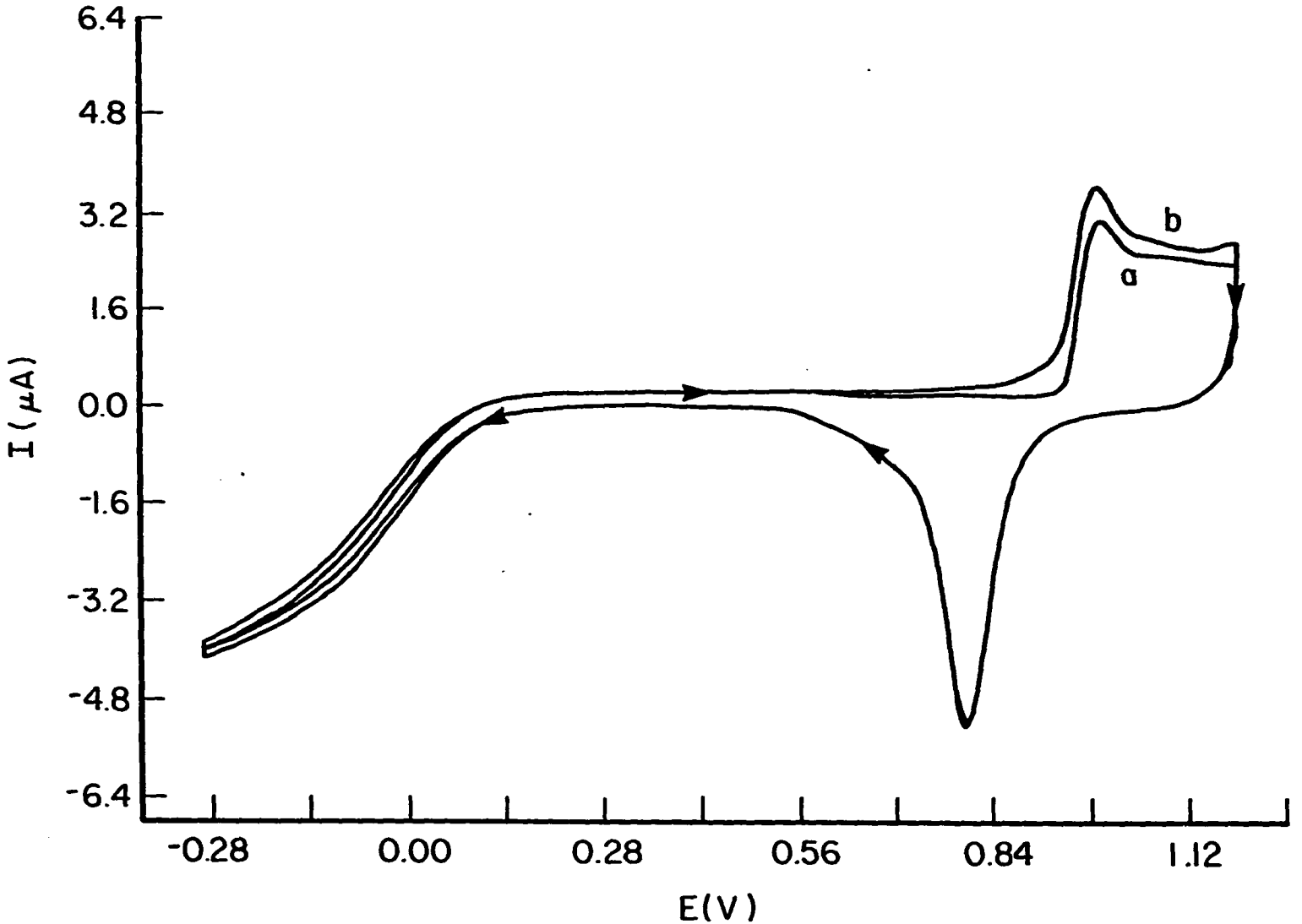
6.4
4.8
3.2
1.6
0.0
-1.6
-3.2
-4.8
-6.4
I (μA)
-0.28
0.00
0.28
0.56
0.84
1.12
E(V)
a
b

in 0.1 M NaOH and the results were compared to the predicted response for mass transport limited reactions for a RDE given by the Levich equation (9) shown below.

$$I_{d,lim} = 0.62nFA_d D^{2/3} v^{-1/6} w^{1/2} C^b \quad (1)$$

In Equation 1, $I_{d,lim}$ is the limiting disc current (mA), A_d is the geometric area of the disk electrode (cm^2), C^b is the concentration (M) of analyte in the solution bulk, and the remaining terms have their usual significance for rotated disk electrodes (9). A plot of the maximum current for glucose measured at 0.1 V and with w = 168 rad sec^{-1} versus glucose concentration (0.1 - 1.0 mM) in 0.1 M NaOH was linear with slope = 37.03 ± 0.21 mA M^{-1}, y-intercept = -0.05 ± 0.11 mA, standard error = 24.90 mA, and correlation coefficient (r) = 0.99987 (N = 10). Uncertainties given are ± one standard deviation. Therefore, the oxidation of glucose is concluded to proceed at an apparent mass transfer limited rate for $C^b \leq 1.0$ mM. The experiment was repeated four times and the average value of n was calculated from the slopes of the respective I_d - C^b plots to be 7.9 ± 0.5 equiv mol^{-1}, using the value D = 6.7 x 10^{-6} cm^2 sec^{-1} for glucose and v = 0.01023 cm^2 sec^{-1} for 0.1 M NaOH (10). We propose Equation 2 as the primary anodic reaction for glucose at 0.1 V in 0.1 M NaOH.

$$\text{glucose} + 3H_2O \rightarrow \text{formic acid} + \text{arabinaric acid} + 8H^+ + 8e^- \quad (2)$$

This proposed reaction is reasonable based on results of a previous study of the action of O_2 on glucose in alkaline solution in which

formic acid and arabinonic acid were determined to be the primary reaction products (11). A more rigorous investigation of the mechanism of glucose oxidation at Au electrodes in highly alkaline solutions is in process.

The strong dependence of the kinetics of the electrochemical oxidation of glucose on solution pH is easily rationalized on the basis of the large number of protons generated in Reaction 2. Furthermore, the importance of a high buffer capacity for alkaline supporting electrolytes also is obvious. The production of 8 protons in the 8-electron reaction requires a sufficient flux of base from the bulk solution to the diffusion layer so that the electrode surface pH is not changed as a result of the electrode reaction. It is conceivable in a solution of high pH, but low buffer capacity, that the pH in the diffusion layer of the Au RDE can be shifted substantially toward neutral values which can significantly decrease the rate of the heterogeneous process so that the reaction is no longer transport limited for glucose.

The effect of a decrease in NaOH concentration on the plot of $I_{d,lim}$ vs. C^b is shown for glucose in Figure 2. The anodic process in the presence of excess NaOH displays the linear $I_{d,lim}$ - C^b response predicted by Equation 1 for reactions limited by mass transport of the analyte. However, for the more dilute NaOH solution, significant deviation from the predicted Levich response was observed when the ratio of glucose to NaOH concentrations was increased above ca. 1:5 (glucose > 0.3 mM). For glucose:NaOH > 1:5, the glucose signal was virtually constant in spite of increases in glucose concentration and the signal

Figure 2. Voltammetric current for glucose as a function of glucose concentration. Conditions: $w = 105$ rad sec^{-1}, $v = 6.0$ V min^{-1}, $A_d = 0.008$ cm^2; current measured at 0.1 V, air-saturated solution. Curves: (●) 0.1 M NaOH, (O) 1.5 mM NaOH + 50 mM $NaNO_3$

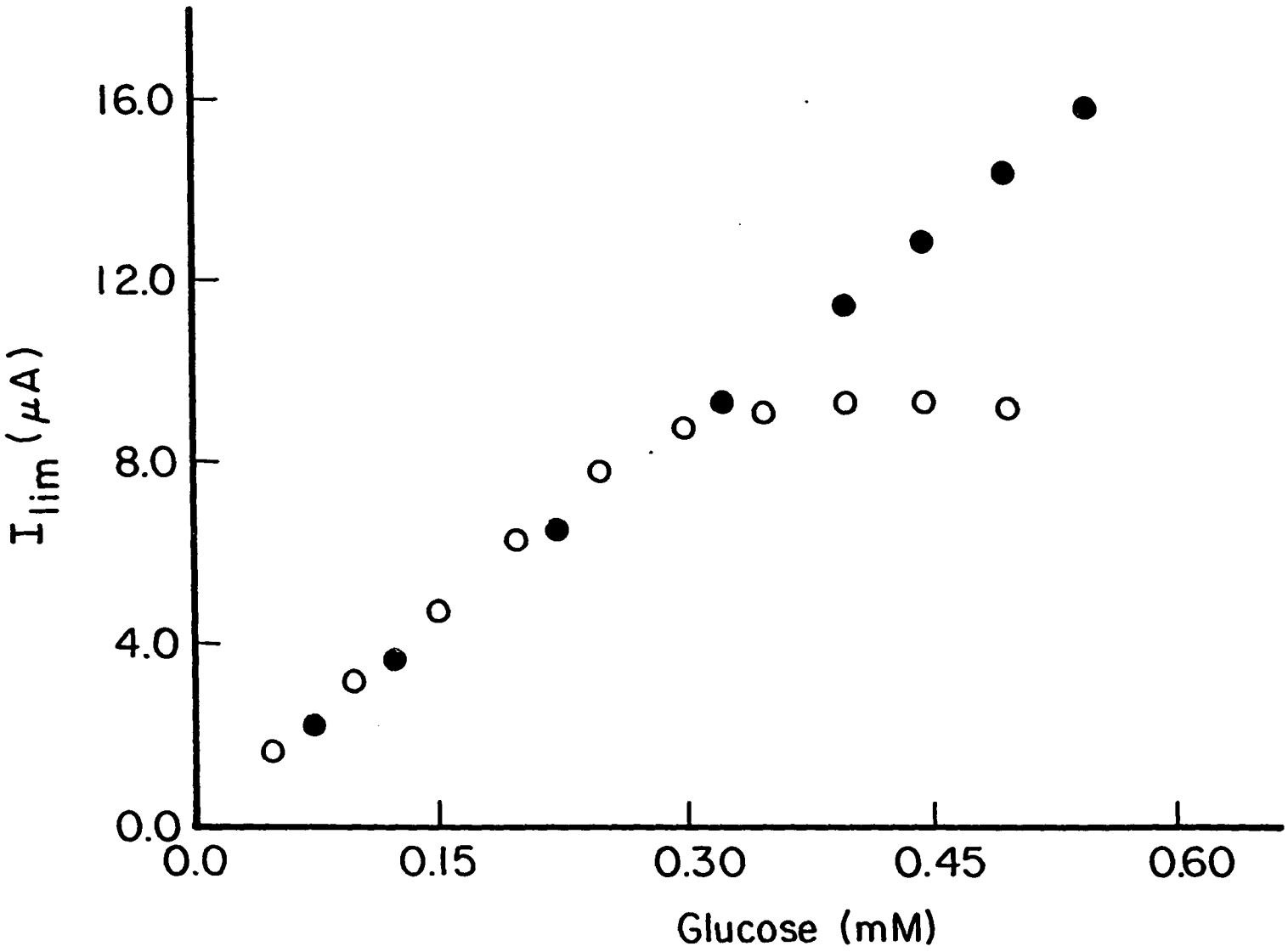
16.0
12.0
8.0
4.0
0.0
I_{lim} (μA)
0.0
0.15
0.30
0.45
0.60
Glucose (mM)

is concluded to be limited by the flux of OH^-. Using the value D = 5×10^{-5} cm^2 sec^{-1} for OH^- (12), it is predicted from Equation 1 that the OH^- flux is equivalent to the flux of H^+ produced by glucose oxidation for glucose:NaOH = ca. 1:2. For equal fluxes of OH^- and H^+ in the NaOH solution, the pH of the diffusion layer would be ca. 7. However, because of the rapid attenuation of the anodic glucose reaction with decreasing pH, the anodic signal should be expected to deviate from the transport limited value for glucose:NaOH < 1:2, as was observed. In addition to decreasing pH in the diffusion layer, factors which can cause loss of reactivity for glucose include electrode fouling by adsorption of reaction products.

Electrochemical Generation of Hydroxide

Hydroxide ion is generated in the diffusion layer by the cathodic reduction of both the Au-oxide film and dissolved oxygen, as described by Equations 3 and 4, respectively (13,14).

$$6e + Au_2O_3 + 3H_2O \rightarrow 2Au + 6OH^- \quad (3)$$

$$4e + O_2 + 2H_2O \rightarrow 4OH^- \quad (4)$$

Voltammetric experiments were performed in neutral and acidic solutions to examine the extent to which these reactions are capable of increasing the diffusion layer pH.

Voltammetric results are shown in Figure 3A for a Au RDE in acetate buffer solutions (pH 4.8) as a function of decreasing buffer capacity (Curves a-e). For comparison, the voltammetric curve for 0.1 M NaOH (pH ca. 13) is included (Curve f). As is readily seen, the cathodic wave for Au-oxide stripping has the characteristic peak shape at a high buffer

Figure 3A. Au-oxide stripping peaks obtained by cyclic voltammetry as a function of buffer capacity. Conditions: A_d = 0.008 cm^2, v = 10 V min^{-1}, w = 94.2 rad sec^{-1}. Curves: (a) 100 mM sodium acetate + 50 mM $NaNO_3$ (pH 4.8); others same as (a) except: (b) 10.0, (c) 7.0, (d) 3.0 and (e) 1.0 mM sodium acetate; (f) 0.1 M NaOH.

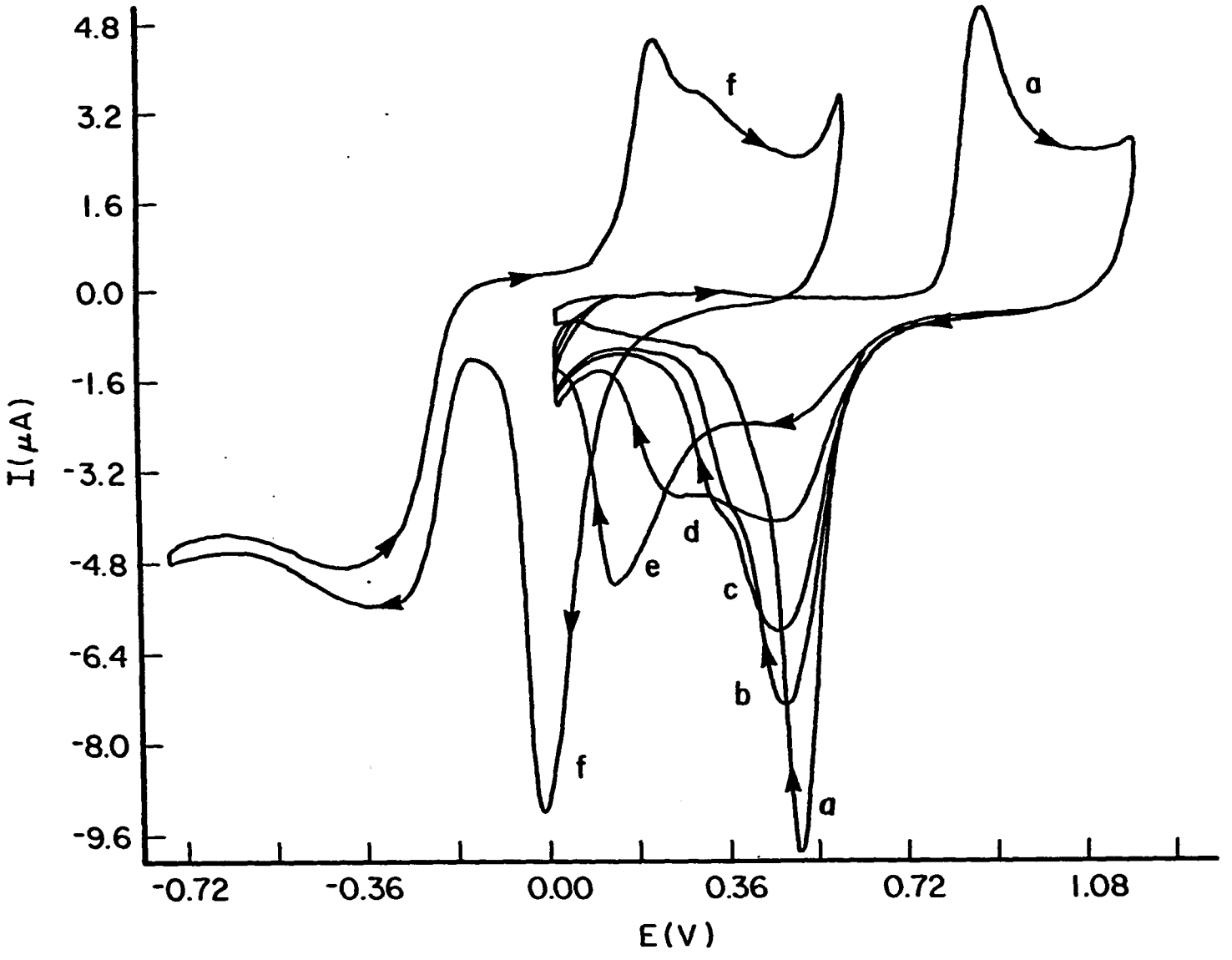
4.8
3.2
1.6
0.0
-1.6
-3.2
-4.8
-6.4
-8.0
-9.6
I(μA)
-0.72
-0.36
0.00
0.36
0.72
1.08
E(V)
a
b
c
d
e
f
f

capacity (Curve a). As the buffer capacity is decreased (Curves b-e), the stripping process commences at approximately the same potential value as for a well-buffered solution; however, the peak current decreases and the cathodic process is extended to more negative potential values, even though the bulk solution remains at a constant pH of 4.8. The shift in the cathodic peak potential is ca. -0.4 V going from 100.0 mM to 1.0 mM acetate buffer. Voltammetric results are shown in Figure 3B for acidic solutions of decreasing HNO_3 concentration. As the acidity is decreased from 0.8 mM to 0.05 mM HNO_3 (compare Curves a and j), the peak potential for the Au-oxide stripping process is shifted by ca. -0.5 V. The negative shifts in the potential for Au-oxide stripping are the result of a significant increase in the diffusion layer pH caused by OH^- produced by the reaction shown in Eq. 3. The OH^- generated in the solutions of low buffer capacity consumes all of the acetic acid (Fig. 3A) and H^+ (Fig. 3B) transported into the diffusion layer by the convective-diffusional processes. For solutions of extremely low buffer capacity, the pH of the diffusion layer is estimated to be ca. 11, based on the most negative peak potential observed for oxide stripping (Curve e in Figure 3A and Curves h-j in Figure 3B).

The transition in the stripping peak potential in Figures 3A and 3B appears as a smooth and continuous function of decreasing buffer capacity. In fact, pseudo current plateaus are observed for intermediate values of buffer capacity. We conclude for the plateau regions that the reduction current is limited by the flux of acid transported to the electrode surface. The presence or absence of dissolved O_2 did not effect the

Figure 3B. Au-oxide stripping peaks obtained by cyclic voltammetry as a function of acid concentration. Conditions: A_d = 0.008 cm^2, v = 10 V min^{-1}, w = 41.8 rad sec^{-1}. Curves: (a) 0.8 mM HNO_3 + 50 mM $NaNO_3$; others same as (a) except: (b) 0.6, (c) 0.5, (d) 0.4, (e) 0.3, (f) 0.25, (g) 0.2, (h) 0.15, (i) 0.1, (j) 0.05, (k) 0.0 mM HNO_3

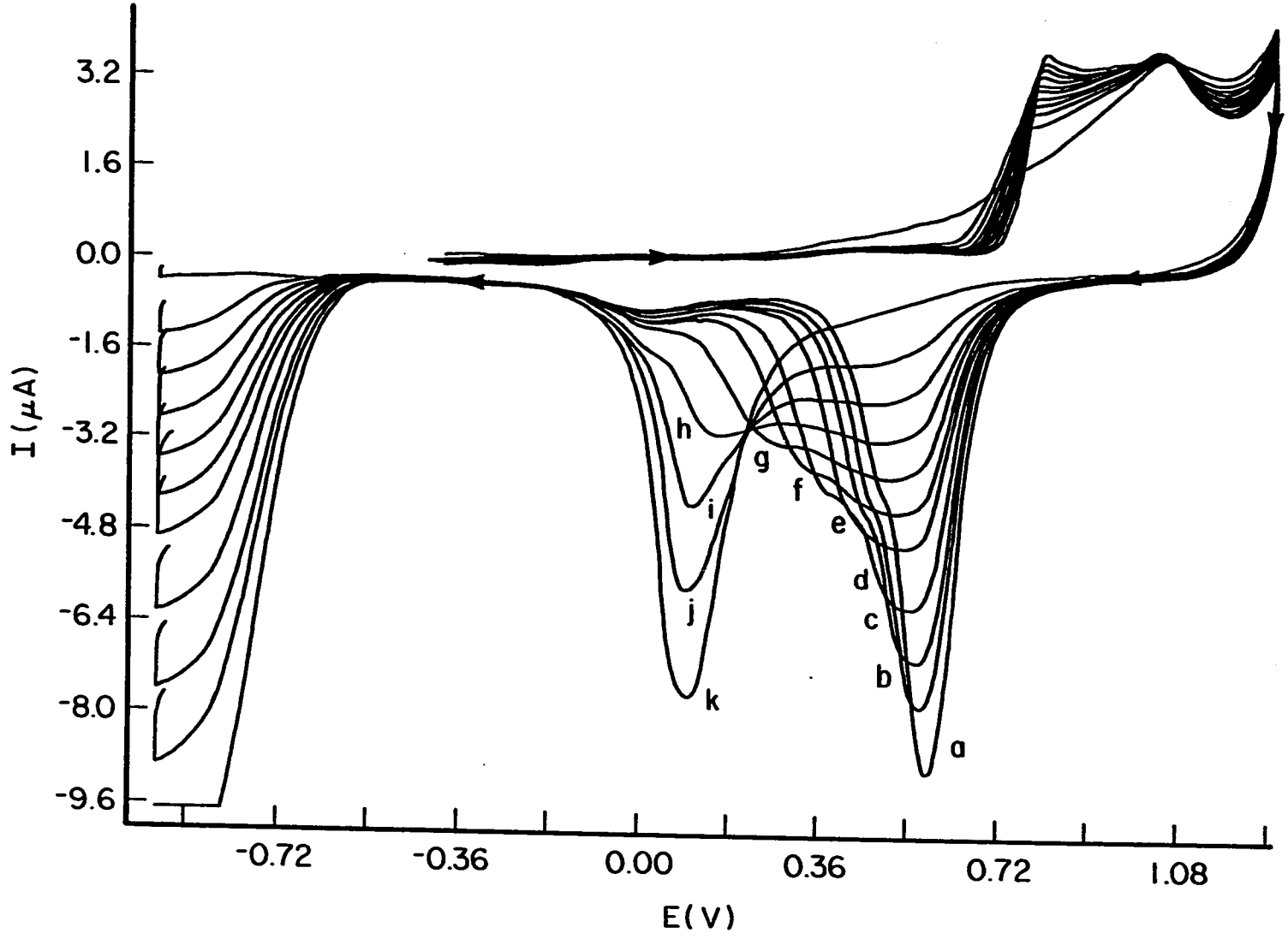
3.2
1.6
0.0
-1.6
-3.2
-4.8
-6.4
-8.0
-9.6
I (μA)
-0.72
-0.36
0.00
0.36
0.72
1.08
E(V)
a
b
c
d
e
f
g
h
i
j
k

voltammetric characteristics of the stripping wave for any of the solutions. This is because OH^- generated by O_2 reduction in the previous cyclic scan has either escaped from the diffusion layer, by mass transport, or has been neutralized during the time interval between production and the subsequent oxide stripping process.

The anodic generation of the Au-oxide film during the positive potential scan produces an amount of H^+ equivalent to the quantity of OH^- generated by the subsequent Au-oxide stripping process. Hence, there would be no net change in the pH of the bulk solution of a very low capacity buffer even from extended applications of either cyclic voltammetry or the PAD waveform. The time delay between the successive anodic and cathodic processes, as determined by the potential scan rate (v) in cyclic voltammetry or the period t_2 in the PAD waveform, allows a substantial amount of the H^+ from the anodic process to be transported out of the diffusion layer prior to the subsequent cathodic generation of OH^-.

The effect of increased potential scan rate (v) on the Au-oxide stripping peak was studied in dilute acid solutions. The i_d-E curves obtained for the negative potential scans are shown in Figure 4 as a function of v. As shown in Figure 4A for a high acid concentration, the potential range in which oxide stripping occurs is independent of v. The oxide stripping peak is symmetrical with a peak potential (E_p) of 0.80 V and a half-peak width ($dE_{p,1/2}$) of ca. 0.04 V. Furthermore, the peak current (I_p) increased with increasing v, as is expected for a surface-controlled process. As shown in Figure 4B for a low acid concen-

Figure 4A. Au-oxide stripping waves obtained by voltammetry in air-saturated 0.2 M HNO_3 as a function of potential scan rate. Conditions: $w = 41.8$ rad sec^{-1}; $A_d = 0.008$ cm^2. Curves; scan rate (V min^{-1}): (a) 10.0, (b) 7.5, (c) 5.0, (d) 2.5

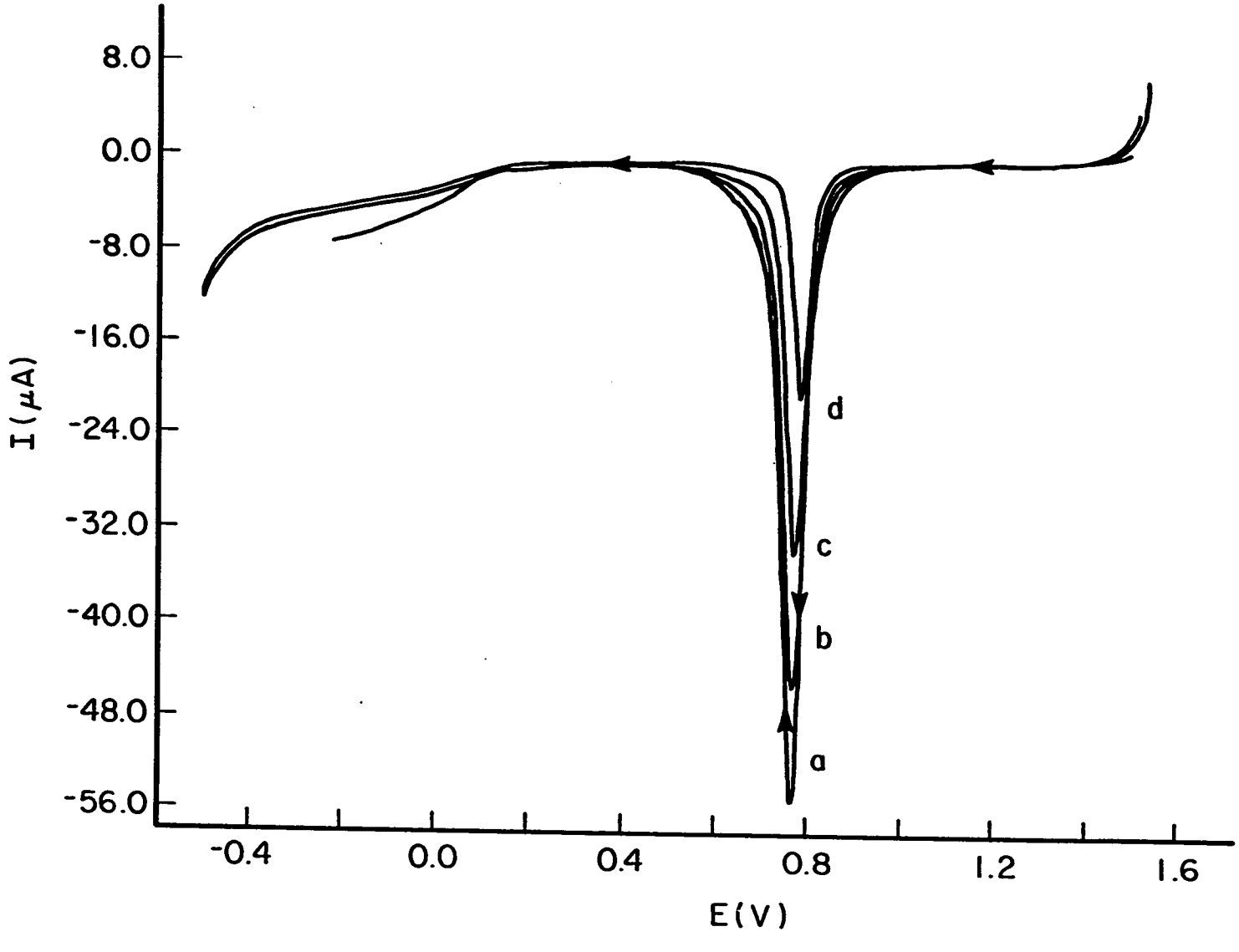
8.0
0.0
-8.0
-16.0
-24.0
-32.0
-40.0
-48.0
-56.0
I(μA)
-0.4
0.0
0.4
0.8
1.2
1.6
E(V)
d
c
b
a

Figure 4B. Au-oxide stripping waves obtained by voltammetry in air-saturated 50 mM $NaNO_3$ + 0.5 mM HNO_3 as a function of potential scan rate. Conditions: $w = 41.8$ rad sec^{-1}, $A_d = 0.196$ cm^2. Curves; scan rate (V min^{-1}): (a) 6, (b) 12, (c) 18, (d) 24

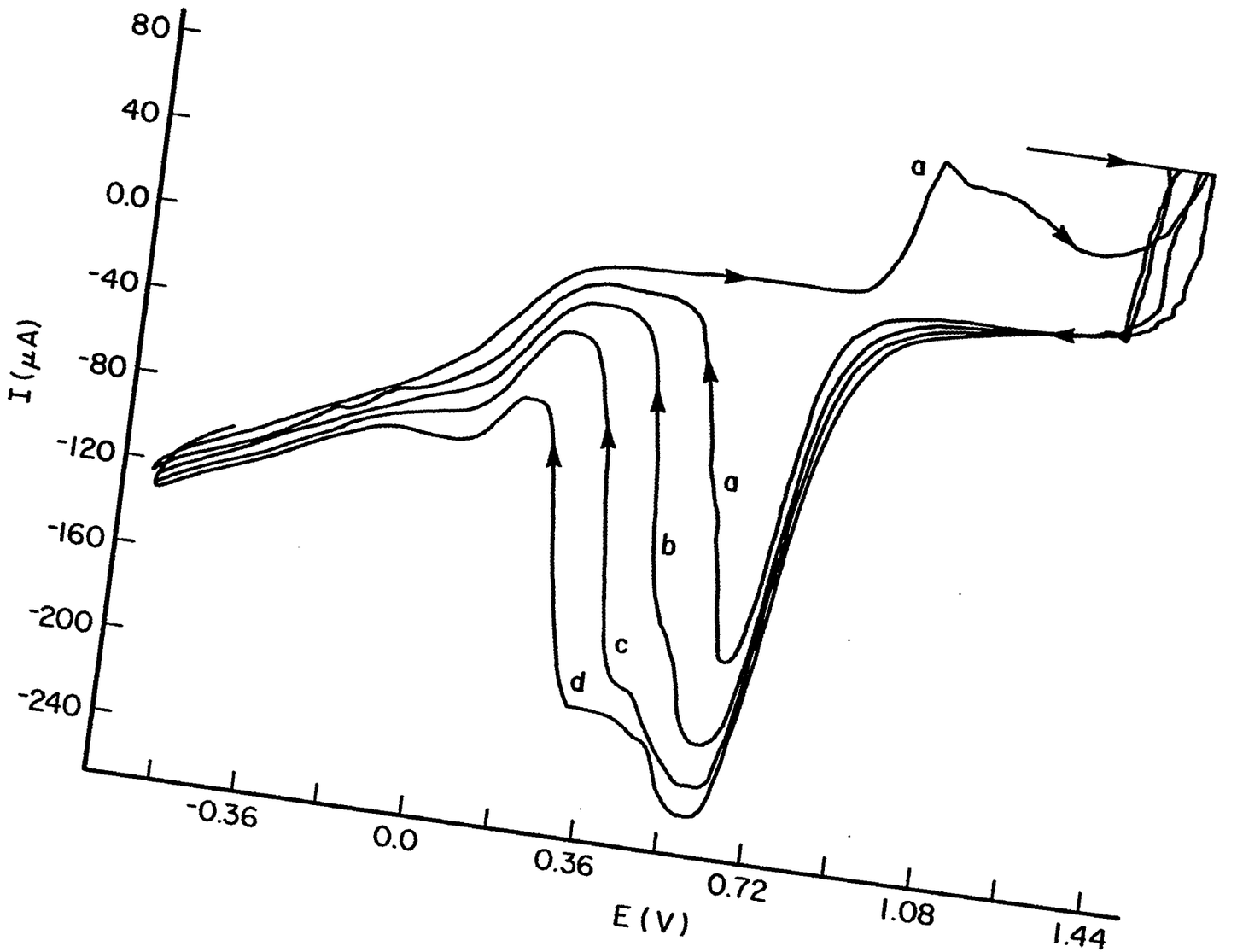
80
40
0.0
-40
-80
-120
-160
-200
-240
I (μA)
-0.36
0.0
0.36
0.72
1.08
1.44
E (V)
a
a
b
c
d

tration, the stripping peak becomes quite unsymmetrical and the stripping process is shifted toward more negative potential values for large v. The stripping peak obtained at v = 6 V min^{-1} is characterized by the values E_p = 0.65 V and $dE_{p,1/2}$ = 0.17 V. However, when v is doubled (12 V min^{-1}), the stripping peak is broadened to $dE_{p,1/2}$ = 0.28 V, with reduction continuing to 0.35 V. For v = 24 V min^{-1}, the stripping process continues well into the region of oxygen reduction with $dE_{p,1/2}$ = 0.50 V. The severe increase in $dE_{p,1/2}$ as a function of v shown in Figure 4B results from the transient increase in the diffusion layer pH above the bulk value because the high flux of OH^- generated for large values of v exceeds the flux of H^+ transported from the solution bulk.

The transport-limited flux of H^+ at the electrode surface also is a function of rotational velocity (w). Hence, for a constant value of v, a decrease in w has virtually the same effect as a decrease in buffer capacity to cause distortion in the oxide stripping peak. To illustrate, the i-E curves recorded for the negative scans of the cyclic voltammograms are shown in Figure 5 as a function of w for 0.5 mM HNO_3. Whereas the stripping peak obtained in 0.2 M HNO_3 is independent of w, because of the large flux of H^+ for this concentrated solution, the peak shape is highly sensitive to decreases in w for the dilute acidic solution. The peak at 83.7 rad s^{-1} was similar in position and shape to those obtained in more concentrated acid with $dE_{p,1/2}$ = ca. 0.20 V; however, a decrease to w = 10.5 rad sec^{-1} causes a 25% decrease in I_p with an increase in $dE_{p,1/2}$ to 0.40 V. This increase in peak width with decrease in w is the result of the decrease in the flux of H^+. Similar results for

Figure 5. Au-oxide stripping waves obtained by voltammetry as a function of rotational velocity. Conditions: same as Figure 4B (b). Curves; rotation velocity (rad sec^{-1}): (a) 83.7, (b) 31.4, (c) 20.9, (d) 10.5

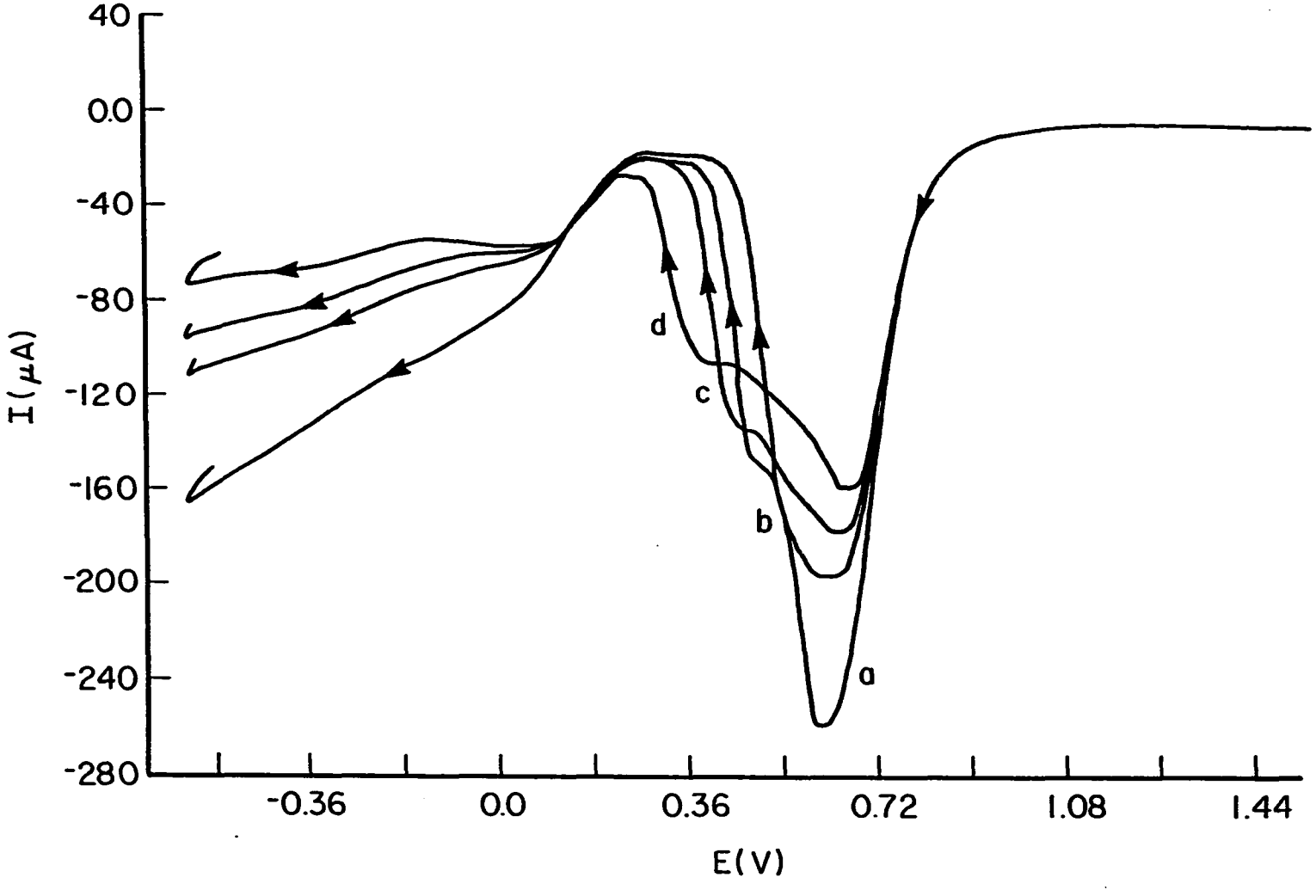
40
0.0
-40
-80
-120
-160
-200
-240
-280
I(μA)
-0.36
0.0
0.36
0.72
1.08
1.44
E(V)
a
b
c
d

changes in v and w were obtained in the dilute acetate buffer (pH 4.8).

Glucose Detection in Neutral and Acidic Solutions

The local condition of high alkalinity generated within the diffusion layer by Reactions 3 and 4 can be used to produce a transient increase in the rate of glucose oxidation in low capacity buffers of neutral and acidic pH. Current-potential curves obtained on the positive scan are shown in Figure 6 for glucose at a Au RDE in dilute acetate buffer (pH 4.8). Under the prevailing conditions, glucose oxidation occurs at the oxide-free electrode in the potential range ca. 0.0 - 0.6 V, with a maximum response at ca. 0.2 V. The anodic signal is completely attenutated at ca. 0.7 V, perhaps as a result of the onset of oxide formation. An additional anodic signal for glucose is observed in the range 0.8 - 1.2 V which occurs simultaneously with Au-oxide formation. Detection of glucose at 0.2 V is preferred because of the small background current. It is apparent from the figure that the anodic current for glucose at 0.2 V is not a linear function of glucose concentration.

The possibility of anodic detection of glucose at Au electrodes in neutral and slightly acidic solutions is highly dependent upon buffer capacity. As the concentration of buffer is increased, the higher flux of the acid component of the buffer being transported to the electrode results in more rapid consumption of the OH^- generated electrochemically. Consequently, the pH of the diffusion layer does not experience a strong transient shift to alkaline values as a result of Reactions 3 and 4. To illustrate, the change in current sensitivity as a function of buffer capacity is given in Table 1 for solutions containing acetate buffer (pH

Figure 6. Voltammetric response for glucose in air-saturated 50 mM $NaNO_3$ + 1.0 mM sodium acetate (pH 4.8). Conditions: same as Figure 3A (e). Curves; glucose concentration (mM): (a) 0.0, (b) 1.0, (c) 2.0, (d) 4.0, (e) 8.0, (f) 15.0

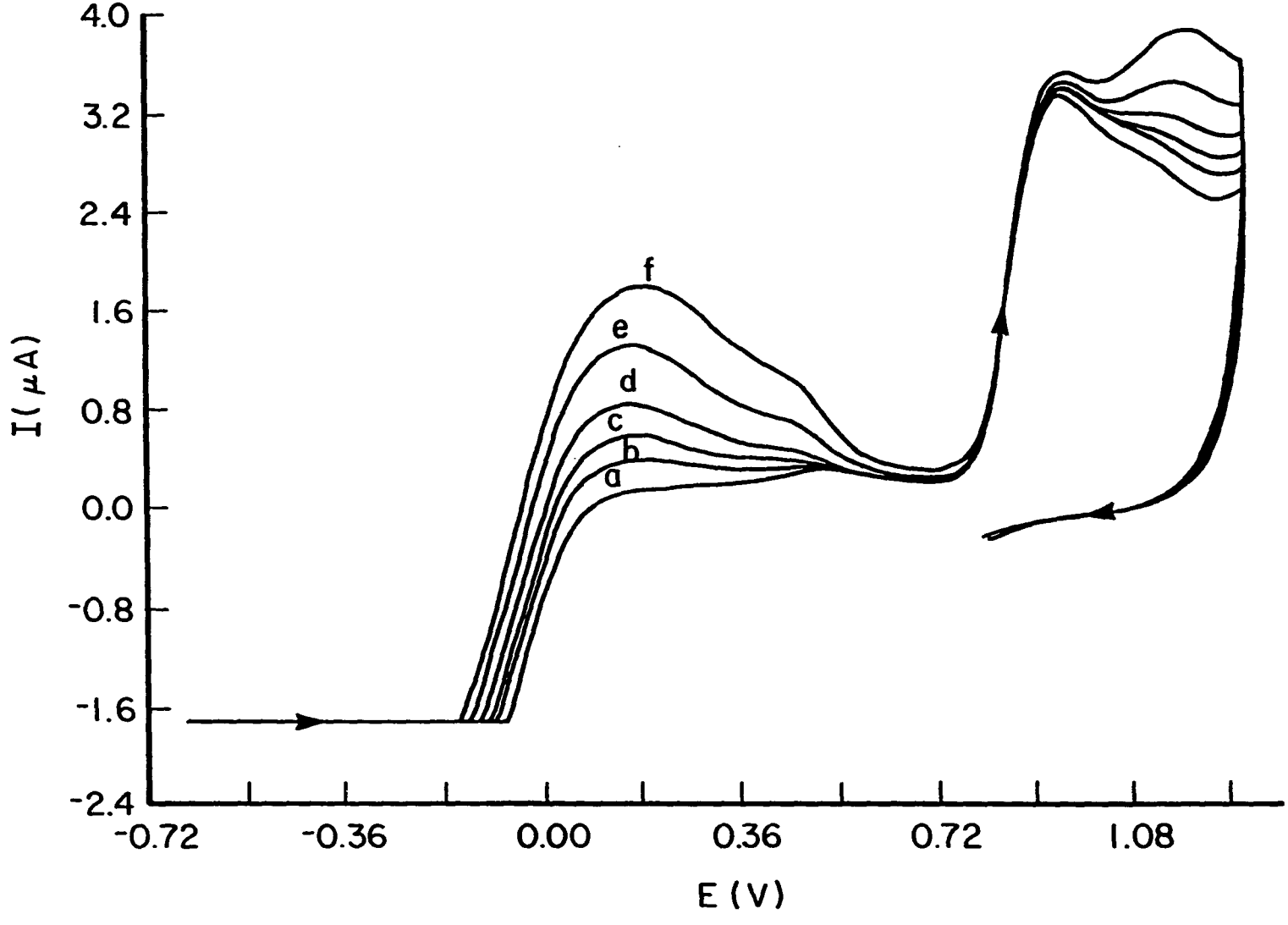
4.0
3.2
2.4
1.6
0.8
0.0
-0.8
-1.6
-2.4
I(μA)
-0.72
-0.36
0.00
0.36
0.72
1.08
E (V)
a
b
c
d
e
f

Table 1. Effect of buffer concentration on glucose oxidation at the Au RDE

Buffer[a]	Buffer Concentration (mM)	Current[b] Sensitivity (uA per M glucose)
Acetate (pH 4.8)	1.0	145
	5.0	42
	10.0	18
	20.0	10
	40.0	6
	200.0	0
Phosphate (pH 6.8)	3.0	726
	30.0	263
	300.0	21
Nitric Acid	0.5	758
	5.0	232
	50.0	17
	200.0	5

A_d = 0.008 cm^2, w = 94.2 rad sec^{-1}, v = 10 V min^{-1}.

[a]Buffers also contained 50 mM $NaNO_3$.

[b]Current measured at potential of maximum signal; C^b = 10.0 mM glucose.

4.8), phosphate buffer (pH 6.8), and HNO_3. As shown, glucose signals decrease in the order phosphate > HNO_3 >> acetate. At equal buffer concentrations, the dibasic phosphate can consume more protons than the monobasic acetate. The anodic signals in Table 1 are to be compared to a sensitivity of 37 mA M^{-1} for glucose in 0.1 M NaOH. The extremely small current sensitivity in the acetate buffer could also be the result partially from adsorption of the organic acetate ion with the consequential interference in the glucose detection mechanism. However, we have no direct evidence to support the conclusion of interference by adsorbed acetate.

The anodic current resulting from glucose oxidation in 0.1 M NaOH changes only slightly with increased values of v. This result, plus the transport limited nature of the detection reaction at high pH (see Fig. 2), support the conclusion that the anodic reaction is not under the control of a priori adsorption of glucose. However, as shown in Table 2, the glucose signal for dilute acetate buffers is highly dependent on v, which is commonly taken as evidence for a surface-controlled reaction mechanism. This result is explained as the consequence of the transient nature of surface alkalinity, as already discussed. The highest signal for glucose, then, is expected for the highest value of v for which the flux of generated OH^- is greatest.

Equation 1 predicts a linear dependence of I_d on $w^{1/2}$ for transport limited reactions at a RDE. The plot of I_d vs. $w^{1/2}$ for 0.5 mM glucose in 0.1 M NaOH was linear with a positive slope of 1.23 ± 0.01 uA $sec^{1/2}$ $rad^{-1/2}$, an intercept of 2.50 ± 0.11 uA, standard error of 102 uA, and a

Table 2. Effect of increasing potential scan rate on glucose oxidation at the Au RDE

Solution	Scan Rate ($V\ min^{-1}$)	Percentage[a] increase in anodic current for glucose
5.0 mM acetate, 50 mM $NaNO_3$ (pH 4.8), 9.5 mM glucose	5.0	41
	7.5	81
	10.0	107
0.1 M NaOH, 0.5 mM glucose	5.0	1
	7.5	3
	10.0	3

A_d = 0.008 cm^2, w = 41.9 rad sec^{-1}.

[a]Percentage increase compared to value for v = 2.5 V min^{-1}: 0.27 uA in acetate solution, 10.16 uA in NaOH solution.

correlation coefficient (r) of 0.99985 (N = 5, v = 5.0 V min^{-1}, w from 10.5 to 209.3 rad sec^{-1}, and A_d = 0.008 cm^2). The I_d-$w^{1/2}$ plot for a dilute acetate buffer is shown in Figure 7. As is seen, I_d decreases rather than increases as w is increased. This behavior is the direct consequence of the more rapid consumption of the generated OH^- at higher values of w, with the resultant decrease in glucose signal, as the flux of buffer is increased; see also Fig. 5 and the accompanying discussion.

The reduction of dissolved O_2 (Reaction 4) also generates OH^-. Furthermore, the process does not have the transient nature as is seen for reduction of the Au-oxide film (Reaction 3). The contribution of dissolved O_2 to surface alkalinity was investigated by obtaining i-E curves for glucose in dilute acetate buffer (pH 4.8) before and after purging the solution with dispersed He. As shown in Figure 8, the anodic current from glucose decreased by 35% when O_2 was removed. Thus, Reaction 4 can contribute significantly to alkalinity in the diffusion layer which allows for an increased rate of glucose oxidation.

Pulsed Amperometric Detection (PAD)

PAD was performed for glucose at a Au RDE in dilute acetate buffer (pH 4.8) and the results were compared to those obtained in 0.1 M NaOH. As shown in Figure 9A, the increase in PAD signal is a nonlinear function of glucose concentration in dilute acetate buffer. The sensitivity (i.e., current/concentration) at 10 uM glucose is only 2.4 times larger than that at 100 uM. For comparison, a plot of PAD current versus glucose concentration in 0.1 M NaOH is shown in Figure 9B. The current increased linearly with glucose concentration from 10 - 270 uM with a

Figure 7. Voltammetric current measured at 0.10 V for 9.5 mM glucose as a function of rotational velocity. Conditions: same as Figure 3A (d)

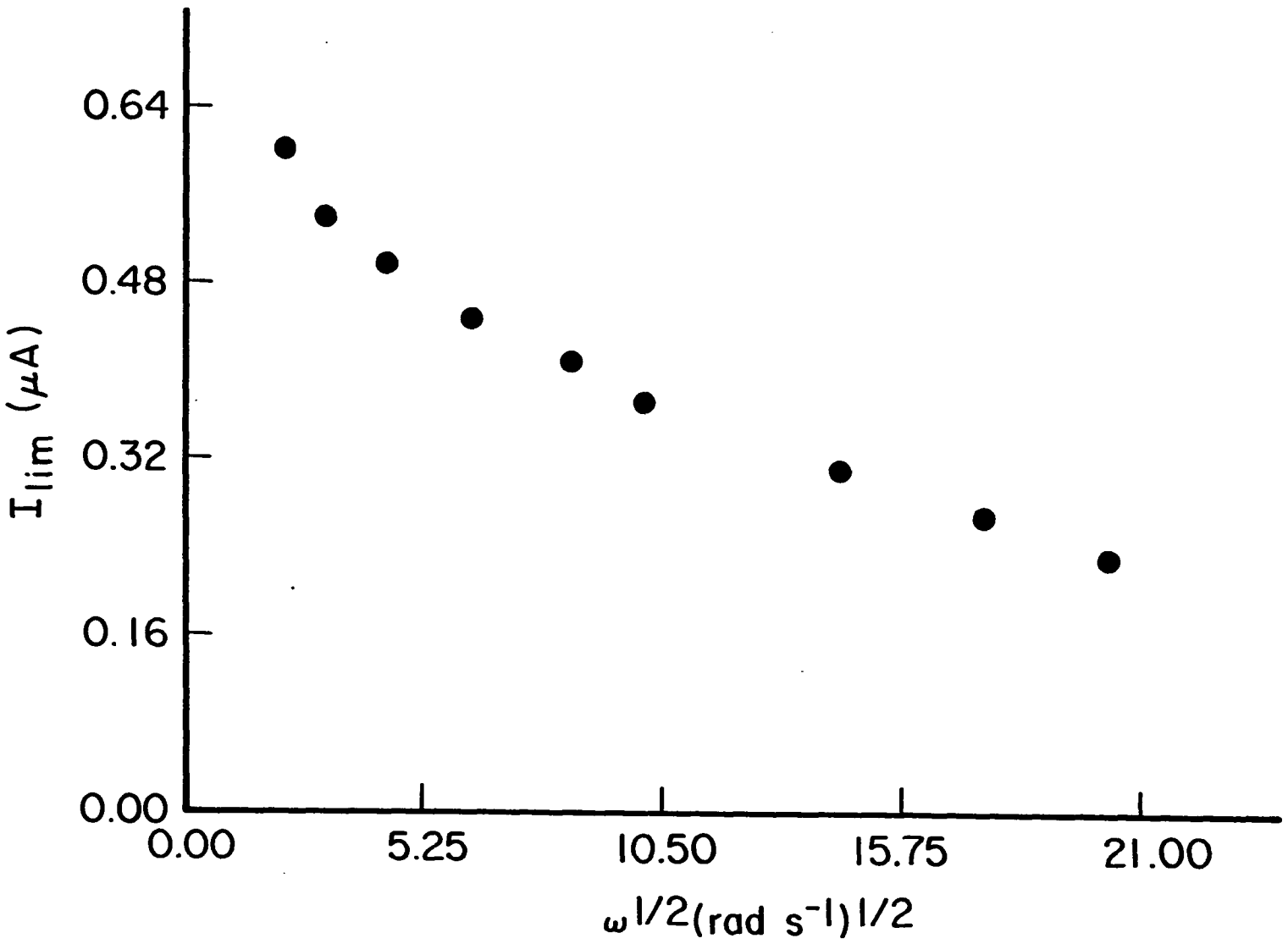
0.64
0.48
0.32
0.16
0.00
I_{lim} (μA)
0.00
5.25
10.50
15.75
21.00
$\omega^{1/2}$(rad s^{-1})$^{1/2}$

Figure 8. The effect of the removal of dissolved O_2 on the voltammetric response of glucose. Conditions: same as Figure 6. Curves: (a) air-saturated supporting electrolyte, (b) same as (a) except; 10.0 mM glucose, (c) same as (b) except; He-saturated

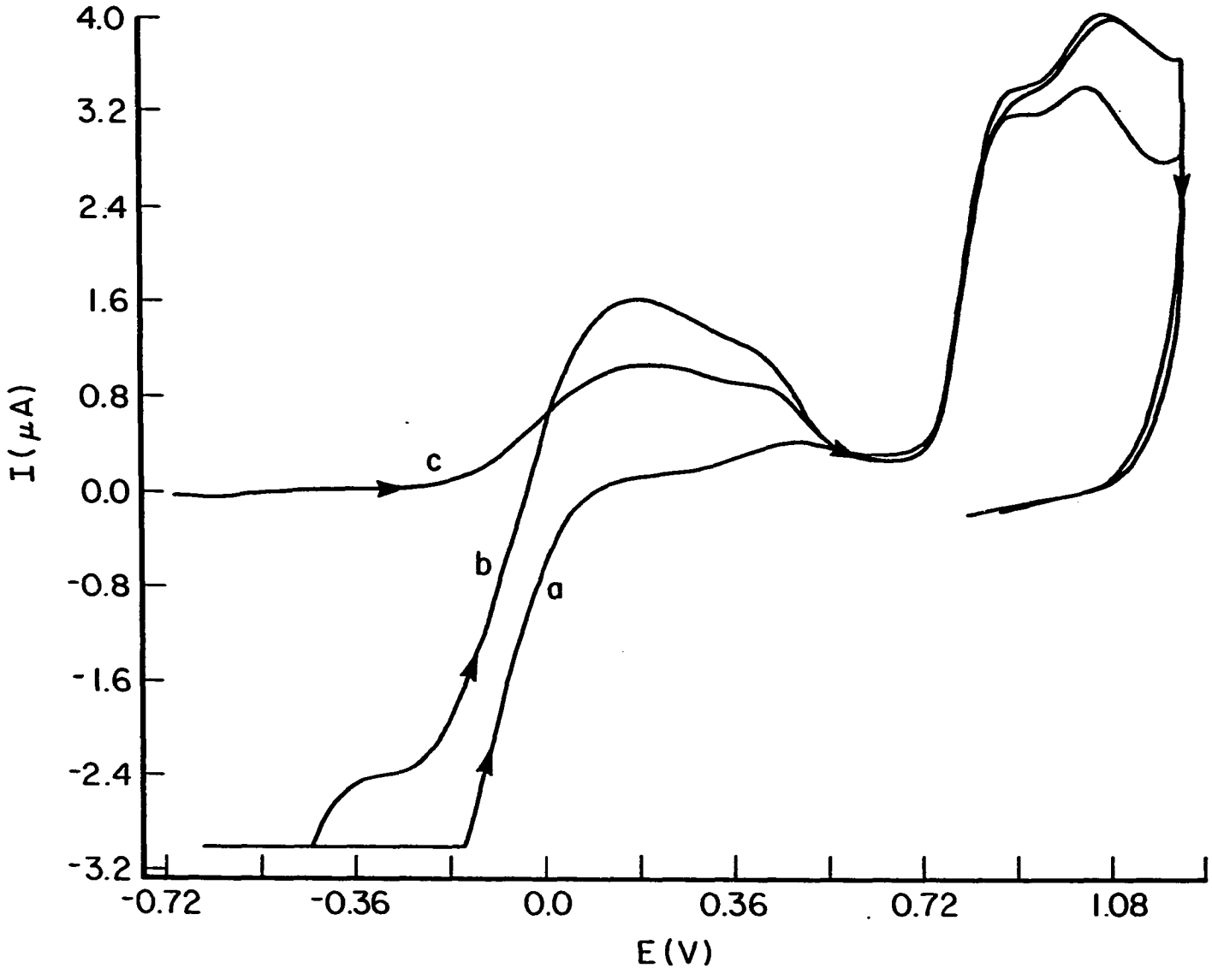
4.0
3.2
2.4
1.6
0.8
0.0
-0.8
-1.6
-2.4
-3.2
I(μA)
-0.72
-0.36
0.0
0.36
0.72
1.08
E(V)
a
b
c

Figure 9A. PAD signal for glucose as a function of glucose concentration in 1.0 mM sodium acetate + 50 mM $NaNO_3$ (pH 4.8). Conditions: air-saturated solution, $w = 94.2$ rad sec^{-1}, $A_d = 0.008$ cm^2

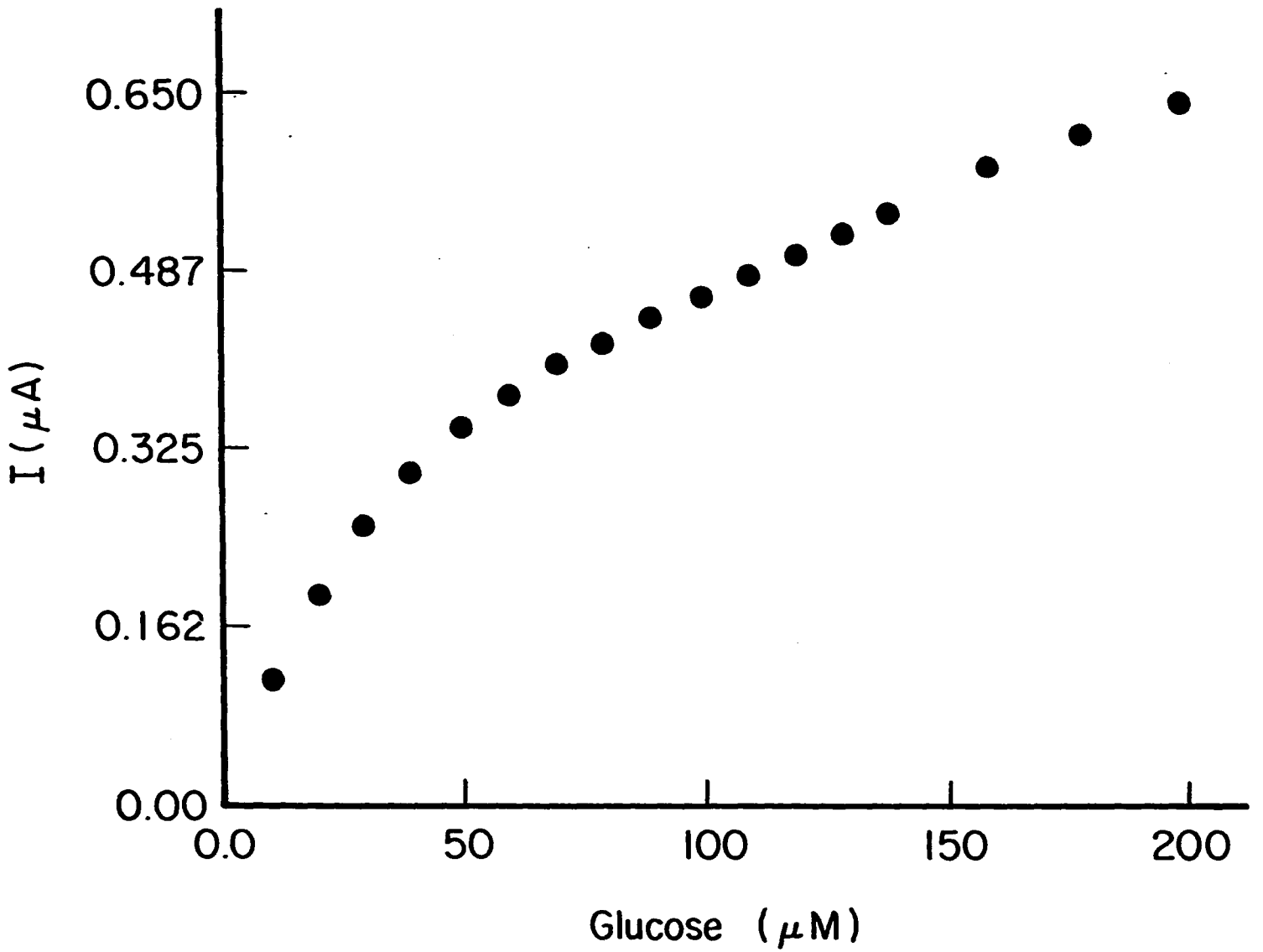
0.650
0.487
0.325
0.162
0.00
I (μA)
0.0
50
100
150
200
Glucose (μM)

Figure 9B. PAD signal for glucose as a function of glucose concentration in 0.1 M NaOH. Conditions: air-saturated solution, $w = 94.2$ rad sec^{-1}, $A_d = 0.008$ cm^2

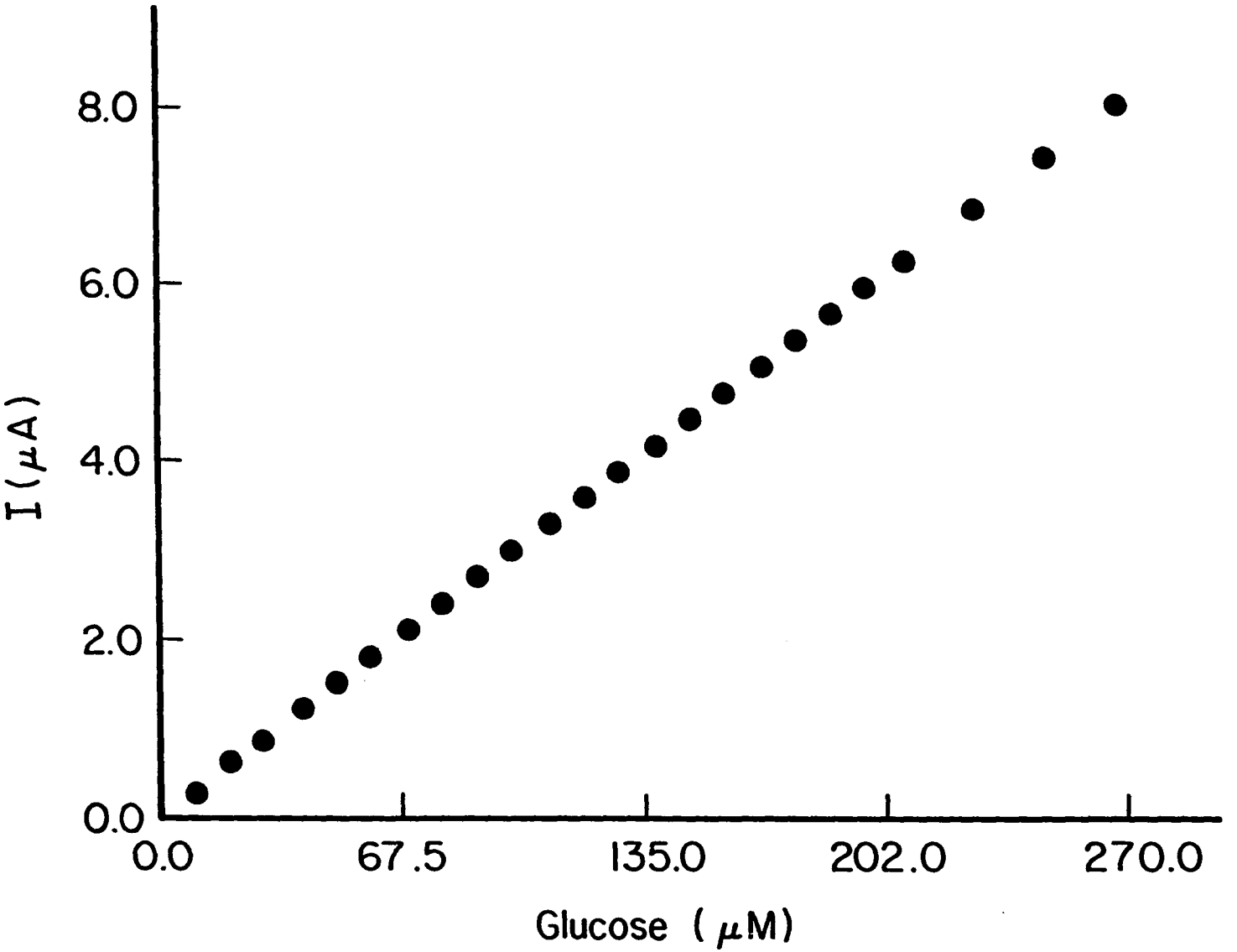
8.0
6.0
4.0
2.0
0.0
I (μA)
0.0
67.5
135.0
202.0
270.0
Glucose (μM)

slope of 0.030 ± 0.001 uA uM^{-1}, intercept of 0.010 ± 0.005 uA, standard error of 3817 uA, and a correlation coefficient of 0.99997 (N = 24). A different PAD waveform was required for each solution. In both cases, the PAD waveform which gave the maximum current for 10 uM glucose was chosen. The optimized waveform for acetate buffer was unsymmetrical in that the time allowed for oxide stripping (t_3) was greater than the time allowed for oxide formation (t_2). The effect of variations in t_2 and t_3 upon the glucose signal in acetate buffer is shown in Figure 10. Making t_2 smaller resulted in less available oxide for the generation of OH^- during the subsequent reduction step. Thus, the PAD current sensitivity for glucose decreased when t_2 was made smaller. At long t_2, the PAD current from glucose oxidation was constant independent of the value of t_3. Thus, Reaction 4 was not a significant source of OH^- at long t_2. However, at short t_2, the PAD current from glucose oxidation decreased when t_3 was made smaller. Thus, OH^- generated from Reaction 4 is significant at short t_2. From examination of Figure 10, it would appear that large values of t_2 would be desirable for the PAD waveform in dilute buffers of neutral pH. However, baseline instability was greatest for long t_2. Because of the baseline stability and reasonably high sensitivity, the optimum PAD waveform for detection of glucose in dilute buffers was chosen with t_2 = 120 msec and t_3 = 480 msec. The cause of the unstable baseline at long t_2 is not known.

In voltammetric experiments, the maximum anodic signal for 10 uM glucose in dilute acetate buffer (pH 4.8) was 250 times less than that obtained in 0.1 M NaOH. However, the PAD current sensitivity for 10 uM

Figure 10. Dependence of the PAD signal for 30 uM glucose as a function of t_3 for two values of t_2 in the waveform. Conditions: same as Figure 9A. Curves; value of t_2 (ms): (O) 120 and (●) 480

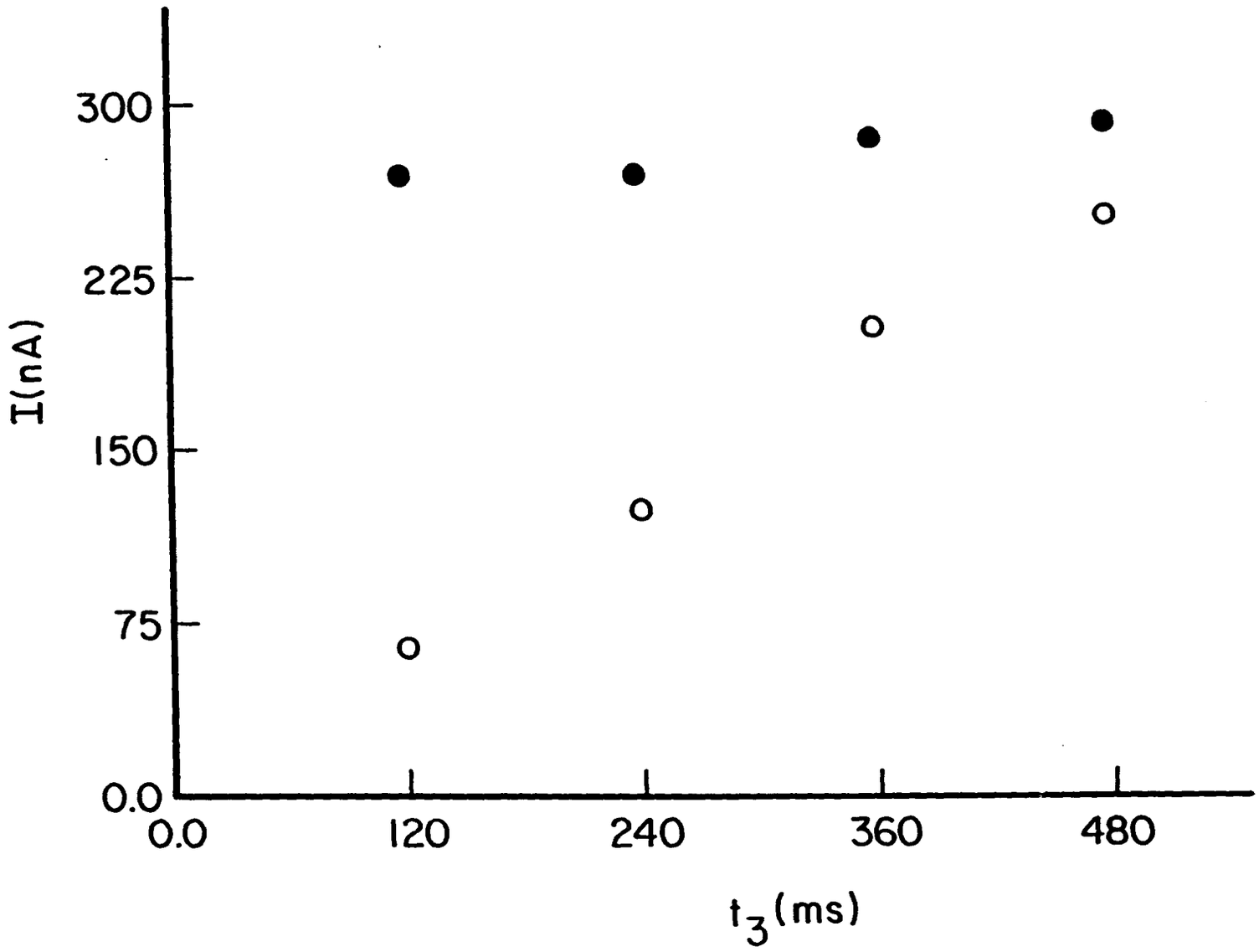
300
225
150
75
0.0
I(nA)
0.0
120
240
360
480
t_3(ms)

glucose in the equivalent acetate buffer was only 2.5 times less than the PAD sensitivity in 0.1 M NaOH. This observation of increased current sensitivity for glucose in dilute buffers for PAD as compared to voltammetric detection was the result of the very small time interval (ca. 200 msec) allowed for the OH^- generated electrochemically in PAD to be transported out of the diffusion layer prior to glucose detection. In the voltammetric experiments, the analogous time interval was ca. 5 sec. The estimated limit of detection (S/N = 3) for glucose by PAD was 2 nM in 0.1 M NaOH and 0.8 uM in dilute acetate buffer. The nonlinearity of PAD response for glucose in dilute acetate buffer, shown in Figure 9A, is the result of consumption of the transient alkalinity by the glucose oxidation reaction. The alkali generated by Reactions 3 and 4 is constant for each cycle of the PAD waveform. Thus, the increase in glucose concentration, with a concomitant increase in electrode current, results in more rapid consumption of the generated OH^- with attenuation of the specific rate of the detection reaction.

The ability to detect glucose by PAD in dilute acetate buffer is highly dependent upon buffer capacity, as was the case in voltammetric detection. The decrease in PAD current sensitivity with increase in acetate buffer concentration is shown in Table 3. The decrease in sensitivity results in higher limits of detection for glucose by PAD in more concentrated buffer solutions. The limit of detection (S/N = 3) for glucose in 10.0 mM acetate buffer was 15 uM.

Table 3. Effect of buffer concentration on glucose oxidation by PAD at a Au RDE

Buffer[a]	Buffer Concentration (mM)	PAD Current[b] Sensitivity (uA per M Glucose)
Acetate (pH 4.8)	1.0	8300
	2.0	4700
	4.0	1300
	10.0	300
	200.0	0
NaOH	100.0	30000

A_d = 0.008 cm^2, w = 94.2 rad sec^{-1}.

[a]Buffers also contained 50 mM $NaNO_3$.

[b]Sensitivity given for 30 uM glucose.

Direct Assay for Enzyme Activity by PAD

Glucoamylase catalyzes the hydrolysis of *a*-(1,4) and *a*-(1,6) glucosidic bonds of di- and oligosaccharides producing free glucose from the nonreducing end of the polymer chain (15). The activities of starch hydrolyzing enzymes (i.e., the amylases) have traditionally been determined with discontinuous assays. Examples include: saccharogenic assays wherein the enzyme reaction is followed by measuring the increase in reducing materials formed; amyloclastic assays in which the reaction is followed by measuring the decrease in starch substrate; chromolytic assays wherein the reaction is followed by measuring the release of dye-labeled products; and multi-enzyme assays in which the reaction is followed using indicator enzymes which convert the amylase products to a form that can be detected (16). All of these assays are discontinuous because the amylase reaction must be stopped prior to measuring the reaction products (or substrates). Consequently, these assays are time consuming, especially when heating and color development are involved. Also, these assays can be quite expensive when chemically derivatized substrates or multi-enzyme systems are used. There are few assays which allow the activity of amylases to be measured continuously (17,18) and these also require multi-enzyme systems or derivatized substrates. But, until now, no continuous <u>in situ</u> assay has been developed which detects directly the reaction products (or substrates) in the presence of the active enzyme.

Glucose, the product of the enzymatic hydrolysis, can be determined directly by PAD at a Au RDE in the mixture of the enzyme and its subs-

trate. A typical plot of PAD signal with time is shown in Figure 11A for a mixture of glucoamylase and corn starch at pH 4.8. The increase in PAD signal corresponds with the increase in glucose concentration resulting from glucoamylase activity. For these conditions, the rate of hydrolysis by glucoamylase is known to be constant up to 25 min. Therefore, the nonlinear increase in PAD signal is the result of a nonlinear response of PAD for glucose at this pH. Results of the calibration of PAD response for glucose are shown in Figure 11B for the buffered solution of starch containing no enzyme.

The time required for glucoamylase to produce a PAD response equivalent to 40 uM glucose was used to calculate the enzyme activity. From the results of three enzyme assays by PAD, the initial glucoamylase activity was determined to be 6670 $\pm$ 170 umoles of glucose produced per minute per gram of enzyme. This value is in good agreement with that obtained from three ferricyanide assays (6.82 $\pm$ 0.59 mmoles glucose per minute per gram enzyme). The higher standard deviation for the ferricyanide assay was the result of the multi-step procedure. Since the PAD assays were continuous, several assays could be performed in a relatively short period of time. All three assays, plus the glucose calibration of the PAD response, required only 30 min. The three ferricyanide assays required approximately 3 hr. Hence, the PAD assay for glucoamylase is concluded to be accurate, much faster, and more precise than the ferricyanide assay.

It was somewhat surprising to find that glucose could be determined in the presence of a high concentration of starch (a polymer of glucose)

Figure 11A. Starch hydrolysis by glucoamylase monitored by detection of glucose by PAD at a Au RDE in a dilute acetate buffer (pH 4.8). Conditions: same as Figure 9A except solution contained 1.0% (wt/vol) corn starch; 0.105 mg enzyme added to 50 mL solution at time = 0 min

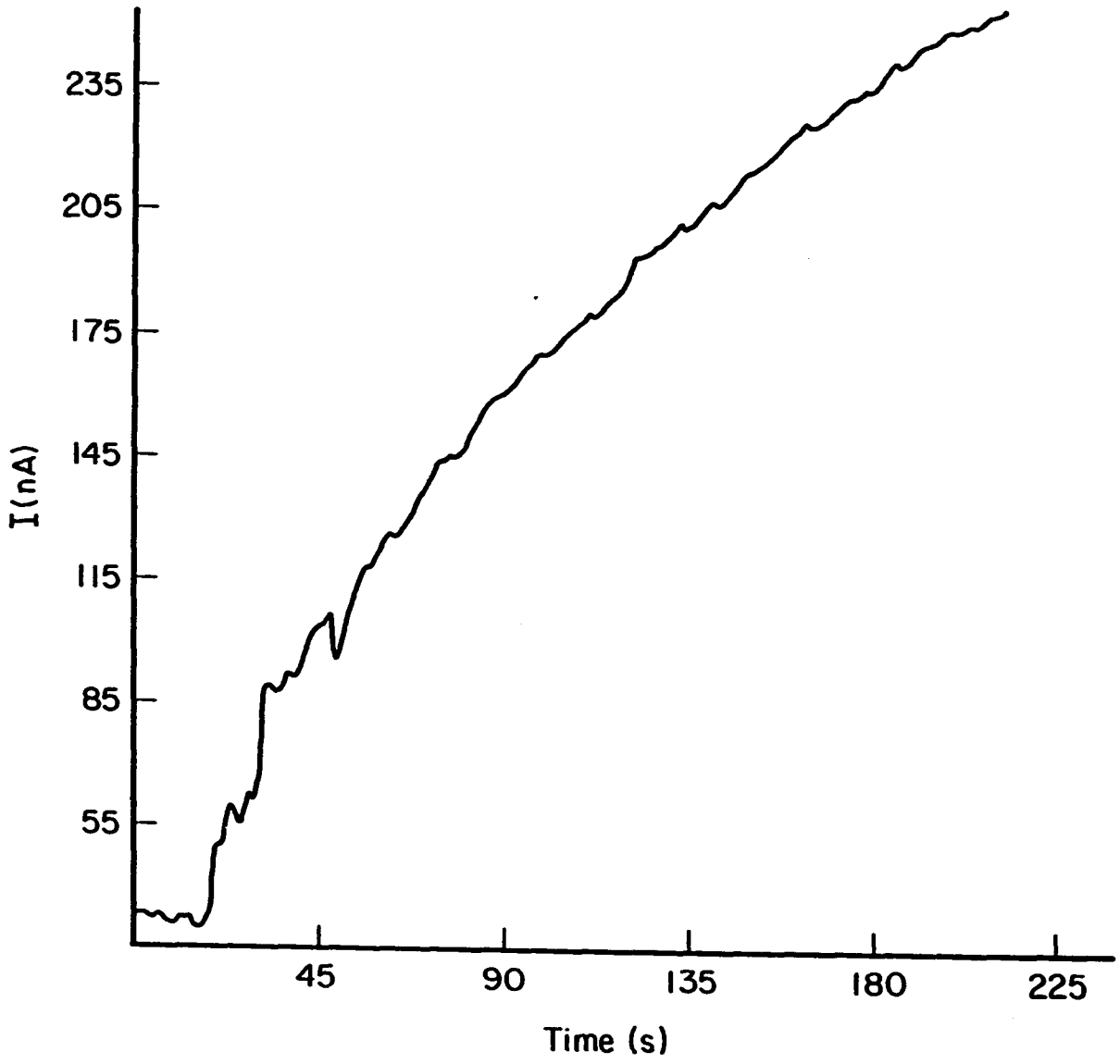
235
205
175
145
115
85
55
I(nA)
45
90
135
180
225
Time (s)

Figure 11B. Calibration of PAD response as a function of glucose concentration. Conditions: same as Figure 11A except no enzyme added to solution. Curves; glucose concentration (uM): (a) 0.0, (b) 10.0, (c) 20.0, (d) 30.0, (e) 40.0, and (f) 50.0

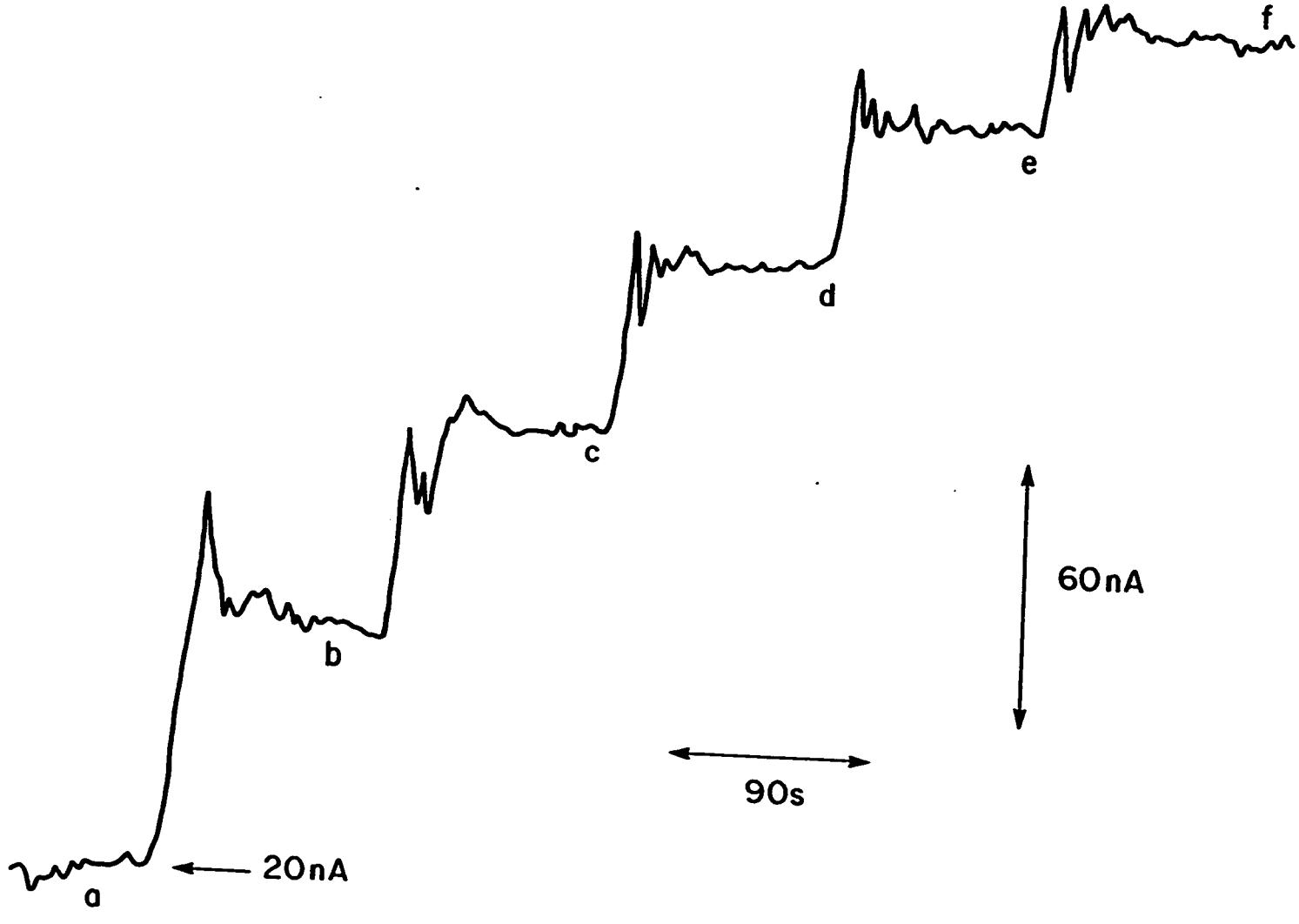
a
b
c
d
e
f
20nA
90s
60nA

with little interference from direct oxidation of starch. The PAD signal for glucose in the presence of starch was 1.8 times less than the signal in the same solution but without the starch. This is concluded to be the result of the decrease in effective electrode surface area caused by adsorption of some starch to the electrode surface. However, as shown in Figure 11B, glucose concentrations as low as 10 uM were easily detected in the presence of starch. Voltammograms obtained for the assay solution, but without the addition of the enzyme, showed no oxidation wave for starch. Therefore, the glucose units of the polymer are not accessible to the electrode surface and the smaller sensitivity was not the result of higher background current. Corn starch exists in solution as a colloidal sol (19). Starch in this state apparently does not have direct interaction with the electrode surface. It is still not explained why the presence of starch caused a decrease in the sensitivity of PAD for glucose detection. It should be noted that other soluble starches have been detected by PAD (20). Thus, the ability to oxidize starch at a Au electrode depends on the type and size distribution of the starch molecules.

It is believed that direct assays by PAD can be developed for many enzymes of clinical, biological and industrial significance which involve substrates and products that are not easily detected by UV/VIS spectrophotometry. Direct enzyme assays by PAD should be much faster, more precise and less expensive than discontinuous assays based on indicator enzymes or derivatized substrates. Work is currently in progress to develop a direct PAD assay for the clinically important human enzyme *a*-amylase.

ACKNOWLEDGMENTS

The authors thank Peter Reilly for supplying the glucoamylase. This work was supported by the National Science Foundation under Contract CHE-8612314.

REFERENCES

1. D. C. Johnson, Nature, 321 (1986), 451.
2. J. D. Olechno, S. R. Carter, W. T. Edwards and D. G. Gillen, Am. Biotech. Lab., 5 no. 5 (1987), 38.
3. D. C. Johnson and T. Z. Polta, Chromatogr. Forum, 1 (1986), 37.
4. G. G. Neuburger and D. C. Johnson, Anal. Chem., 59 (1987), 203.
5. G. G. Neuburger and D. C. Johnson, Anal. Chem., 59 (1987), 150.
6. L. A. Larew and D. C. Johnson, Anal. Chem., in press (1988).
7. J. Osteryoung and E. Kirowa-Eisner, Anal. Chem., 52 (1980), 62.
8. M. Wojciechowski and J. Osteryoung, Anal. Chem., 57 (1985), 927.
9. A. J. Bard and L. R. Faulkner, "Electrochemical Methods: Fundamentals and Applications", John Wiley & Sons, New York, 1980, chapt. 8.
10. R. C. Weast (Ed.), "CRC Handbook of Chemistry and Physics", 64th ed., CRC Press, Boca Raton, 1983, pp. F-46 and D-261.
11. B. Warshowsky and W. M. Sandstrom, Arch. Biochem. Biophys., 37, (1952), 46.
12. A. T. Kuhn and C. Y. Chan, J. Appl. Electrochem., 13 (1983), 189.
13. L. D. Burke and G. P. Hopkins, J. Appl. Electrochem., 14 (1984), 679.
14. R. W. Zurilla, R. K. Sen and E. Yeager, J. Electrochem. Soc., 125 (1978), 1103.
15. P. J. Reilly, in G. M. A. van Beynum and J. A. Roels (Eds.), "Starch Conversion Technology", Marcel Dekker, New York, 1985, chapt. 5.

16. N. W. Tietz (Ed.), "Textbook of Clinical Chemistry", W.B. Saunders Co., Philadelphia, 1986, pp. 729 - 735.

17. G. Strnad, R. Renneberg and F. Scheller, J. Electroanal. Chem., 194 (1985), 123.

18. R. Renneberg, G. Kaiser, F. Scheller and Y. Tsujisaka, Biotech. Lett., 7 (1985), 809.

19. D. French, in W. J. Whelan (Ed.), "Biochemistry of Carbohydrates", University Park Press, Baltimore, 1975, p. 299.

20. L. A. Larew, D. A. Mead, Jr. and D. C. Johnson, Anal. Chim. Acta, 204 (1988), 43.

SECTION III.

QUANTITATION OF CHROMATOGRAPHICALLY SEPARATED MALTOOLIGOSACCHARIDES WITH A SINGLE CALIBRATION CURVE USING A POST-COLUMN ENZYME REACTOR AND PULSED AMPEROMETRIC DETECTION

SUMMARY

Maltooligosaccharides were separated by anion exchange chromatography and determined with an on-line immobilized enzyme reactor followed by pulsed amperometric detection. The molar sensitivities of pulsed amperometry for maltooligosaccharides were found to increase with each additional glucose added to the polymer chain. The molar sensitivity for maltoheptaose was 2.7 times larger than that for glucose. Glucoamylase, immobilized onto porous silica and packed into a short stainless steel column, was capable of converting maltooligosaccharides nearly quantitatively (96%) to glucose. After enzymatic conversion, the peak area (coulombs) from pulsed amperometry for maltooligosaccharides was within 10% of that for the equivalent amount of glucose. The enzyme reactor with pulsed amperometric detection was coupled to an anion exchange column for the separation and determination of maltooligosaccharides found in corn syrup. A single calibration curve for glucose based on peak area was used to quantify each maltooligosaccharide. The limit of detection for maltoheptaose, after conversion to glucose, was 1.1×10^{-10} mol (50-uL sample).

INTRODUCTION

Immobilized enzyme reactors, when used in tandem with high-performance liquid chromatography (HPLC), provide increased sensitivity for selected sample components prior to their detection (1). This is made possible by the specificity that the immobilized enzyme has for its substrates (1,2). Many other advantages along with limitations of this technique have been reported recently (3).

The identification and quantitation of maltooligosaccharides are of primary importance in the food processing (4), brewing (5), and starch processing (6) industries. High-performance anion exchange chromatography, using alkaline eluents, has recently been shown to be an effective separation technique for resolving complex mixtures of monosaccharides and maltooligosaccharides (7,8). Pulsed amperometric detection (PAD) has been applied with great success to the detection of many organic compounds, including carbohydrates, which are considered to be electroinactive under conditions of dc detection (9,10). Furthermore PAD has been easily coupled to liquid chromatography for the direct detection of carbohydrates (8-11). This method of detection overcomes many of the difficulties associated with the more traditional methods of carbohydrate detection (11,12).

Glucoamylase catalyzes the hydrolysis of *a* - (1,4), *a* - (1,3) and *a* - (1,6) glucosidic bonds of di- and oligosaccharides producing free glucose from the nonreducing end of the polymer chain (13). Glucoamylase immobilized reactors of large capacity have been used for the continuous conversion of starch to glucose in the starch processing industry (4, 14).

Recently, we reported the use of an immobilized glucoamylase reactor coupled to PAD for the determination of starch and total carbohydrate in beer (15).

Here we describe an immobilized glucoamylase reactor used in tandem with high performance anion exchange chromatography and PAD for the quantitation of eight maltooligosaccharides using only the single calibration curve for glucose.

MATERIALS AND METHODS

Apparatus

Schematic diagrams of the two chromatographic configurations used in this work are shown in Figure 1. The chromatographic system consisted of a gradient liquid chromatograph (Beckman, Model 344; Berkeley, CA), two solvent delivery systems (Rainin, Rabbit-HP; Woburn, MA), an injection valve equipped with a 50-uL sample loop (Rheodyne, Model 7010; Cotati, CA), a 10-uL solvent mixer (The Lee Company, Visco Mixer; Westbrook, CT), a guard column (Dionex, AG6A; Sunnyvale, CA), an anion-exchange column (Dionex, AS6A), a string-bead mixer (Dionex), and a potentiostat with a flow-through detector cell (Dionex, Model PAD-2). The flow-through cell was equipped with a gold working electrode and a glassy carbon counter electrode. The Ag/AgCl reference electrode was replaced with a saturated calomel reference electrode (SCE). Data were collected and processed with an Apple IIe computer and ADALAB interface (Interactive Microware; State College, PA). A circulating water bath (Lauda, Model K-2/RD from Brinkman; Westbury, NY) was used for temperature control.

Reagents

Glucoamylase (EC 3.2.1.3, *a* -(1,4) glucan glucohydrolase, ex. Aspergillus niger) was from Novo Industri (Bagsvaerd, Denmark). Glucose was from Fisher Scientific (Fair Lawn, NJ). Maltotriose and 1,1'-carbonyldiimidazole were from Aldrich Chemical Company (Milwaukee, WI). Maltose, maltotetraose, maltopentaose, maltohexaose, maltoheptaose and corn syrup maltooligosaccharides were from Sigma Chemical Company (St. Louis, MO). *g*-Glycidoxypropyltrimethoxysilane was from Petrarch (Bristol, PA).

Figure 1A. Schematic diagram of the system used to determine the enzyme reactor efficiency

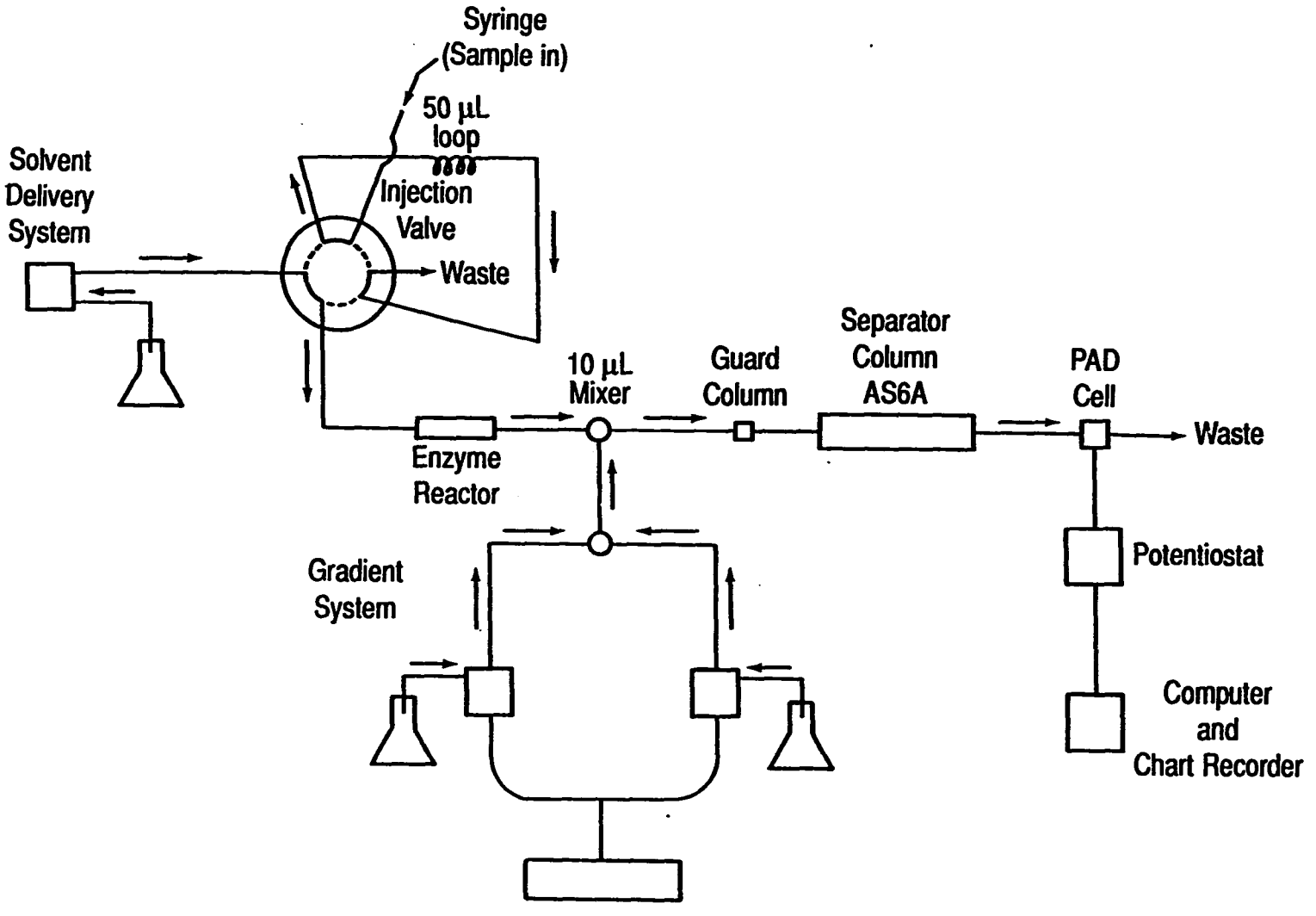
Syringe
(Sample in)
50 µL
loop
Solvent
Delivery
System
Injection
Valve
Waste
10 µL
Mixer
Guard
Column
Separator
Column
AS6A
PAD
Cell
Waste
Enzyme
Reactor
Gradient
System
Potentiostat
Computer
and
Chart Recorder

Figure 1B. Schematic diagram of the system used to quantify malto-oligosaccharides

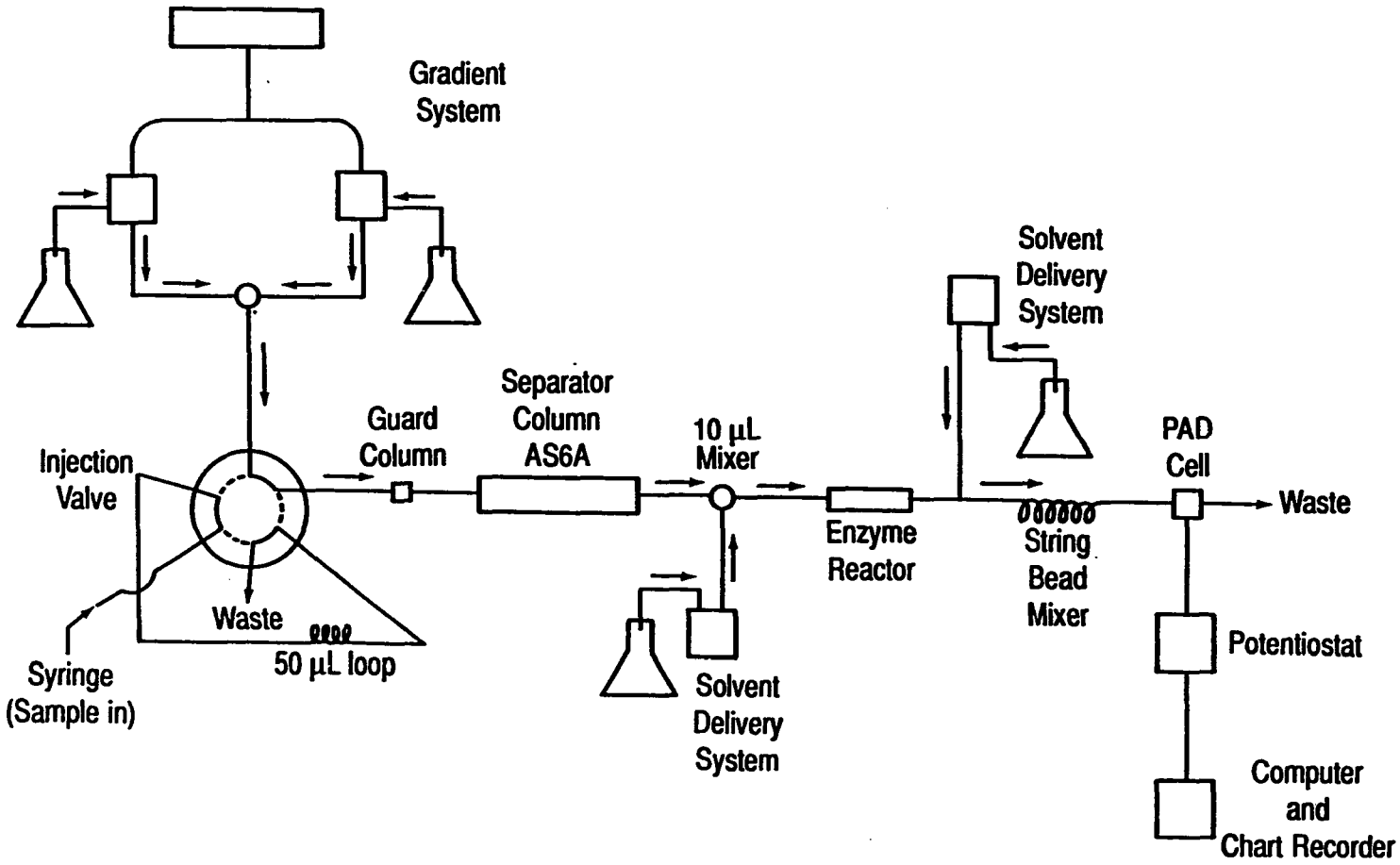
Gradient System
Solvent Delivery System
Separator Column AS6A
Guard Column
10 µL Mixer
PAD Cell
Injection Valve
Waste
Enzyme Reactor
String Bead Mixer
Waste
50 µL loop
Syringe (Sample in)
Solvent Delivery System
Potentiostat
Computer and Chart Recorder

Nucleosil 300 (10 um diameter) was from Alltech (Deerfield, IL). All other chemicals were reagent grade. Water was condensed from steam and purified further by a Milli-Q system (Millipore; Bedford, MA).

Procedures

Preparation of Enzyme Reactor

Glucoamylase was immobilized onto the Nucleosil support following the procedure of Crowley et al. (16). The enzyme was first dissolved at a concentration of 50 mg mL^{-1} in 0.2 M sodium acetate buffer (pH 4.8). A 10 mL aliquot of this solution was added to 1.0 g of activated support and shaken for 6 days at 4.0° C. The enzyme-linked support was then washed by centrifugation with 2 M NaCl, followed by acetate buffer, and stored under refrigeration in the buffer.

The immobilized glucoamylase reactor was prepared by vacuum slurry-packing (17) the enzyme-linked support into a 2.5 cm x 2.1 mm i.d. column. The column was of a published design with the outer connector modified as a water jacket (18).

Determination of Reactor Efficiency

A schematic diagram of the chromatographic system used to determine the immobilized enzyme reactor efficiency is shown in Fig. 1A. Standard maltooligosaccharides were dissolved in 0.2 M sodium acetate buffer (pH 4.8) and injected into the immobilized enzyme reactor at the following concentrations: 90 uM maltose, 113 uM maltotriose, 98 uM maltotetraose, 91 uM maltopentaose, 105 uM maltohexaose, and 97 uM maltoheptaose. The immobilized enzyme reactor was continuously eluted with 0.05 M acetate buffer (pH 4.5) at a flow rate of 0.5 mL min^{-1}. The eluate from the en-

zyme reactor was mixed with the chromatographic eluent at the 10 uL Visco mixer. The total flow rate through the chromatographic column was 1.0 mL min^{-1}. The chromatographic column was eluted with a linear gradient from 0.1 M NaOH plus 0.025 M sodium acetate to 0.1 M NaOH plus 0.525 M sodium acetate in 15 min. The maltooligosaccharides were injected into the immobilized enzyme reactor 1.5 min after the start of the gradient. The enzyme reactor temperature was held constant at 50° C. All eluents were prepared with water free of carbonates and stored under helium. The PAD cell was operated under the following conditions (all potentials versus SCE): detection at 150 mV with a sampling time of 200 ms at the end of a 420 ms period, oxidative cleaning at 750 mV for 120 ms, and oxide reduction at -1.0 V for 120 ms. The detector output was filtered with a 3.0 s time constant to suppress noise.

Determination of Corn Syrup Maltooligosaccharides

The chromatographic system used to determine the maltooligosaccharides from corn syrup is shown in Fig. 1B. The samples analyzed contained 70 ug mL^{-1} and 490 ug mL^{-1} corn syrup maltooligosaccharide in 0.2 M sodium acetate buffer (pH 4.8). The more concentrated sample was used for the determination of glucose and maltose. The samples were injected into the chromatographic column at a flow rate of 0.5 mL min^{-1} in 0.1 M NaOH plus 0.06 M sodium acetate. Following a two minute hold at this eluent concentration, the samples were eluted from the chromatographic column with a linear gradient to 0.1 M NaOH plus 0.36 M sodium acetate in 50 minutes. The eluate from the chromatographic column was mixed with 2.0 M sodium acetate buffer (pH 4.5) in the 10 uL Visco mixer prior to elution through

the enzyme reactor. The total flow rate through the reactor was 0.7 mL min^{-1}. The eluate from the enzyme reactor was combined with 0.35 M NaOH at a 3-way valve and mixed with a string-bead mixing tube prior to the detector cell. The total flow rate through the detector cell was 1.7 mL min^{-1}. Peak areas were measured by computer integration. The system response was calibrated with standards containing 300, 250, 200, 150, 94, 71, 47, 31, and 24 uM glucose. The immobilized enzyme reactor was thermostated at 50° C and the PAD cell was operated at the same conditions as those given above.

Determination of PAD Sensitivity for Maltooligosaccharides

The sensitivity of PAD for maltooligosaccharides with and without the enzyme reactor was determined using the system shown in Fig. 1A with the following modifications: the guard and chromatographic columns were removed, the enzyme reactor was eluted with 0.2 M sodium acetate buffer (pH 4.8) at a flow rate of 0.7 mL min^{-1}, the eluate from the enzyme reactor was mixed with 0.35 M NaOH at the Visco mixer, the string-bead mixing tube was inserted between the Visco mixer and the detector cell, and the total flow rate through the detector cell was 1.7 mL min^{-1}. Carbohydrate standards were injected at the following concentrations: 94 uM glucose, 45 uM maltose, 30 uM maltotriose, 25 uM maltotetraose, 18 uM maltopentaose, 18 uM maltohexaose, and 14 uM maltoheptaose.

Determination of Enzyme Activity

The system used to determine glucoamylase activity is shown in Fig. 2. The reaction flask contained 500 mL of 1.0% (wt/vol) soluble starch and 0.2 M sodium acetate (pH 4.8) at 25° C. The flask solution was

Figure 2. Schematic diagram of the system used to determine glucoamylase activity

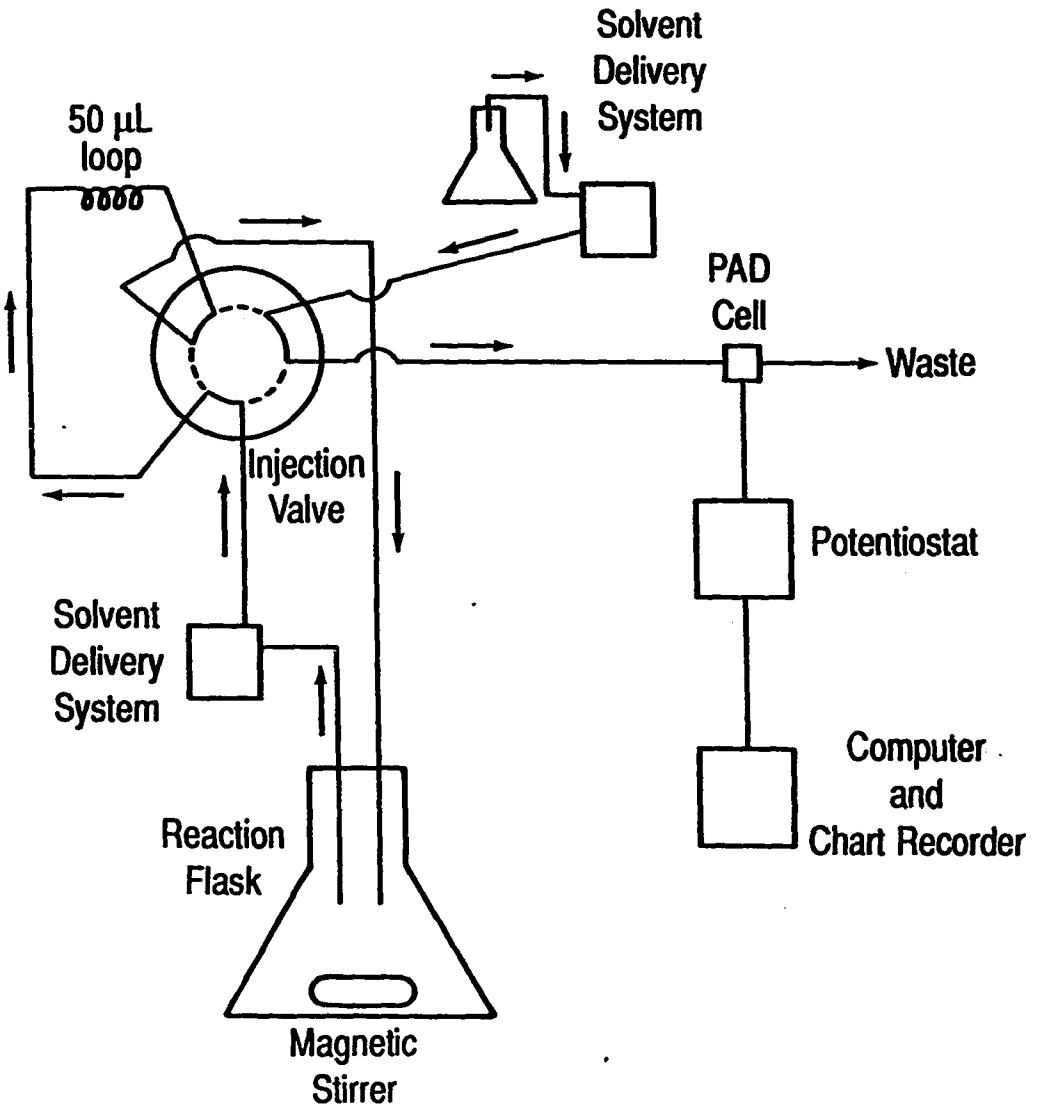
Solvent
Delivery
System
50 µL
loop
PAD
Cell
Waste
Injection
Valve
Potentiostat
Solvent
Delivery
System
Computer
and
Chart Recorder
Reaction
Flask
Magnetic
Stirrer

continuously mixed by magnetic stirring (100 rev min^{-1}) and pumped through the injection loop at a flow rate of 2.0 mL min^{-1}. The loop contents were injected into a stream of 0.2 M NaOH flowing at 1.0 mL min^{-1} and detected at the PAD cell using the same conditions as those given above. The background peak current from the flask contents was determined prior to addition of enzyme. The system response to glucose was determined by adding 20 umoles of standard glucose. Glucoamylase (1.5 mg) was added to the flask and the increase in peak current with increase in time was observed. To determine the activity of immobilized glucoamylase, the experiment was repeated with the addition of 70 mg of enzyme-linked silica to the reaction flask. A porous frit attached to the inlet tube prevented silica from entering the pump.

RESULTS AND DISCUSSION

Enzyme Immobilization

The effectiveness of the enzyme immobilization procedure was evaluated by comparing the rates of glucose production by both free and immobilized glucoamylase. For a well-stirred mixture, a steady-state condition exists and the plot versus time of the concentration of glucose generated is expected to be linear with a zero intercept and a slope which is equivalent to the initial rate of glucose production. Experimental plots were linear with virtually zero intercepts for both the free and immobilized enzyme. For six measurements made for the free enzyme over the period 0 - 20 min, the linear regression statistics were: slope = 16.2 $\pm$ 0.3 uM min^{-1}, intercept = -4.6 $\pm$ 3.8 uM, standard error = 3820 uM, and correlation coefficient (r) = 0.99924. For six measurements made for the immobilized enzyme over the period 0 - 15 min, the regression statistics were: slope = 27.1 $\pm$ 0.7 uM min^{-1}, intercept = - 4.1 $\pm$ 6.0 uM, standard error = 3510 uM, and correlation coefficient (r) = 0.99859. Uncertainties given represent one standard deviation. As determined by a BCA protein assay (16), 59 mg of glucoamylase were immobilized per 1.0 g of support. Therefore, of the 4.1 mg of immobilized glucoamylase added to the reaction flask, 2.5 mg maintained its original activity.

Sensitivity of PAD

Immobilized glucoamylase has its maximum activity at pH 4.5 - 5.0 (19). Working under conditions of maximum enzyme activity was desired so that the conversion of maltooligosaccharide to glucose would be rapid

and complete. PAD has its greatest sensitivity for glucose at alkaline pH (11). Thus, NaOH was added to the enzyme reactor effluent prior to the PAD cell to increase the pH sufficiently for the sensitive detection of carbohydrate. Because of the large difference in pH between these two solutions, the eluent mixing systems had to be good enough to provide uniform mixing and, thus, prevent air bubble formation which would have caused an unstable baseline current to be produced in the detector cell. The mixing systems also had to have small dead volumes to minimize the extra-column band spreading. Furthermore, immobilized glucoamylase has its maximum activity at temperatures between 50^{o} and 55^{o} C (19). Hence, the enzyme reactor temperature was thermostated at 50^{o} C.

The molar and weight sensitivities of PAD determined without the immobilized enzyme reactor are shown in Fig. 3 for glucose and each of the six standard maltooligosaccharides. Each experimental point represents the average of three determinations. The molar and weight sensitivities were calculated for each carbohydrate by dividing the peak area (uCoul) by the concentration or mass of carbohydrate, respectively, in the sample injected. The abscissa in Figure 3 designates the degree of polymerization (DP). Accordingly, DP1 is glucose, DP2 is maltose, DP3 is maltotriose, DP4 is maltotetraose, etc. As shown in Figure 3, the molar sensitivity increases with increasing value of DP. It is concluded that this increase is the result of an increasing value of n (equiv mol^{-1}) for the detection process. However, the increase in n for each unit change in DP should not be calculated literally from the molar sensitivities shown in Figure 3 without accounting for decreases in the

Figure 3. Molar sensitivities (●) and weight sensitivities (O) of PAD for glucose and glucose polymers without elution through the enzyme reactor

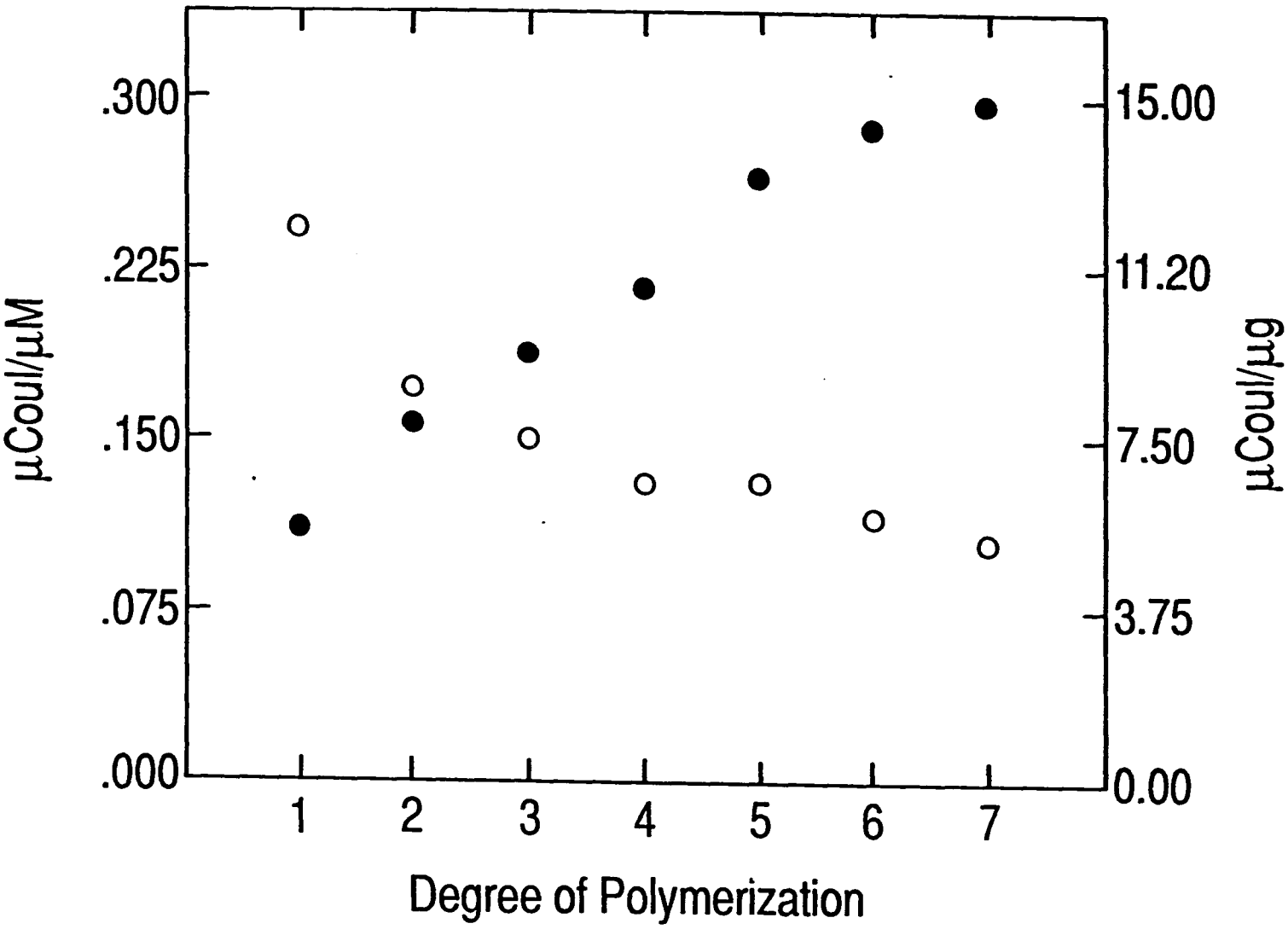
.300
.225
.150
.075
.000
μCoul/μM
15.00
11.20
7.50
3.75
0.00
μCoul/μg
1
2
3
4
5
6
7
Degree of Polymerization

mass transport rate which result from decreasing values of diffusion coefficient as DP is increased (20). The molar sensitivity (Figure 3) did not increase as a linear function of DP; hence, the weight sensitivity was observed to decrease with increases in DP value, as is shown also in Figure 3.

The molar and weight sensitivities are shown in Figure 4 for glucose and each of the six standard maltooligosaccharides as determined by PAD following conversion by passage through the immobilized enzyme reactor. The value of molar sensitivity given for each carbohydrate is a normalized value calculated by dividing the detection peak area (uCoul) by the product of the concentration and the corresponding DP value. The weight sensitivity was calculated by dividing peak area by the mass of carbohydrate injected. The DP value was not involved in calculations of weight sensitivity since, theoretically, one gram of maltooligosaccharide is converted to ca. one gram of glucose regardless of the DP value. The sensitivity values for all maltooligosaccharides tested were within the range 90 - 110% of the theoretical values for the equivalent amounts of glucose. On this basis, we conclude that the quantitation of maltooligosaccharides, using the single calibration curve for glucose, is satisfactory when based on conversion in the enzymatic reactor followed by pulsed amperometric detection.

It must be emphasized that for the chromatographic determinations of maltooligosaccharides using enzymatic conversion to glucose, quantitation based on the single glucose calibration curve is to be considered valid only when peak areas (charge) are used rather than peak

Figure 4. Molar (●) and weight (O) sensitivities of PAD for glucose and glucose polymers after elution through the enzyme reactor

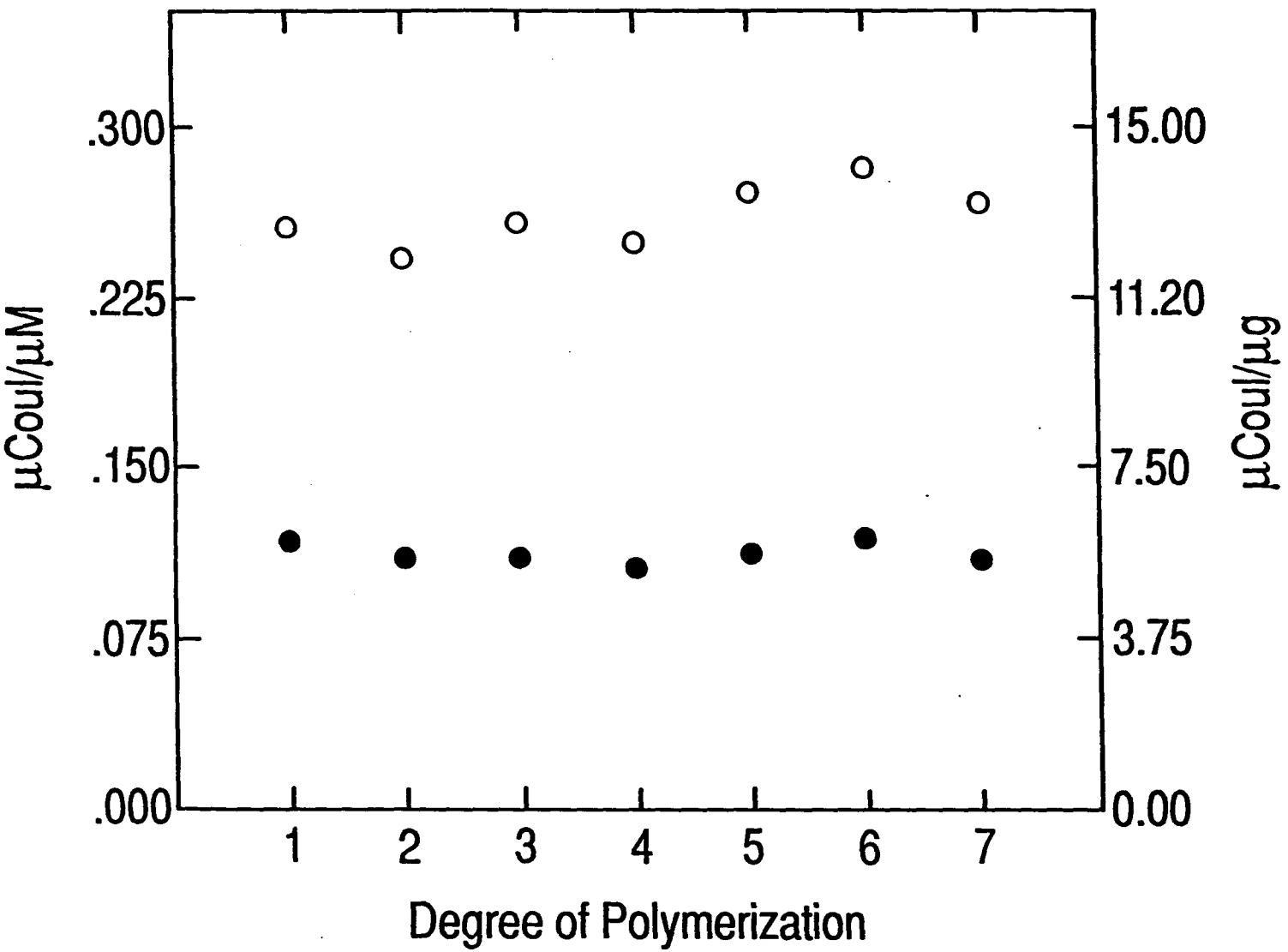
.300
.225
.150
.075
.000
μCoul/μM
15.00
11.20
7.50
3.75
0.00
μCoul/μg
1
2
3
4
5
6
7
Degree of Polymerization

height (current). Peak areas are independent of the extent of peak dispersion which occurs within the separator and reactor columns. Conversely, peak height is a sensitive function of peak dispersion and use of the single calibration curve applied to peak heights would require the normalization of current values by the dispersion coefficient for each peak.

Reactor Efficiency

A chromatogram showing the separation of glucose and the six standard maltooligosaccharides without elution through the enzyme reactor is shown in Fig. 5A. To determine the efficiency of glucose production from maltooligosaccharides by the enzyme reactor, the mixture of maltooligosaccharides was first eluted through the enzyme reactor and then through the anion exchange column to separate any unconverted maltooligosaccharides from the glucose produced. The resulting chromatogram is shown in Fig. 5B. By comparing the two chromatograms, it was concluded that maltotetraose, maltopentaose, maltohexaose and maltoheptaose were virtually quantitatively converted to glucose with a small amount of maltotriose or maltose being produced also. This is consistent with the known rates of glucoamylase hydrolysis of maltooligosaccharides (13), the rates of hydrolysis being faster for the larger maltooligosaccharides. The extent of hydrolysis of maltose and maltotriose, however, could not be estimated by comparing these two chromatograms. The small shoulder on the maltotriose peak shown in Fig. 5A is believed to be a triose impurity, perhaps panose or isopanose, which also would be hydrolyzed by glucoamylase.

Figure 5A. Chromatogram of glucose and glucose polymers without elution through the enzyme reactor prior to separation. Peaks: G1, glucose (61 uM); G2, maltose (55 uM); G3, maltotriose (58 uM); G4, maltotetraose (45 uM); G5, maltopentaose (65 uM); G6, maltohexaose (70 uM); G7, maltoheptaose (75 uM)

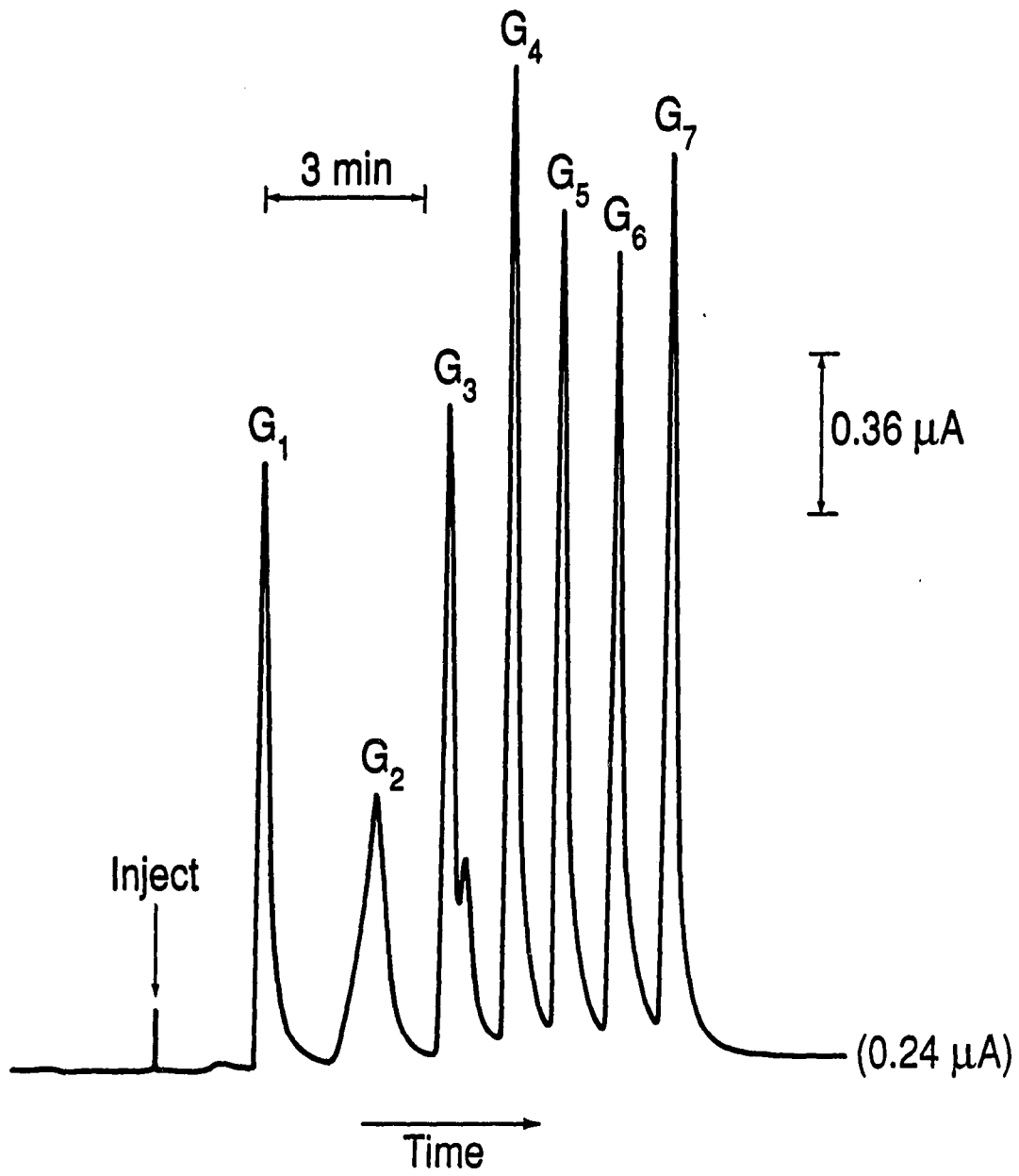
G4
G7
3 min
G5
G6
G3
G1
0.36 µA
G2
Inject
(0.24 µA)
Time

Figure 5B. Chromatogram of glucose and glucose polymers with elution through the enzyme reactor prior to separation. Peaks: G1, glucose; G2 maltose; G3, maltotriose

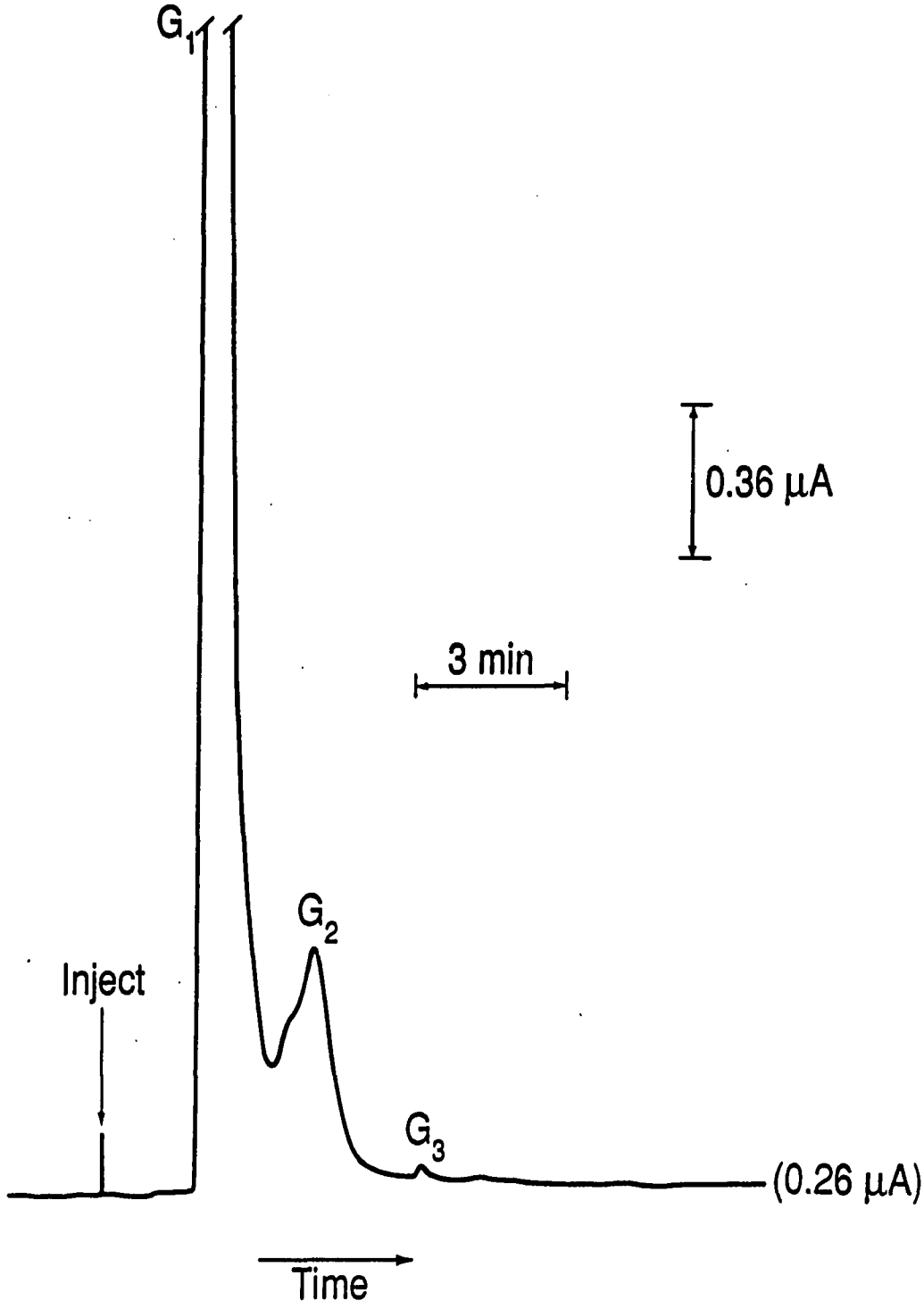
G1
0.36 μA
3 min
G2
Inject
G3
(0.26 μA)
Time

To determine the exact extent of hydrolysis for each maltooligosaccharide, the maltooligosaccharides were eluted individually through the enzyme reactor followed by the separator column. To illustrate, a chromatogram of standard maltohexaose without elution through the enzyme reactor is shown in Fig. 6A. The purity of the maltohexaose standard was quite good; only a small amount of maltopentaose appeared in the chromatogram. A chromatogram of the same sample, under identical conditions, but eluted through the enzyme reactor prior to the separator column is shown in Fig. 6B. By comparison of these two chromatograms, it is concluded that the conversion of maltohexaose to glucose was nearly complete and only a small amount of maltose was produced. Such comparisons were repeated for each of the maltooligosaccharides and the amount of maltose and maltotriose produced was determined from the system response to standard maltose and maltotriose as determined without elution through the immobilized enzyme reactor. The results are shown in Table 1. As can be seen in Table 1, the conversion of the maltooligosaccharides to glucose was within 4% of completion for maltotetraose, maltopentaose, maltohexaose and maltoheptaose. Maltotriose and maltose were converted to glucose within 7% and 13% of completion, respectively. Again, since the residence time in the enzyme reactor was the same for each maltooligosaccharide, the percent converted to glucose is consistent with the known rates of glucoamylase hydrolysis of maltooligosaccharides.

Figure 6A. Chromatogram of standard maltohexaose without elution through the enzyme reactor prior to separation. Peaks: G5, maltopentaose; G6, maltohexaose

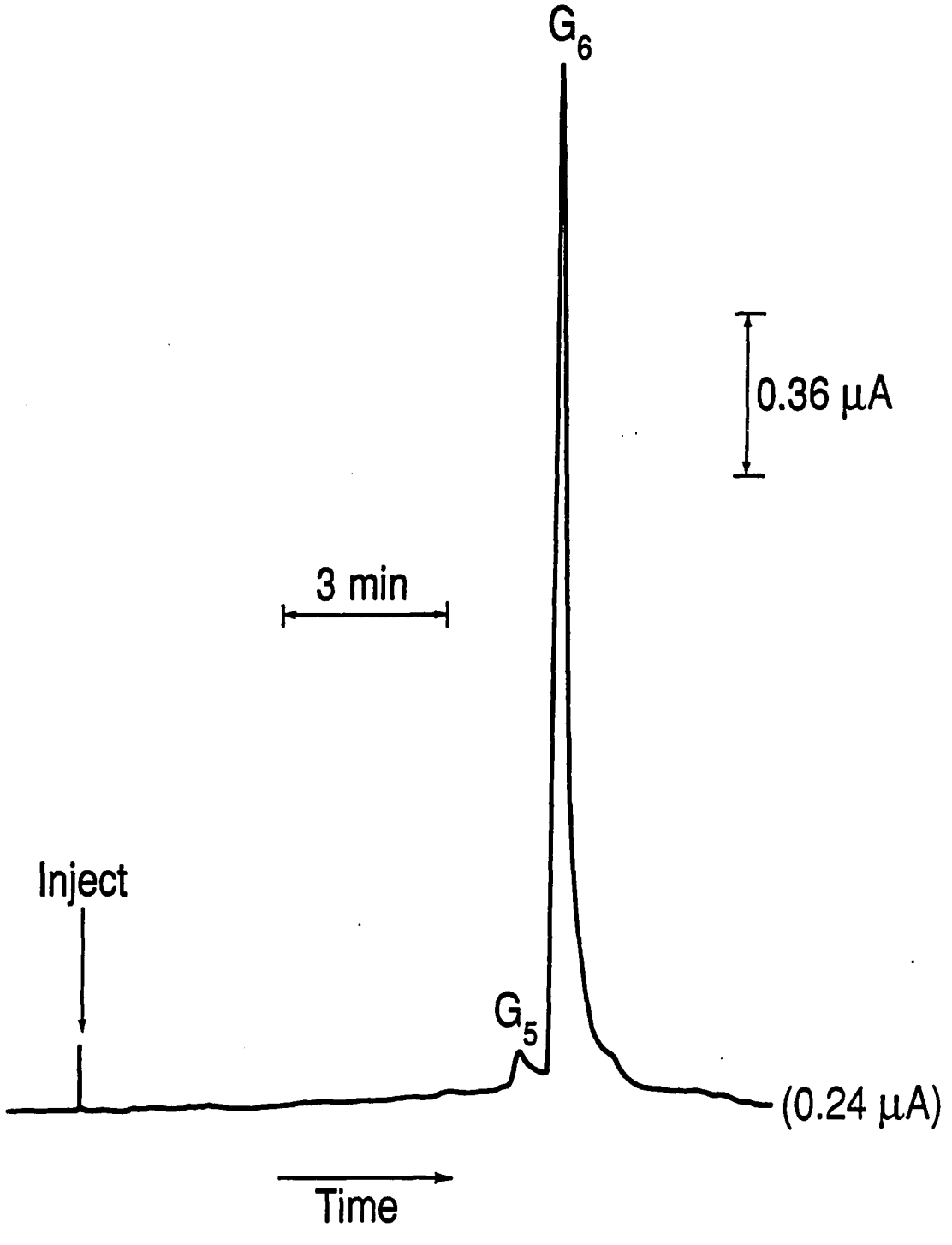
G6
0.36 µA
3 min
Inject
G5
(0.24 µA)
Time

Figure 6B. Chromatogram of standard maltohexaose with elution through the enzyme reactor prior to separation. Peaks: G1, glucose; G2, maltose

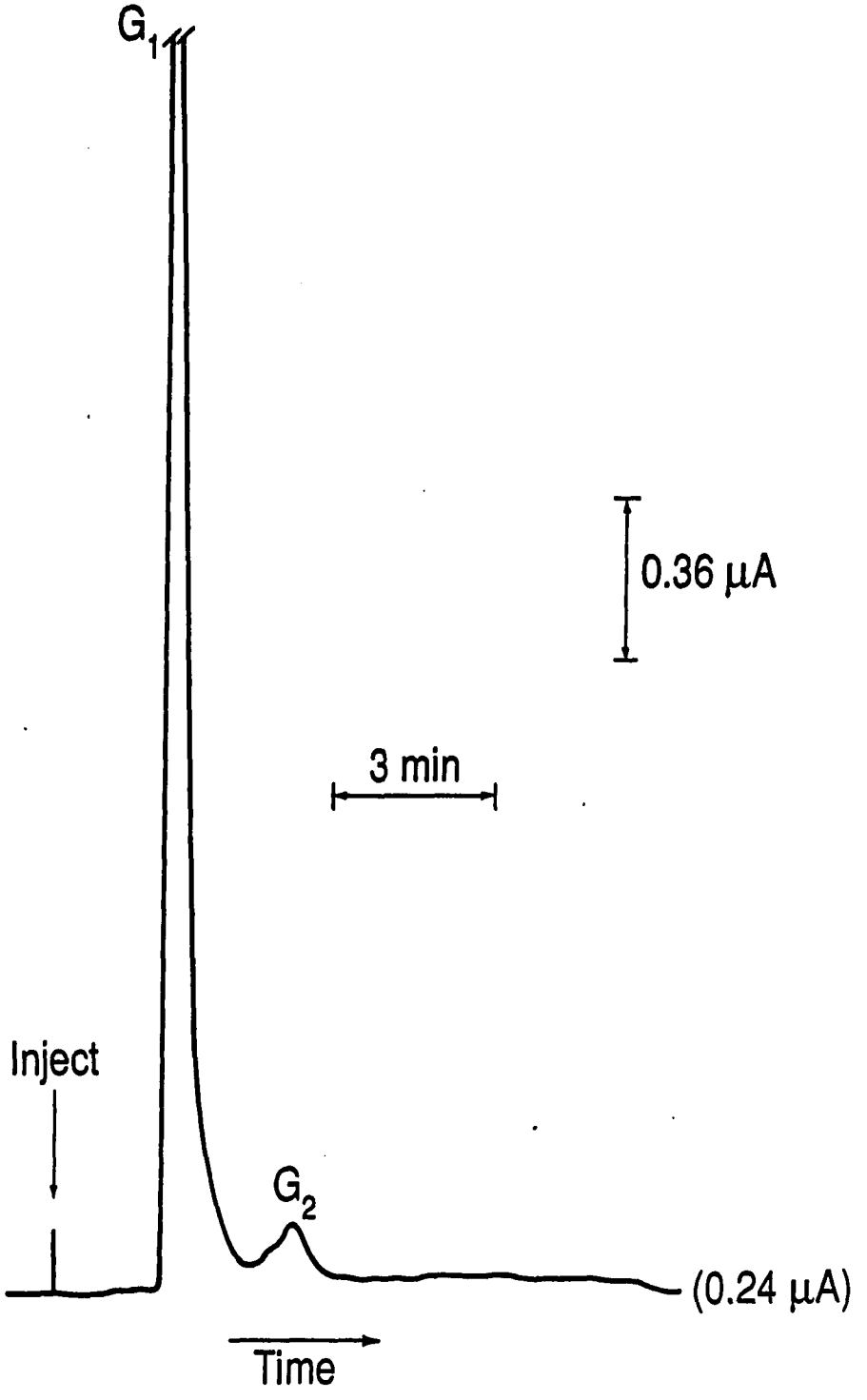
G1
0.36 μA
3 min
Inject
G2
(0.24 μA)
Time

Table 1. Efficiency of hydrolysis of maltooligosaccharides by immobilized glucoamylase reactor

Maltooligosaccharide degree of polymerization	Molar percent converted to: maltotriose	maltose	glucose
2	---	13	87
3	2	5	93
4	---	4	96
5	---	4	96
6	---	4	96
7	---	4	96

Quantitation of Maltooligosaccharides

The post-chromatographic conversion of maltooligosaccharides to glucose by the enzyme reactor required that the chromatographic eluate be brought into the pH range necessary for maximum glucoamylase activity. To do this, an additional solvent pump and mixer were added to the system. Sodium acetate buffer (pH 4.5) was mixed with the chromatographic eluate at a mole ratio of 8 to 1 prior to the enzyme reactor. This produced an eluent pH of 5.0 and maintained maximum enzyme activity in the reactor.

A chromatogram showing the separation of glucose and the six standard maltooligosaccharides using the system described for the quantitation of maltooligosaccharides, but without elution through the enzyme reactor, is shown in Fig. 7A. The two minute holding period after sample injection and before the start of the gradient caused the glucose and maltose peaks to elute isocratically. This caused the maltose peak to be very flat and broad. But, the two minute hold was necessary for the baseline resolution of the larger malto-oligosaccharides. The estimated limit of detection (S/N = 3) for glucose was 15 uM. This is 30 times larger than the previous limit of detection reported for glucose using anion exchange chromatography with PAD (21). Because the system described here required the addition of two solvent pumps, two mixing systems and an immobilized enzyme reactor, a significantly higher limit of detection for glucose was expected due to additional extra-column band spreading and additional "pump noise" caused by the mixing of solutions with large differences in pH.

Figure 7A. Chromatogram of glucose and glucose polymers without elution through the enzyme reactor after separation. Peaks: G1, glucose (61 uM); G2, maltose (22 uM); G3, maltotriose (24 uM); G4, maltotetraose (28 uM); G5, maltopentaose (25 uM); G6, maltohexaose (24 uM); G7, maltoheptaose (31 uM)

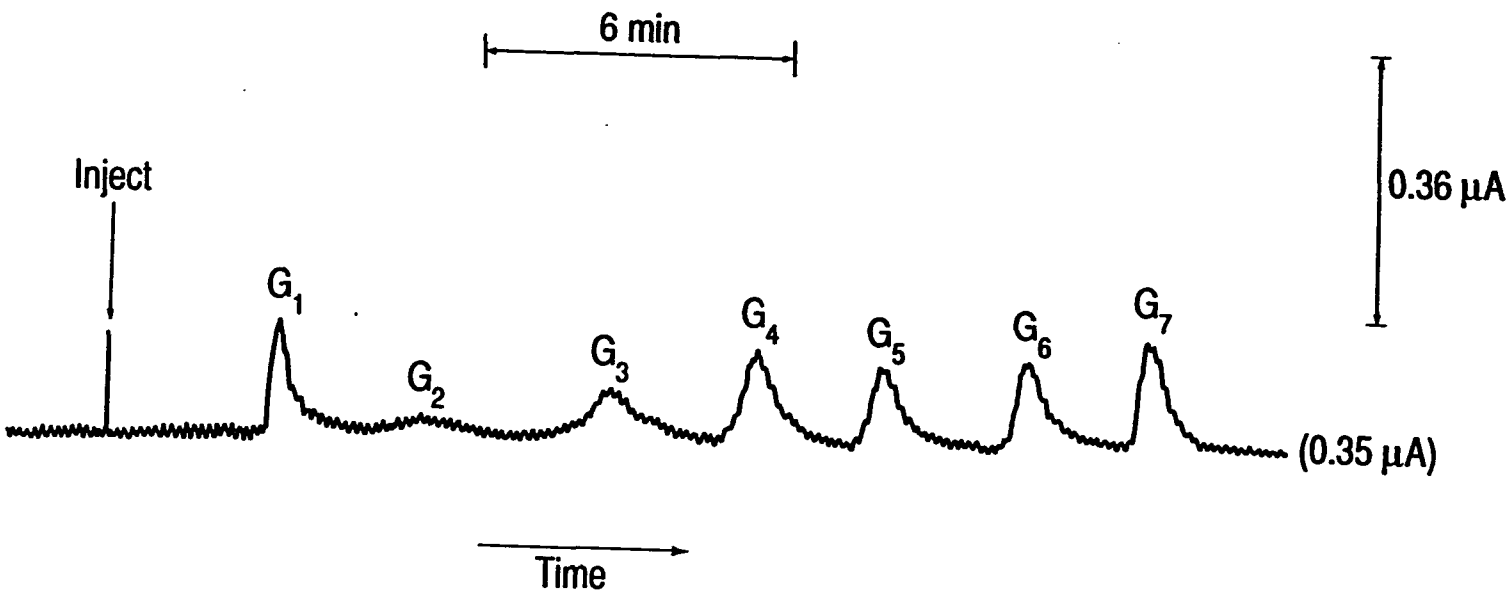
6 min
Inject
0.36 µA
G1
G2
G3
G4
G5
G6
G7
(0.35 µA)
Time

A chromatogram for the same sample separated under identical conditions but eluted through the enzyme reactor is shown in Fig. 7B. The large increases in the maltooligosaccharide peak areas were the result of their conversion to glucose by the enzyme reactor. Since the conversion to glucose is known to be nearly quantitative, the 1.6 nmoles of maltoheptaose injected were converted to 11 nmoles of glucose. Whereas this represents a seven-fold increase in molar concentration, the peak area increased only by a factor of 2.2. This is in approximate agreement with the observation in Figure 3 that the molar sensitivity for maltoheptaose was 2.7 times larger than that for glucose.

Although desirable, it is not necessary that calibration curves be linear for precise and accurate quantitative analytical work. The calibration curve based on peak area was carefully determined for PAD applied to glucose in the concentration range 25 - 300 uM. The curve was linear in the range 0 - 150 uM as described by the following linear regression statistics: for 18 measurements, slope = 0.11 $\pm$ 0.0012 uCoul uM^{-1}, intercept = 0.00014 $\pm$ 0.14 uCoul, standard error = 1227 uCoul, and correlation coefficient (r) = 0.99977. The uncertainties given correspond to one standard deviation. Negative deviation from linearity occurred for concentrations above 150 uM which is explained tentatively as the result of electrode fouling caused by adsorbed detection products (12). It should be noted that in the study of PAD sensitivity versus DP value of the maltooligosaccharides, the concentration values were chosen to be within the linear range of response both before and after enzymatic conversion. Likewise, in studies of enzyme reactor efficiency,

Figure 7B. Chromatogram of glucose and glucose polymers with elution through the enzyme reactor after separation. Peaks: G1, glucose; G2, maltose; G3, maltotriose; G4, maltotetraose; G5, maltopentaose; G6, maltohexaose; G7, maltoheptaose

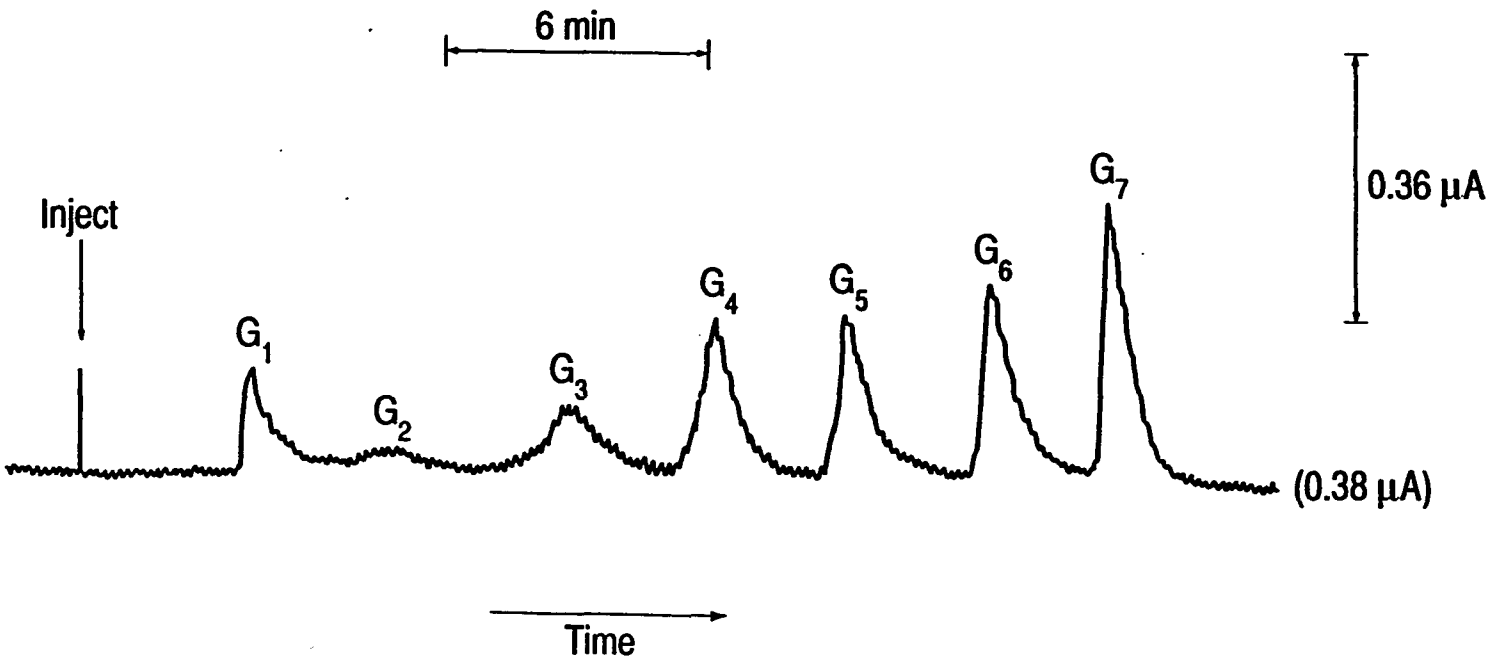
6 min
0.36 µA
Inject
G1
G2
G3
G4
G5
G6
G7
(0.38 µA)
Time

the resulting maltose and maltotriose concentrations also were within the linear range of response.

To test the accuracy of using a single glucose calibration curve to quantify the chromatographically separated maltooligosaccharides which are converted in the enzymatic reactor following separation, the actual concentrations of the maltooligosaccharides shown in Figure 7B were compared to the concentrations calculated from the plot of glucose concentration versus peak area. As shown in Table 2, the relative accuracy of the method ranged from 0.31 for maltotriose to -0.04 for maltopentaose. The deviations in the calculated concentrations from the known concentrations can be attributed to several factors. First, the relatively large peak dispersions, as well as the baseline fluctuations which resulted from the mixing of solutions with large differences in pH, made it difficult to accurately measure peak areas, particularly for maltose and maltotriose. Second, conversion of the maltooligosaccharides to glucose was assumed to be complete and was not corrected for the known conversion efficiencies given in Table 1. When the peak areas were corrected for the differences in the conversion efficiencies and molar sensitivities, the relative accuracies were calculated to be as follows: maltose, 0.00; maltotriose, 0.22; maltotetraose, 0.09; maltopentaose, -0.07; maltohexaose, -0.10; maltoheptaose, 0.04. Standard maltooligosaccharides with DP > 7 (maltoheptaose) are not readily available from chemical sources. Also, pure standards for DP4-7 are quite expensive. In view of these factors, we conclude that the method described here represents a significant improvement in accuracy

Table 2. Accuracy of using a single glucose calibration curve to quantify chromatographically separated maltooligosaccharides eluted through a glucoamylase reactor prior to their detection

Carbohydrate	(A)[a] True Concentration After Conversion (uM)	(B)[b] Apparent Concentration (uM)	Relative Accuracy [(B)-(A)]/(A)
glucose	61	60	-0.02
maltose	44	45	0.02
maltotriose	72	94	0.31
maltotetraose	112	124	0.11
maltopentaose	125	120	-0.04
maltohexaose	144	131	-0.09
maltoheptaose	217	233	0.07

[a]Assuming 100% conversion to glucose by the immobilized enzyme reactor, e.g., 31 uM maltoheptaose hydrolyzed to 217 uM glucose.

[b]Calculated from the areas of the peaks shown in Fig. 7B using a calibration plot of glucose concentration versus glucose peak area.

and economy for quantifying maltooligosaccharides present in mixtures, e. g., corn syrups, dextrins, etc.

Recently it was reported that the PAD signal per carbohydrate molecule for the series of sugars from glucose through maltopentaose was the same (8). However, no results supporting that statement were given. As shown in Figure 3, the PAD signal per carbohydrate molecule is not the same. The glucose calibration plot was used to directly quantify the chromatographically separated maltooligosaccharides shown in Figure 7A assuming equivalent peak area sensitivities of PAD for each carbohydrate. The relative accuracies obtained were quite poor: maltose, 0.8; maltotriose, 2.0; maltotetraose, 1.9; maltopentaose, 1.5; maltohexaose, 1.8; maltoheptaose, 1.9. The apparent concentrations were all much larger than the true concentrations due to the increase in molar sensitivity with increase in degree of polymerization. Thus, a single calibration curve for glucose cannot be used to quantify maltooligosaccharides unless the immobilized enzyme reactor (or an equivalent method) is used which produces equivalent peak area sensitivities.

The system described here was used to determine the amount of each maltooligosaccharide found in corn syrup. The sample was a commercial product recommended as a substrate for *a*-amylase determinations. It was reported to contain maltooligosaccharides with DP = 4-10 and to be essentially free of glucose, maltose and maltotriose. The actual amounts of each maltooligosaccharide component was not specified. Two concentrations of the corn syrup maltooligosaccharide were analyzed.

The higher concentration (490 ug mL^{-1}) was used to quantify glucose and maltose and the lower concentration (70 ug mL^{-1}) was used to quantify maltotetraose and larger maltooligosaccharides. The samples were analyzed under the same conditions as those described above for the standard maltooligosaccharides. The single calibration curve for glucose was used to determine the quantity of each maltooligosaccharide present. The results of the analysis of corn syrup maltooligosaccharides are given in Table 3. It was determined that the sample contained 82% total carbohydrate by weight. To check this result, a phenol-sulfuric acid test for total carbohydrate (22) was performed on the sample; 86% total carbohydrate by weight was found (95% agreement). Therefore, the analytical system described is concluded to be valid for the determination of corn syrup maltooligosaccharides.

Table 3. Amounts of maltooligosaccharides found from corn syrup

Maltooligosaccharide degree of polymerization	[a]Percent by weight	Percent relative standard deviation
1	1.6	63
2	5.9	37
3	---	--
4	2.9	31
5	6.6	11
6	15.9	8
7	19.6	5
8	14.3	3
9	9.3	8
10	6.3	11

[a]The average of four determinations except for glucose and maltose which were determined in duplicate.

ACKNOWLEDGMENTS

The authors thank Dr. Peter Reilly for supplying the glucoamylase and for many helpful discussions. This work was supported by the National Science Foundation under Contract CHE-8612314.

REFERENCES

1. L. D. Bowers, in I. S. Krull (Ed.), "Reaction Detection in Liquid Chromatography", Marcel Dekker, New York, 1986, Chapter 4.
2. G. G. Guilbault, "Analytical Uses of Immobilized Enzymes", Marcel Dekker, New York, 1984, Chapter 1.
3. L. D. Bowers, Anal. Chem., 58 (1986), 513A.
4. B. E. Norman, in G. G. Birch, N. Blakebrough and K. J. Parker (Eds.), "Enzymes and Food Processing", Applied Science, London, 1981, Chapter 2.
5. G. K. Buckee and R. Hargitt, J. Inst. Brew., 84 (1978), 13.
6. D. French, in W. J. Whelan (Ed.), "Biochemistry of Carbohydrates", University Park Press, Baltimore, 1975, Chapter 6.
7. R. E. Reim and R. M. Van Effen, Anal. Chem., 58 (1986), 3203.
8. J. D. Olechno, S. R. Carter, W. T. Edwards and D. G. Gillen, Am. Biotech. Lab., 5 no. 5 (1987), 38.
9. D. S. Austin, J. A. Polta, T. Z. Polta, A. Tang, T. D. Cabelka and D. C. Johnson, J. Electroanal. Chem., 168 (1984), 227.
10. D. C. Johnson and T. Z. Polta, Chromatogr. Forum, 1 (1986), 37.
11. D. C. Johnson, Nature, 321 (1986), 451.
12. G. G. Neuburger and D. C. Johnson, Anal. Chem., 59 (1987), 150.
13. P. J. Reilly, in G. M. A. van Beynum and J. A. Roels (Eds.), "Starch Conversion Technology", Marcel Dekker, New York, 1985, Chapter 5.

14. D. D. Lee, Y. Y. Lee, P. J. Reilly, E. V. Collins, Jr. and G. T. Tsao, Biotech. Bioeng., 18 (1976), 253.

15. L. A. Larew, D. A. Mead and D. C. Johnson, Anal. Chim. Acta, 204 (1988), 43.

16. S. C. Crowley, K. C. Chan and R. R. Walters, J. Chromatogr., 359 (1986), 359.

17. L. A. Larew and R. R. Walters, Anal. Biochem., 164 (1987), 537.

18. R. R. Walters, Anal. Chem., 55 (1983), 591.

19. D. R. Marsh, Y. Y. Lee and G. T. Tsao, Biotech. Bioeng., 15 (1973), 483.

20. C. R. Cantor and P. R. Schimmel, "Biophysical Chemistry", Part 2, W. H. Freeman and Co., San Francisco, 1980, Chapt. 10.

21. L. E. Welch, D. A. Mead and D. C. Johnson, Anal. Chim. Acta, 204 (1988), 323.

22. M. Dubois, K. A. Gilles, J. K. Hamilton, P. A. Rebers, and F. Smith, Anal. Chem., 28 (1956), 350.

SECTION IV.

FLOW INJECTION DETERMINATION OF STARCH AND TOTAL CARBOHYDRATE USING A GLUCOAMYLASE IMMOBILIZED REACTOR WITH PULSED AMPEROMETRIC DETECTION

SUMMARY

Starch and total carbohydrate were determined using a flow injection system comprised of an immobilized glucoamylase reactor followed by pulsed amperometric detection of the glucose produced. Glucoamylase, immobilized onto porous silica and packed into a short stainless steel column, was capable of nearly quantitative (98%) conversion of the starch to glucose. The sensitivity of pulsed amperometric detection for soluble starch was increased 26-fold by first passing the starch through the immobilized glucoamylase reactor. This system was successfully used to determine total carbohydrate in beer samples. The method is simple, rapid and sensitive for starch.

INTRODUCTION

The determination of total carbohydrate, including mono-, di- and oligosaccharides, is of primary importance in the brewing (1) and food processing (2) industries. Traditionally, carbohydrates have been determined colorimetrically using such reagents as ferricyanide for measuring total reducing end groups, and anthrone or phenol with sulfuric acid to measure total saccharide units (1). While these methods can be quite accurate (3), they suffer from poor precision (4) and are time consuming.

The use of immobilized enzyme reactors in flow injection analysis (FIA) combines the selectivity of enzyme reactions with the speed and simplicity of FIA (5). Recent applications of this technique for carbohydrate determination includes glucose and sucrose in soft drinks using invertase, mutarotase and glucose oxidase (6); fructose in fruit samples using fructose 5-dehydrogenase (7); and lactose in milk using galactose oxidase and peroxidase (8).

Glucoamylase catalyzes the hydrolysis of *a*-(1,4) and *a*-(1,6) glucosidic bonds of di- and oligosaccharides producing free glucose from the nonreducing end of the polymer chain (9). Glucoamylase immobilized reactors of large capacity have been used for the continuous conversion of starch to glucose in the starch processing industry (2,9,10). Some of the past analytical applications of glucoamylase have included starch determination in cereal brans using the enzyme in free solution (11), maltose determination using an immobilized glucoamylase/glucose oxidase electrode (12) and the determination of maltose and starch using the

enzyme immoblized onto tubular (13) or thin layer (14) flow-through reactors. The glucose liberated in these starch and maltose determinations was determined indirectly based on detection of the hydrogen peroxide produced by glucose oxidase. The hydrogen peroxide was detected colorimetrically (11,13), amperometrically (12) and titrimetrically (14).

Pulsed amperometric detection (PAD) of carbohydrates has become increasingly popular since it was first reported in 1981 (15,16,17). This method allows direct electrochemical detection of carbohydrates without the need for chemical or enzymatic transformation prior to detection. Pulsed amperometric detection also provides detection limits at the part-per-million level and excellent sensitivity for mono- and disaccharides (18). However, as the degree of polymerization (DP) of the oligosaccharide increases, the amperometric response decreases, resulting in the relatively poor sensitivity and high detection limits for DP > 3, as compared to glucose (18,19). This paper describes a method which combines an immobilized glucoamylase reactor with PAD for the determination of oligosaccharides having a degree of polymerization >> 2. The method is simple, rapid and sensitive and has been applied to the determination of soluble starch and to total carbohydrate in beer samples.

MATERIALS AND METHODS

Reagents

Glucoamylase (EC 3.2.1.3, *a*-(1,4) glucan glucohydrolase, ex. Aspergillus niger) was from Novo Industri (Bagsvaerd, Denmark). Glucose and soluble starch were from Fisher Scientific (Fair Lawn, NJ). *g*-Glycidoxypropyltrimethoxysilane was from Petrarch (Bristol, PA). 1, 1'-Carbonyldiimidazole was from Aldrich (Milwaukee, WI). LiChrospher Si-4000 silica (10 uM diameter) was from Merck (Darmstadt, Germany). All other chemicals were reagent grade. Water was condensed from steam and purified further by a Milli-Q system from Millipore (Bedford, MA).

Apparatus

The flow injection system consisted of a gradient liquid chromatograph (Beckman, Model 344; Berkeley, CA), a solvent delivery system (Rainin, Rabbit-HP; Woburn, MA), an injection valve equipped with a 50-uL sample loop (Rheodyne, Model 7010; Cotati, CA), a potentiostat (Dionex, Model PAD-2; Sunnyvale, CA), and eluent mixing system (Dionex, Model GM-2). The PAD-2 detector system included a flow-through cell equipped with a gold working electrode, glassy carbon counter electrode and saturated calomel reference electrode (Dionex, Model PAD-2). Data were collected and processed with an Apple IIe computer and ADALAB interface (Interactive Microware; State College, PA). The immobilized enzyme reactor was packed with an air-driven pump (Haskel from Alltech; Deerfield, IL) and a stirred-slurry column packer (Micromeritics, Model 705; Norcross, PA). A circulating water bath (Lauda, Model K-2/RD from Brinkman; Westbury, NY) was used for temperature control.

Procedures

Preparation of Enzyme Reactor

Glucoamylase was immobilized onto the LiChrospher support following the procedure of Crowley et al. (20). The enzyme was first dissolved at a concentration of 10 mg mL^{-1} in 0.2 M sodium acetate buffer (pH 4.8). A 10 mL aliquot of this solution was added to 1.0 gram of activated support and shaken for 6 days at 4.0° C. The enzyme-linked support was then washed by centrifugation with 2 M NaCl followed by acetate buffer and stored under refrigeration in the buffer.

The immobilized glucoamylase reactor was prepared by slurry-packing the enzyme-linked support into a 5 cm x 4.1 mm i.d. column at 3000 p.s.i. using the acetate buffer. The column was of a published design with the outer connector modified as a water jacket (21).

Flow Injection System and Oligosaccharide Determination

A schematic diagram of the flow-injection system is shown in Figure 1. The gradient system, composed of a controller (A) and two pumps (B,C), provided simple generation of calibration plots by varying the amount of standard or sample pumped through the sample loop (SL) of the sample injection valve (IJ). Samples and standard were dissolved in 0.2 M sodium acetate buffer (pH 4.8). The standard was 0.50 mM glucose and the samples included soluble starch at a concentration of 0.0083% (wt/vol), and two popular brands of beer each diluted 250-fold. The flow rate through the injection loop was held constant at 1.0 mL min^{-1}. The immobilized enzyme reactor was continuously eluted with the

Figure 1. Schematic diagram of the flow injection system.

Components: (A) gradient controller; (B,C) gradient pumps: (B) sample or standard, (C) 0.2 M acetate buffer; (D,E) carrier pumps: (D) 0.2 M acetate buffer (0.6 mL min-1), (E) 0.1 M NaOH (1.0 mL min-1); (V) 3-way valve; (M) eluent mixer; (IJ) injection valve; (SL) sample loop; (ER) enzyme reactor; and (PAD) pulsed amperometric detector cell

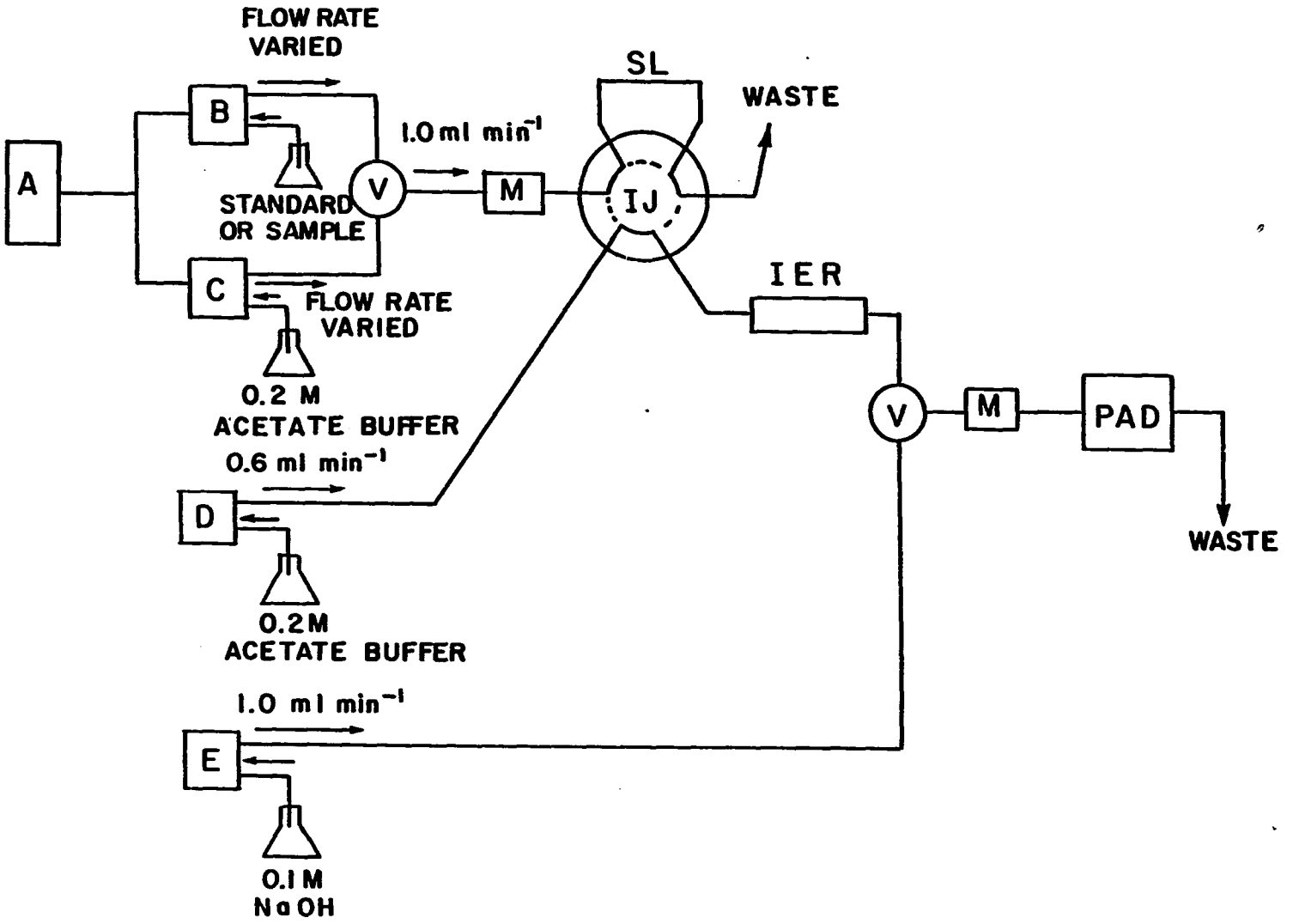
FLOW RATE
VARIED
SL
WASTE
B
1.0 ml min⁻¹
A
V
M
IJ
STANDARD
OR SAMPLE
C
IER
FLOW RATE
VARIED
0.2 M
ACETATE BUFFER
V
M
PAD
0.6 ml min⁻¹
D
WASTE
0.2M
ACETATE BUFFER
1.0 ml min⁻¹
E
0.1 M
NaOH

acetate buffer (pump D) at a flow rate of 0.6 mL min^{-1}. Standard or sample was injected onto the enzyme reactor at various dilutions. The reactor temperature was held constant at 40° C. A carrier stream of 0.1 M NaOH was continuously pumped (E) at a flow rate of 1.0 mL min^{-1} and combined with the eluate from the reactor at a 3-way valve (V). The streams were mixed by an eluent mixer (M) which was placed before the detector cell (PAD). The NaOH was required to raise the pH sufficiently for the highly sensitive detection of carbohydrates in the PAD cell (i.e., pH > 10). The PAD cell was operated under the following conditions (all potentials versus SCE): detection at 150 mV with a sampling time of 200 ms at the end of a 420 ms period, oxidative cleaning at 750 mV for 120 ms, and oxide reduction at -1.0 V for 120 ms. The detector output was filtered with a 3.0 s time constant to eliminate noise.

RESULTS AND DISCUSSION

Enzyme Immobilization

Prior to immobilization the glucoamylase had an initial activity of 6600 units at 25° C, where one unit is equivalent to 1 umol of glucose produced per minute per gram of enzyme in a 1.0% (wt/vol) solution of soluble starch. The initial activity was measured using a ferricyanide assay for the glucose produced. As determined by a BCA protein assay (20), 7.0 mg of glucoamylase were immobilized per 1.0 g of support. One gram of enzyme-linked support had an initial activity at 25° C of 22 umoles of glucose produced per minute, as determined using a continuously stirred batch reactor and PAD for the glucose produced from a 1.0% (wt/vol) solution of soluble starch. Thus, the immobilized glucoamylase maintained 48% of its original activity.

Preliminary Testing and Calibration

Soluble starch was used as the enzyme substrate for testing the proposed system. The starch was found to be 96.4% pure using a phenol-sulfuric acid method for determining total carbohydrate (22). Combining the results of a ferricyanide assay for total reducing end groups with the phenol-sulfuric acid results, the number average degree of polymerization of the starch sample was calculated to be 25. The starch concentrations injected onto the enzyme reactor were chosen so that the total glucose produced was well within a linear range of response for PAD.

The response of the flow-injection PAD system to starch and glucose, with and without the presence of the reactor column, is

shown in Figure 2. The additional peak dispersion caused by the enzyme reaction is readily observed in Fig. 2. The peaks for glucose produced by the immobilized enzyme (peaks B through G) had much greater tailing and required longer times for elution than standard glucose (peak H). The increased peak dispersion produced smaller peak heights but did not change peak areas. Therefore, a comparison of starch and glucose peak heights would have required a correction for the difference in dispersion. Because of this, only peak areas were compared. A plot of starch concentration versus peak area was linear. The equation and regression results for 18 data points are slope = 6600 ± 270 ucoul per wt/vol % starch, Y-intercept = -1.8 ± 1.0 ucoul, standard error = 0.15 ucoul and correlation coefficient = 0.995, where all confidence intervals represent one standard deviation. The large increase in the sensitivity of PAD for soluble starch when the enzyme reactor was used is shown also in Fig. 2. The sensitivity was 26 times larger when the starch was passed through the enzyme reactor prior to PAD. The contribution by the enzyme reactor to total dispersion of the system could presumably be diminished by a decrease in the internal volume of the enzyme reactor. To maintain the goal of 100% conversion by the reactor, any decrease in the amount of enzyme resulting from a decrease in the dimension of the reactor would require an increase in enzyme activity. At first thought, an increase in reactor temperature above 40° C might be expected to increase the activity. However, as demonstrated by Lee et al. (10), a change to 55° C brought about a 2X increase in activity but a 20X decrease in reactor lifetime. For this work,

Figure 2. The response of pulsed amperometric detection to starch and glucose without (A) and with (B-H) the glucoamylase reactor. Soluble starch (% w/v) injected: (A) 0.0083, without enzyme reactor; (B) 0.0016, (C) 0.0024, (D) 0.0032, (E) 0.0040, (F) 0.0048, (G) 0.0056. Peak H: 0.0027% (w/v) glucose injected. Reactor dimensions: 5 cm x 4.1 mm i.d.

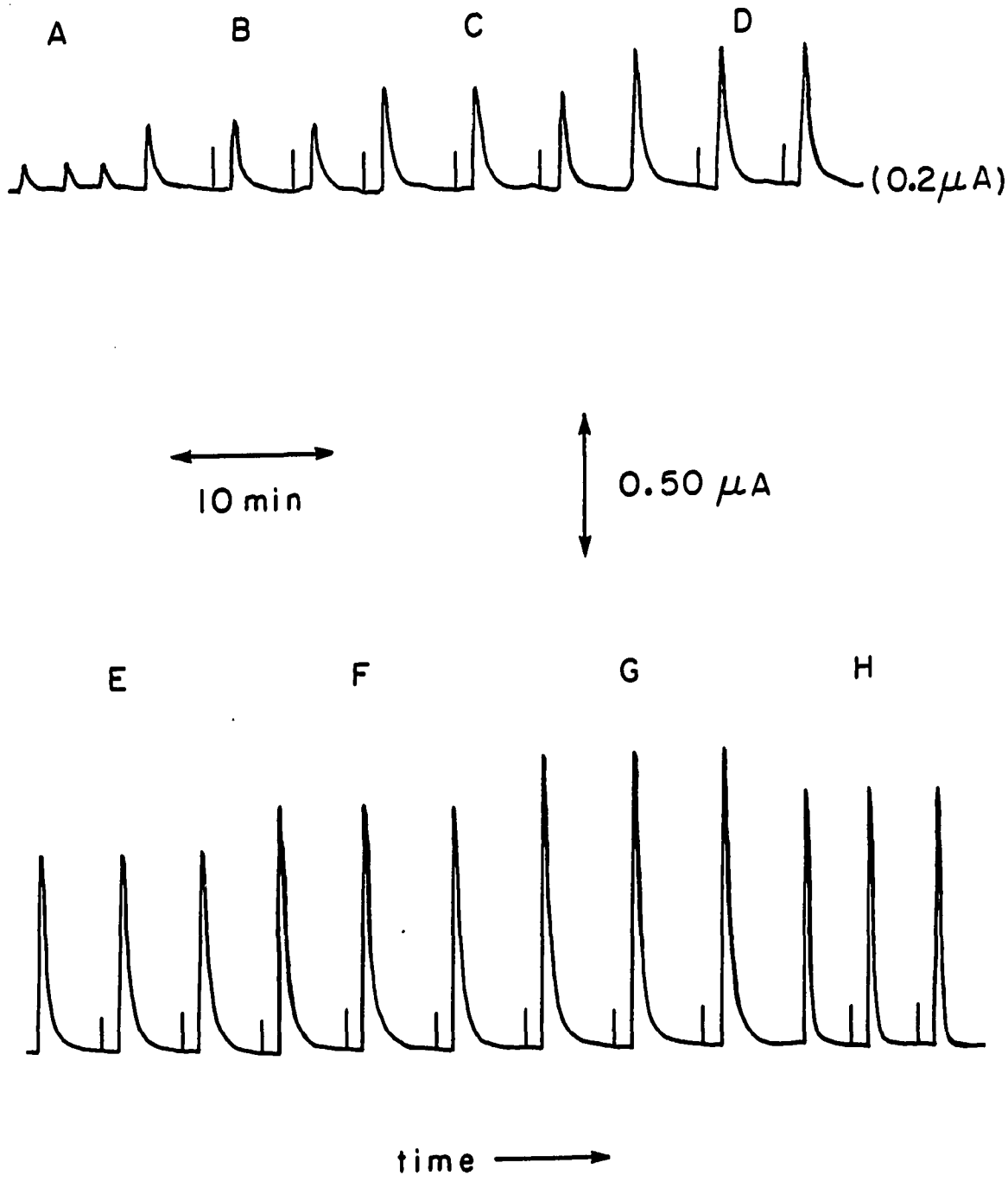
A
B
C
D
(0.2μA)
10 min
0.50 μA
E
F
G
H
time

maintenance of reactor lifetime was given precedence over a slight increase in activity.

Pulsed amperometric detection has its greatest sensitivity and lowest detection limits for monosaccharides. Therefore, it was desired that the enzyme reactor achieve as close to 100% conversion of the starch to glucose as possible. Also, if the column activity is more than sufficient to produce 100% conversion, then the effective conversion is independent of small changes in enzyme activity which may occur with time. The percent conversion was determined by comparing the slopes of peak area calibration plots for soluble starch and glucose. It was assumed that if the conversion of the starch to glucose was complete, then the slopes of the peak area calibration plots would be equal for starch and glucose. The percent conversion was calculated from the ratio of slopes of the starch and glucose calibration plots. The linear regression statistics for the calibration plot of standard glucose are (for 18 data points) slope = 6700 $\pm$ 160 ucoul per wt/vol % glucose, y-intercept = -1.2 $\pm$ 0.6 ucoul, standard error = 0.23 ucoul and correlation coefficient = 0.998. Therefore, 98 $\pm$ 5% of the starch was converted to glucose by the enzyme reactor.

Total Carbohydrate in Beer Samples

Many different types of carbohydrates are found in beer samples (1,23). These are usually classified as fermentable sugars, which include glucose, fructose, sucrose, maltose and maltotriose, and non-fermentable sugars, which include the maltooligosaccharides with a degree of polymerization > 3. The total carbohydrate content of beer

ranges from 0.8 to 6.0 wt/vol %, depending on the type and sample (23). The total fermentable sugar content of beer ranges between 0.2 and 2.0 wt/vol % and the total nonfermentable sugar content ranges between 0.2 and 4.0 wt/vol %. Other types of carbohydrate include *b*-glucans and pentosans (0 - 1.0 wt/vol %). Two beer samples were analyzed in this study. One was a low calorie, or "light" beer, known to contain not more than 1.41 wt/vol % total carbohydrate. The second was a high calorie beer from the same manufacturer for which the carbohydrate content was unknown. The low calorie beer was used as a control sample.

The response of PAD to beer samples with and without the benefit of the enzyme reactor was determined. If it can be assumed that the conversion of the maltooligosaccharides to glucose was complete, then the peaks obtained with the reactor in place were a measurement of the total fermentable and non-fermentable sugar content of the beer. The peaks obtained without the benefit of the reactor were a measurement of the fermentable sugars only. The values for total fermentable sugar and total non-fermentable sugar obtained with this method are given in Table 1. Glucose was the standard used to calibrate the PAD response for carbohydrate; therefore, the values are expressed as wt/vol % glucose. Also given in Table 1 are values for total carbohydrate and total *b*-glucan content of the beers. The total carbohydrate content was determined using the phenol-sulfuric acid method with glucose as the standard. Any *b*-glucan polymers present in the sample were not hydrolyzed by the enzyme reactor and, thus, were not detected by PAD. The *b*-glucan content was determined by the difference between the total

Table 1. Results for the determination of carbohydrate in beers

	CONTENT[a] (%wt/vol)			
	Total Fermentable Sugar	Total Nonfermentable Sugar	Total b-Glucan	Total Carbohydrate
Light Beer	0.99 ± 0.1	0.22 ± 0.09	0.04 ± 0.13	1.3 ± 0.2
Beer	1.4 ± 0.1	1.3 ± 0.1	0.6 ± 0.3	3.3 ± 0.4

[a]Mean and standard deviation for 3 separate determinations.

carbohydrate value and the sum of the values for total non-fermentable and fermentable sugars obtained with the benefit of the enzyme reactor. The values listed in Table 1 are well within the ranges typical for beer samples. The total carbohydrate found in the control sample (light beer) was in good agreement with the known value of < 1.41 wt/vol %. It is interesting to note that the calorie difference between the two beers was the result of the greater starch (non-fermentable sugar) content of the higher calorie beer. The total fermentable sugar was approximately the same for each beer. Also, the much lower *b*-glucan content of the light beer provided this beer with a much lower viscosity and thus a "lighter" quality sensed by the tongue and palate.

To test the assumption that the conversion of the beer malto-oligosaccharides by the enzyme reactor was complete, the slopes of calibration plots for glucose, starch and the beer samples were compared. These results are summarized in Table 2. Again, if the conversion of the maltooligosaccharides to glucose by the enzyme reactor was complete, then the slopes of the peak area calibration plots for the starch and beers would be equal to that for glucose. As can be seen in Table 2, the conversion by the reactor was quantitative, within one standard deviation, for all of the samples. Therefore, the analytical system described is concluded to be valid for determining total fermentable and non-fermentable carbohydrate in beers.

Table 2. The slopes of the calibration plots and the percent conversion by the glucoamylase reactor for glucose, soluble starch and beer samples

	GLUCOSE	STARCH	LIGHT BEER	BEER
Slope[a]	6.7 ± 0.2	6.6 ± 0.3	6.6 ± 0.2	7.0 ± 0.2
CONVERSION BY ENZYME REACTOR (%)	---------	98 ± 5	98 ± 4	104 ± 4

[a] 10^3 uCoul per % (w/v) as glucose.

CONCLUSIONS

This is the first published report of work in which an immobilized enzyme reactor was coupled to pulsed amperometric detection. Many of the substances which are advantageously detected by PAD are products of enzyme reactions. These include alcohols, carbohydrates, amines, amino acids, aldehydes and organic sulfur compounds. Thus, many systems based on the combination of enzyme reactors with pulsed ampermometric detection can be envisioned. Future studies involving the glucoamylase-PAD system described in this paper include: using the system as a post-column detector for size-exclusion and reversed-phase chromatographic separations of starches; the determination of the kinetic parameters of the immobilized enzyme; and the determination of the lifetime and stability of the enzyme reactor under various conditions. While no detailed study of the long-range stability of the enzyme reactor has yet been done, the reactor described here was packed 4 months after the enzyme was first immobilized to the support. In a previous study the half life of immobilized glucoamylase was estimated to be over 500 days (10). Therefore, immobilized glucoamylase appears to be stable over reasonably long times.

ACKNOWLEDGMENTS

The authors thank Dr. Peter Reilly for supplying the glucoamylase and for many helpful discussions. This work was supported by the National Science Foundation under Contract CHE-8612314.

REFERENCES

1. G. K. Buckee and R. Hargitt, J. Inst. Brew., 84 (1978), 13.
2. B. E. Norman, in G. G. Birch, N. Blakebrough and K. J. Parker (Eds.), "Enzymes and Food Processing", Applied Science, London, 1981, p. 15.
3. J. Weiner, J. Inst. Brew., 84 (1978), 222.
4. J. R. Brooks, V. K. Griffin and M. W. Kattan, Cereal Chem., 63 no. 5 (1986), 465.
5. G. Johansson, L. Ogren and B. Olsson, Anal. Chim. Acta, 145 (1983), 71.
6. M. Masoom and A. Townshend, Anal. Chim. Acta, 171 (1985), 185.
7. K. Matsumoto, O. Hamada, H. Ukeda and Y. Osajima, Anal. Chem., 58 (1986), 2732.
8. H. Lundback and B. Olsson, Anal. Lett., 18 no. B7 (1985), 871.
9. P. J. Reilly, in G. M. A. van Beynum and J. A. Roels (Eds.), "Starch Conversion Technology", Marcel Dekker, New York, 1985, p. 101.
10. D. D. Lee, Y. Y. Lee, P. J. Reilly, E. V. Collins, Jr. and G. T. Tsao, Biotech. Bioeng., 18 (1976), 253.
11. F. R. Dintzis and C. C. Harris, Cereal Chem., 58 no. 5 (1981), 467.
12. P. R. Coulet and C. Bertrand, Anal. Lett., 12 no. B6 (1979), 581.
13. D. J. Inman and W. E. Hornby, Biochem. J., 137 (1974), 25.
14. J. M. Brillouet, P. R. Coulet and D. C. Gautheron, Biotech. Bioeng., 18 (1976), 1821.

15. S. Hughes and D. C. Johnson, Anal. Chim. Acta, 132 (1981), 11.

16. D. C. Johnson, Nature, 321 (1986), 451.

17. D. C. Johnson and T. Z. Polta, Chromatogr. Forum, 1 (1986), 37.

18. R. D. Rocklin and C. A. Pohl, J. Liq. Chromatogr., 6 no. 9 (1983), 1577.

19. R. E. Reim and R. M. Van Effen, Anal. Chem., 58 (1986), 3203.

20. S. C. Crowley, K. C. Chan and R. R. Walters, J. Chromatogr., 359 (1986) 359.

21. R. R. Walters, Anal. Chem., 55 (1983), 591.

22. M. Dubois, K. A. Gilles, J. K. Hamilton, P. A. Rebers and F. Smith, Anal. Chem., 28 (1956), 350.

23. G. K. Buckee and R. Hargitt, J. Inst. Brew., 83 (1977), 275.

GENERAL SUMMARY

The results from cyclic voltammetric studies of the oxidations of glucose and glucose derivatives at gold electrodes were presented in Section I. A mechanism was presented to explain the observed experimental facts. Amperometric detection of carbohydrates was concluded to result from the oxidation of the carbonyl and/or hydroxyl groups of adsorbed carbohydrate molecules. These oxidations were concluded to be catalyzed by a hydrous gold oxide which was formed on the surface of the electrode in alkaline solutions at potential values between - 0.4 and 0.6 V versus the normal hydrogen electrode. Based upon these results, the response of PAD for different types of carbohydrates is predicted to depend upon the arrangements of the carbonyl and hydroxyl groups; the presence of electrochemically active (or inactive) derived functionalities (i.e., carboxyl, amino, thiol and hydrogen groups); and upon the molecular size (diffusion coefficient) of each type of carbohydrate. Therefore, the quantitation of significantly different carbohydrates by PAD will require a calibration of the PAD response for each different carbohydrate.

Pulsed amperometric detection of glucose was extended to solutions of low buffer capacity having neutral and acidic pH values in Section II. A transient condition of alkalinity was generated within the diffusion layer of a gold electrode by application of the PAD potential waveform. This allowed the catalytic hydrous gold oxide to form prior to the application of the detection potential for glucose. The hydrolysis of starch by glucoamylase was directly followed by performing PAD for

glucose in the presence of the active enzyme and the starch substrate at pH 4.8. This method for glucoamylase activity was found to be accurate, more precise, and much faster than the traditional ferricyanide assay. It is believed that direct assays by PAD can be developed for many other enzymes of clinical, biological and industrial importance. Many of the substances which can advantageously be detected by PAD are the products of enzyme reactions. These include alcohols, carbohydrates, amines, amino acids, aldehydes and thiols. Thus, a direct enzyme assay by PAD should be an attractive alternative to discontinuous enzyme assays based upon indicator enzymes or derivatized substrates. If interference from chloride ions can be eliminated, then direct assays by PAD of serum glucose or *a*-amylase should be possible.

The use of an immobilized glucoamylase reactor, placed before the detector cell, allowed the flow injection (Section IV) and chromatographic (Section III) determinations of starch and maltooligosaccharides to be performed with a single glucose calibration curve. The conversions of these polymers to glucose were approximately quantitative in the reactor. Use of a single glucose calibration curve for the determination of these polymers without the enzyme reactor produced large errors in the estimates of the polymer concentrations. Pure standards for these maltooligosaccharides are not readily available from chemical suppliers to calibrate the PAD response. Therefore, the methods described in Sections III and IV are concluded to offer a significant improvement in accuracy and economy for the determinations of starch and maltooligosaccharides.

REFERENCES

1. E. L. Smith, R. L. Hill, I. R. Lehman, R. J. Lefkowitz, P. Handler and A. White, "Principles of Biochemistry: General Aspects", McGraw-Hill, New York, 1983, Chapter 6.
2. W. Pigman and D. Horton, in W. Pigman and D. Horton (Eds.), "The Carbohydrates: Chemistry and Biochemistry", Vol. 1A, Academic Press, New York, 1972, Chapter 1.
3. J. W. Green, in W. Pigman and D. Horton (Eds.), "The Carbohydrates: Chemistry and Biochemistry", Vol. 1B, Academic Press, New York, 1980, Chapter 22.
4. O. Theander, in W. Pigman and D. Horton (Eds.), "The Carbohydrates: Chemistry and Biochemistry", Vol. 1B, Academic Press, New York, 1980, Chapter 23.
5. D. Horton and J. D. Wander, in W. Pigman and D. Horton (Eds.), "The Carbohydrates: Chemistry and Biochemistry", Vol. 1B, Academic Press, New York, 1980, Chapter 16.
6. D. Horton and J. D. Wander, in W. Pigman and D. Horton (Eds.), "The Carbohydrates: Chemistry and Biochemistry", Vol. 1B, Academic Press, New York, 1980, Chapter 18.
7. N. Williams and J. Wander, in W. Pigman and D. Horton (Eds.), "The Carbohydrates: Chemistry and Biochemistry", Vol. 1B, Academic Press, New York, 1980, Chapter 17.
8. M. L. Wolfrom and W. A. Szarek, in W. Pigman and D. Horton (Eds.), "The Carbohydrates: Chemistry and Biochemistry", Vol. 1A, Academic Press, New York, 1972, Chapter 7.

9. J. H. Pazur, in W. Pigman and D. Horton (Eds.), "The Carbohydrates: Chemistry and Biochemistry", Vol. 2A, Academic Press, New York, 1970, Chapter 30.

10. I. Danishefsky, R. L. Whistler and F. A. Bettelheim, in W. Pigman and D. Horton (Eds.), "The Carbohydrates: Chemistry and Biochemistry", Vol. 2A, Academic Press, New York, 1970, Chapter 35.

11. D. French, in W. J. Whelan (Ed.), "Biochemistry of Carbohydrates", University Park Press, Baltimore, 1975, Chapter 6.

12. J. F. Robyt, in Whistler, BeMiller and Paschall (Eds.), "Starch: Chemistry and Technology", Academic Press, New York, 1984, Chapter 4.

13. P. J. Reilly, in van Beynum and Roels (Eds.), "Starch Conversion Technology", Marcel Dekker, New York, 1985, Chapter 5.

14. P. J. Reilly, in L. B. Wingard, E. Katchalski-Katzir and L. Goldstein (Eds.), "Applied Biochemistry and Bioengineering", Vol. 2, Academic Press, New York, 1979, Chapter 6.

15. P. H. Rieger, "Electrochemistry", Prentice-Hall, Englewood Cliffs, New Jersey, 1987.

16. A. J. Bard and L. R. Faulkner, "Electrochemical Methods: Fundamentals and Applications", John Wiley and Sons, New York, 1980.

17. P. T. Kissinger and W. R. Heineman (Eds.), "Laboratory Techniques in Electroanalytical Chemistry", Marcel Dekker, New York, 1984.

18. D. A. Skoog, "Principles of Instrumental Analysis", Saunders College, Philadelphia, 1985.

19. D. P. Shoemaker, C. W. Garland, J. I. Steinfeld and J. W. Nibler, "Experiments in Physical Chemistry", McGraw-Hill, New York, 1981.

20. J. D. Olechno, S. R. Carter, W. T. Edwards and D. G. Gillen, Am. Biotech. Lab., 5 no. 5 (1987), 38.

21. J. M. Elbicki, D. M. Morgan and S. G. Weber, Anal. Chem., 56 (1984), 978.

22. D. C. Johnson, Nature, 321 (1986), 451.

23. J. Giner, Electrochim. Acta, 9 (1964), 63.

24. Y. B. Vassilyev, O. A. Khazova and N. N. Nikolaeva, J. Electroanal. Chem., 196 (1985), 127.

25. E. B. Makovos and C. C. Lui, J. Electroanal. Chem., 211 (1986), 157.

26. D. C. Johnson and T. Z. Polta, Chromatogr. Forum, 1 (1986), 37.

27. G. G. Neuberger and D. C. Johnson, Anal. Chem., 59 (1987), 150.

28. S. Hughes and D. C. Johnson, Anal. Chim. Acta, 132 (1981), 11.

29. G. Halliwell, in H. U. Bergmeyer (Ed.), "Methods of Enzymatic Analysis", Vol. 3, Verlag Chemie Weinheim, Academic Press, New York, 1974, pg. 1132.

30. G. K. Buckee and R. Hargitt, J. Inst. Brew., London, 84 (1978), 13.

31. B. E. Norman, in G. G. Birch, N. Blakebrough and K. J. Parker (Eds.), "Enzymes and Food Processing", Applied Science, London, 1981, pg. 15.

32. W. T. Caraway and N. B. Watts, in N. W. Tietz (Ed.), "Textbook of Clinical Chemistry", W. B. Saunders, Philadelphia, 1986, Chapter 6.

33. D. A. Mead, Jr., M. S. Thesis, Iowa State University, 1988.

34. M. I. Horowitz, in W. Pigman and D. Horton (Eds.), "The Carbohydrates: Chemistry and Biochemistry", Vol. 1B, Academic Press, New York, 1980, Chapter 28.

35. D. Aminoff, W. W. Binkley, R. Schaffer and R. W. Mowry, in W. Pigman and D. Horton (Eds.), "The Carbohydrates: Chemistry and Biochemistry", Vol. 2B, Academic Press, New York, 1970, Chapter 45.

36. L. A. Larew and R. R. Walters, Anal. Biochem., 164 (1987), 537.

ACKNOWLEDGMENTS

It would be impossible to give just credit to all the people who have influenced and shaped my scholarly career. Dr. Phyllis Kingsbury and Dr. Roland Stout at Drake University were the first to inspire my interest in the biological and physical sciences. My brief opportunity to work in Dr. Rodney R. Walters' group provided me with the foundations of my knowledge in analytical and separation science. A special thanks to Dr. Walters for instilling in me the confidence to work independently as a researcher. Credit must also be given to the former members of Dr. Walters' group; this group provided a friendship and comradery which will last a lifetime and was also a source of many valuable ideas and discussions. A special thanks goes to Samuel C. Crowley, who shared with me many of his ideas on immobilized enzyme reactors and predicted their success when combined with PAD.

The person most responsible for my development as a scholar and an analytical chemist is Dr. Dennis C. Johnson. I will be forever grateful to Dr. Johnson for letting me join his group after Dr. Walters left Iowa State. I thank Dr. Johnson for his patience and leadership and for sharing with me the research ideas which resulted in this dissertation.

Of course the members of Dr. Johnson's group are also greatly appreciated for their help and assistance in my endeavor to become an electrochemist. A special thanks to Joe Vitt and Dave Mead, who had to tolerate my presence in the laboratory.

I am also grateful to all the teachers and committee members I have

had the opportunity to learn from here at Iowa State for challenging me in both course work and in preliminary examinations. In striving to meet their challenges, I have extended my limits farther than I would have thought possible 5 years ago. A special thanks goes to Dr. Peter Reilly, who generously provided the glucoamylase used in the work described in this dissertation and whose helpful advice aided in the completion of that work.

Finally, I must thank those people who have influenced and shaped me as an individual. I dedicate this dissertation to all the special people who comprise my family. They have been the source of my strength and courage over the last 5 years. I have spent much time away from the ones I dearly love in achieving this goal and I look forward to spending more time with them. My wife, Jackie; our darling little girl, Ashley; my mother and father; and all the rest; I thank you for your understanding, patience, and love.